ANNUAL REPORT - TUNL XVII

1 January 1978-31 December 1978

TRIANGLE UNIVERSITIES NUCLEAR LABORATORY

Duke University
University of North Carolina at Chapel Hill
North Carolina State University at Raleigh

Duke Station, Durham, North Carolina 27706

BLANK PAGE

We dedicate this Annual Report to

HENRY W. NEWSON

James B. Duke Professor of Physics

November 26, 1909 - May 14, 1978

Henry W. Newson was one of the pioneers of nuclear physics and was noted as a distinguished experimental physicist. He came to Duke University in 1948 and shortly thereafter started the Duke Nuclear Structure Laboratory. This developed into the Triangle Universities Nuclear Laboratory and he was its first director. He, more than any other person, is responsible for the nuclear community which now exists at the three Triangle Universities.

Cyclo-Graaff Laboratory

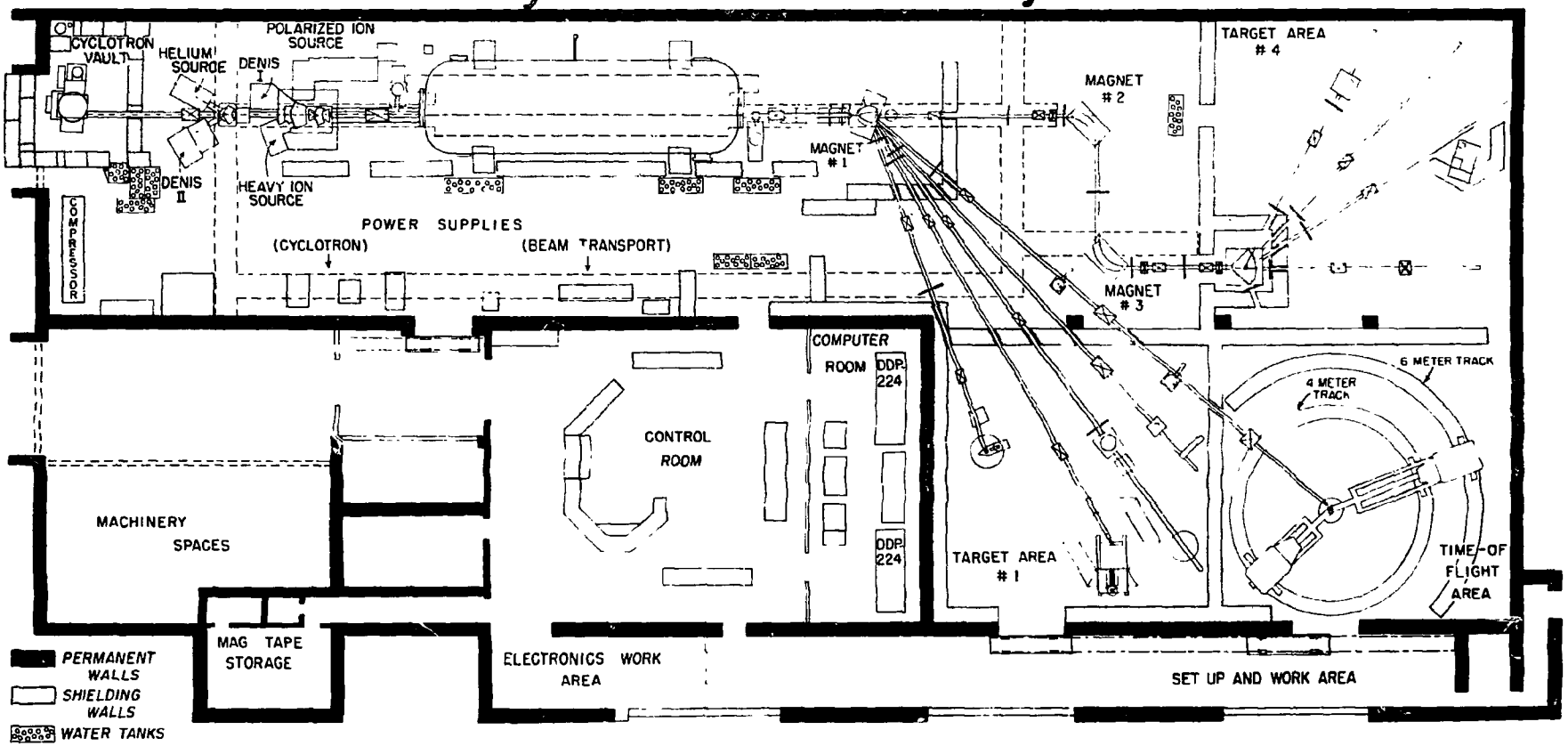

PREFACE

This document, prepared for submission to the U. S. Department of Energy, is the progress report for Triangle Universities Nuclear Laboratory for 1978. The laboratory was initiated and continues to operate as a cooperative research facility of Duke University, the University of North Carolina at Chapel Hill, and North Carolina State University at Raleigh. It is supported principally by the U. S. Department of Energy and by the three Universities.

The major accelerator facilities of the laboratory include a Model FN Tandem Van de Graaff accelerator and a 15 MeV negative-ion fixed-energy cyclotron injector. These machines, when used together, constitute the world's first Cyclo-Graaff. The laboratory has two additional Van de Graaff accelerators with terminal voltage of 4 MV and 3 MV. The latter accelerator, with its related equipment, is an exceptional facility providing intense beams of very high resolution.

While the TUNL research programs are characterized by considerable variety, reflecting the interests of a large permanent staff, the major emphasis is on light ion induced nuclear reactions, particularly those initiated by polarized beams of protons and deuterons, and elastic and inelastic scattering with very high resolution beams. In addition the laboratory has a special commitment to neutron physics--including specifically the measurement of fast neutron differential cross sections relevant to controlled thermonuclear fusion.

During this report period development work continued to emphasize the ion source capabilities serving the TUNL FN tandem. The present arrangement is shown in the new layout of the Cyclo-Graaff laboratory on the facing page.

Major work was concentrated upon the high current direct extraction source, DENIS II in the figure, which is the ion source of choice for pulsed beam experiments. Since it was obtained as surplus equipment, this ion source has undergone major re-design and modifications to improve its performance. Beam current available and beam quality (emittance) have each been improved by approximately factors of two and the source now produces 100 μa of a very high quality proton beam.

Extensive work along several different lines have led to substantial improvements in the TUNL Lamb Shift polarized ion source. Our "best" accelerated beam current has increased from 0.15 μA to 0.37 μA, and target currents of 0.20 to 0.24 μA have been obtained. In addition, major new components for further improving the ion source are being built and tested in Chapel Hill and will be installed during the coming year.

During this period a major effort was also devoted to re-installing the injector cyclotron. New main magnet coils were installed to replace defective coils, the cyclotron was moved to a new location to improve Cyclo-Graaff beam transmission, and most of the associated power supplies and auxiliary equipment were overhauled.

TUNL PERSONNEL

Faculty

Bilpuch, E.G. (director, professor)	Duke
Clegg, T.B. (professor)	UNC
Gould, C.R. (associate professor)	NCSU
Ludwig, E.J. (professor)	UNC
Mitchell, G.E. (professor)	NCSU
Nelson, C.E. (assistant professor)	Duke
Purser, F.O. (senior scientist)	Duke
Roberson, N.R. (professor)	Duke
Seagondollar, L.W. (professor)	NCSU
Shafroth, S.M. (professor)	UNC
Tilley, D.R. (professor)	NCSU
Walter, R.L. (professor)	Duke
Waltner, A.W. (professor)	NCSU
Weller, H.R. (associate professor)	Duke
Wender, S.A. (assistant professor)	Duke

Research Associates and Instructors

Byrd, R.C. (instructor)	Duke
Cadmus, R. (research associate) left 8/78	UNC
Hogue, H.H. (instructor) left 10/78	Duke
Kodre, A. (research associate) left 9/78	UNC
Westerfeldt, C. (research associate)	Duke

Associated Theorists

Biedenharn, L.C. (professor)	Duke
Cotanch, S. (assistant professor)	NCSU
Cusson, R.Y. (professor)	Duke
Kalbach, C. (assistant professor)	Univ. of Tenn.
Merzbacher, E. (professor)	UNC
Park, J. (professor)	NCSU
Thompson, W.J. (professor)	UNC
Way, K. (adjunct professor)	Duke

Visiting Personnel

Buck, B. 8/77-10/78	Oxford
Potokar, M. 4/78-11/78	Ljubljana
Seward, W. 6/78-8/78	Pomona College
Seyler, R. 6/1/78-6/8/78	Ohio State
Blue, R.A. (associate professor) 9/4/78-9/9/78	Florida

TUNL PERSONNEL (Continued)

Graduate Students

Ainsworth, T.L. left 1/78	UNC
Beyerle, A.	NCSU
Bleck, M. left 8/78	Duke
Brown, R.	Duke
Burks, B. (summer 1978)	UNC
Chandler, J. left 6/78	NCSU
Chou, B. H.	NCSU
El Kadi, S.	Duke
Epperson, D. left 12/78	Duke
Feagin, J.	UNC
Fitzpatrick, C.	Duke
Floyd, C.	Duke
Glendinning, S. G.	Duke
Jensen, M.	NCSU
Juelich, R. E. (summer 1978)	UNC
Lipton, G. B. left 5/78	UNC
Manglos, S.	Duke
Mitchell, S. M.	UNC
Murphy, K.	Duke
Putcha, B.	NCSU
Rollison, G.	UNC
Sales, K.	NCSU
Swenson, J.	UNC
Thambidurai, P.	NCSU
Tonsfeldt, S.	UNC
Turner, D. left 8/78	Duke
Varner, R. (summer 1978)	UNC
Ward, L.	NCSU
Watson, W. A.	Duke
Wells, W. K. left 11/78	Duke
Whatley, C. M.	Duke
Wilkerson, J. F.	UNC
Willis, J.	UNC
Wright, M.	Duke
Wu, J. T.	UNC
Wu, T. H. K. left 4/78	UNC

TUNL PERSONNEL (Continued)

Technical Support Staff for TUNL

Bailey, D. M.	Draftswoman
Chermak, C. left 6/78	Electronics Technician
Edwards, S. E.	Computer Maintenance Supervisor
Gibson, P. M.	TUNL Secretary
Harris, E. P.	Instrument Maker
Harward, J. T.	Electronics Technician
Hogan, R. G.	Instrument Maker
Larkins, A.	Electronics Technician
Lovette, A. G. left 9/78	Accelerator Technician
Lovette, A. W.	Shop Foreman, Instrument Maker
McCrary, P. T.	TUNL Secretary
O'Gorman, G. left 9/78	Electronics Technician
Rummel, R. L.	Accelerator Maintenance Supervisor

TABLE OF CONTENTS

BLANK PAGE

A. NEUTRON AND FISSION PHYSICS

1. Fast Neutron Cross Sections (R.L. Walter, C.R. Gould, F.O. Purser, L.W. Seagondollar, C.E. Nelson, H.H. Hogue,* S.G. Glendinning, A. Beyerle, Sadig El Kadi, C. Floyd, E.G. Bilpuch, H.W. Newson**)

a. Experimental

(1) New Electronics Arrangement

The electronics for the neutron time of flight (TOF) detectors have been upgraded to take advantage of the superior pulse shape discrimination (PSD) capabilities of the Canberra Model 2160 NIM modules. The wide dynamic range of these units also permit operation at low bias settings without saturating the electronics for high energy recoil events.

A block diagram of the electronic setup for one of the four TOF scintillators is shown in Fig. A1-1. The anode signal from the photomultiplier

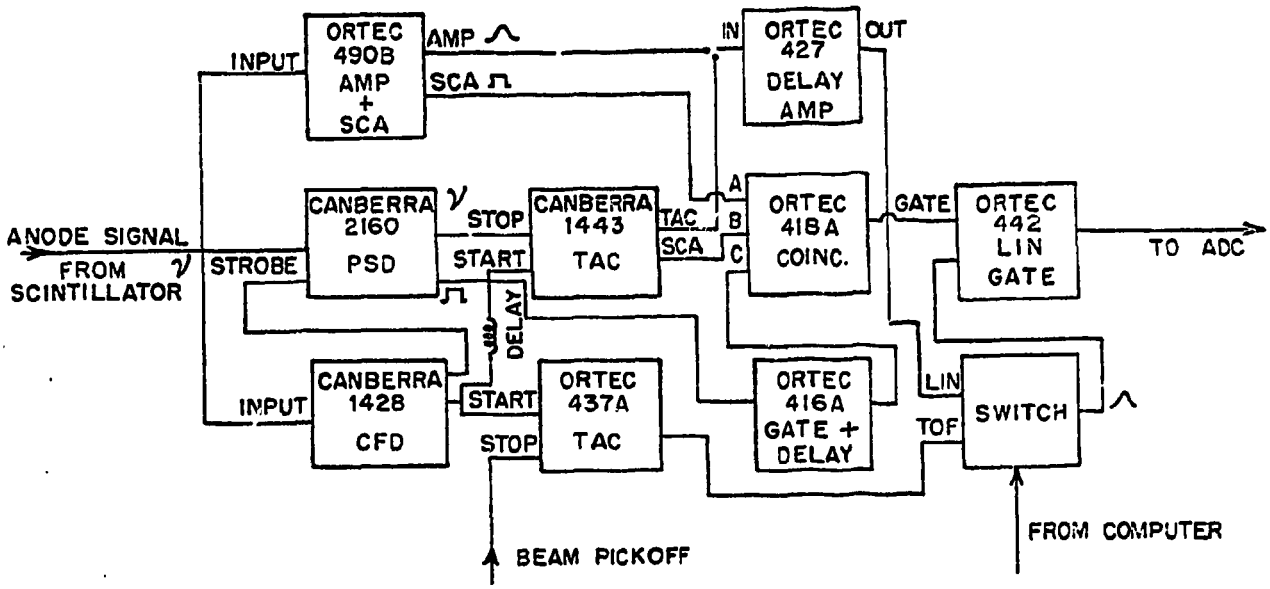

Fig. A1-1 Block diagram of electronics for TOF scintillator.

---

* Now at Oak Ridge National Laboratory

** Deceased

is used for both DSD information and linear information. The single channel analyzer (SCA) in the ORTEC 490B is used for setting the bias level for the experiment. The constant fraction discriminator (CFD) strobes the PSD unit and also provides the start signal for a Canberra 1443 time-to-amplitude converter (TAC). The stop signal comes from the PSD unit which is operated in the n + γ mode, and the SCA output of the TAC is used to select neutron and/or gamma ray events. A separate ORTEC 437A TAC is used for the neutron TOF measurement with the stop signal coming from a capacitive beam pick off. Any of the three signals--neutron TOF, neutron PSD, or the linear neutron energy signal can be gated through to an ADC subject to the logic requirements established in the ORTEC 418A universal coincidence unit. A linear switch operated by the computer permits automatic switching between the energy and TOF signals. This switch, at the same time, activates insertion of a calibration source near the detector permitting automatic checking of the detector bias settings.

Presently four neutron detectors are operational. The two main detectors are in the heavily shielded collimators, usually at flight paths of 4m and 6m respectively for measurements of elastic and discrete inelastic scattering. For low bias continuum measurements these detectors are moved in to flight paths of ~ 3m. Two small scintillators are used to minitor the source reaction. One is at zero degrees and is used to monitor timing variations in the pulsed beam. The other detector is mounted out of the reaction plane at a flight path of 2.0 m and is used for normalizing angular distribution measurements from angle to angle.

(2) Detector Efficiency Studies

As a result of the new electronics setup and in preparation for low bias (≤ 500 keV) measurements of continuum neutrons, new detector efficiency curves have been determined for the two main neutron detectors. Efficiencies for two bias settings were measured by measuring the response functions of the detectors to monoenergetic neutrons produced by the D(d,n) and T(p,n) reactions. Angular distributions were measured for incident particle energies of 6.0 MeV and 10 MeV for the D(d,n) reaction and at 2.5 MeV, 5.0 MeV and 10 MeV for the T(p,n) reaction. The overlapping data sets spanned the neutron energy range from 300 keV to 13 MeV. The energy range was extended to 16.8 MeV by measuring 0° excitation functions for the D(d,n)^{3}He reaction. All cross section data used to convert yields to efficiencies were from the compilation by Drosg[1] except for the 2.5 MeV T(p,n)^{3}He data which were taken from Liskien and Paulsen.[2] Efficiency curves for the two bias conditions are shown in Fig. A1-2.

---

[1] M. Drosg, Nuclear Science and Engineering 67, 190 (1978)

[2] H. Liskien and A. Paulsen, Nuclear Data Tables, Vol. II, no. 7, 1973

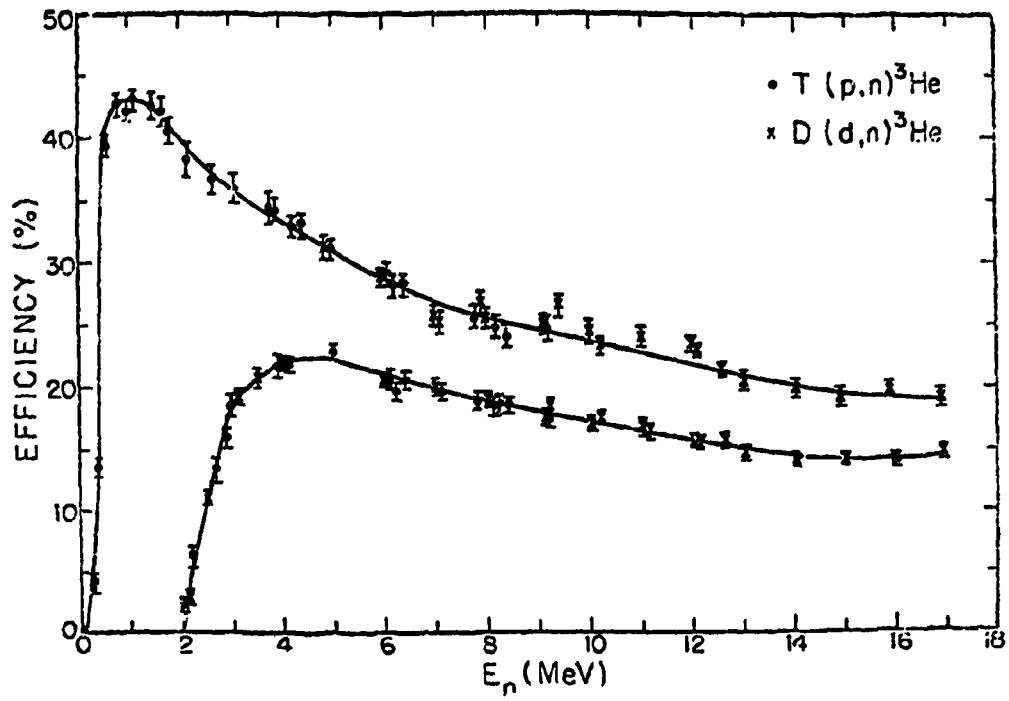

Fig. A1-2 Efficiency curves for two bias conditions.

(3) Comparison of The $D(d,n)^3He$ and $T(p,n)^3He$ Source Reactions

Both of the commonly used reactions for the production of monoenergetic neutrons have the undesirable property of also producing continuum neutrons from three-body breakup processes above the thresholds for the D(d,np)D and T(p,np)D reactions. These thresholds occur at 4.45 MeV deuteron energy and 8.35 MeV proton energy which are approximately equivalent to 7.5 MeV monoenergetic neutron energy in both cases.

For measurements of continuum neutrons from (n,xn) reactions in the presence of these "gas breakup" source neutrons, it is necessary to make four measurements to obtain the proper yields.

$$N(E_n) = [(\text{gas in, sample in}) - (\text{gas in, sample out})]$$
$$- [(\text{gas out, sample in}) - (\text{gas out, sample out})]$$

where gas in and gas out refer to measurements with the target cell filled and evacuated. The spectra resulting from this subtraction process will still contain contributions from gas breakup neutrons scattered from the sample. By measuring the 0° source neutron yield simultaneously with the scattering measurements, we can make corrections for contributions from these "contaminant" neutrons in data analysis pro-

cedures. It is, however, desirable that the magnitude of this correction be kept as small as possible to minimize the computational accuracy required for the correction.

An approximate figure of merit for a neutron source reaction can be constructed by comparing its monoenergetic yield with the integral yield from three and four body breakup processes. Such a signal-to-noise ratio has been measured[1] for the D(d,n) and T(p,n) reactions for monoenergetic neutron energies ranging from 10 to 14 MeV. Since projected neutron measurements at TUNL cover the range from 7 to 14 MeV, we undertook further tests of these reactions from 9 to 10 MeV. For neutron energies of 8.0 MeV and below, the D(d,n) reaction is the obvious selection due to its factor-of-3 additional yield.

Spectra at 0° from the D(d,n) and T(p,n) reactions for 9.2 MeV neutron energy are shown in Fig. A1-3. Gas breakup yields are integrated between the arrows indicated. In Fig. A1-4 our data for the "signal-to-noise" ratio are shown and compared to the LASL measurements. Our data agree quite well with the general trend of the previous results and it is apparent that the T(p,n) reaction retains its superiority over the D(d,n) reaction at 9.0 MeV.

(4) Electro-mechanical Changes in The NTOF Detector System

In our original time-of-flight system inherited from the Wright Patterson AFB laboratory, the massively shielded 4-meter radius detector was moved by hand from one angle to another. Even though the steel track, on which the back of the angular cart rolled, was as level as possible, moving the detector in some areas approached the physical limit of some operators. When the new 6-meter detector, which is even heavier, was installed; one operator could not move it in some areas. This problem has been solved by installation of an electric drive on each angular cart. Standing near the pivot axis where the angular position can be accurately read on a precision vernier scale, one operator now uses a push-button control which activates a high torque drive unit placed between the bottom of the angular cart and its steel track. The unit[2] is a modified "Bar, Pry, Wheeled". A 1/2-hp series-wound 110 vac motor drives, through a 315:1 ratio gear box, a pair of heavy, wide, 4" diameter rubber wheels which are in firm, adjustable contact with the steel track. The unit has a maximum rated thrust of 1900 lbs. and the angular velocity of both the 4-meter cart and the 6-meter cart is high enough that large angles can be traversed in less than a minute and yet the speed is low enough that safe operation occurs and positioning of the carts to a given angle ± 10 minutes is feasible.

---

[1] M. Drosg, et al., Los Alamos Scientific Laboratory, Internal Report LA-6459-MS (1976)

[2] These units, obtained on Federal Surplus ere manufactured for the Defense General Supply Center by Western Gear Corporation, Southwestern Division, 117 North Palmer, Houston, Texas 77003

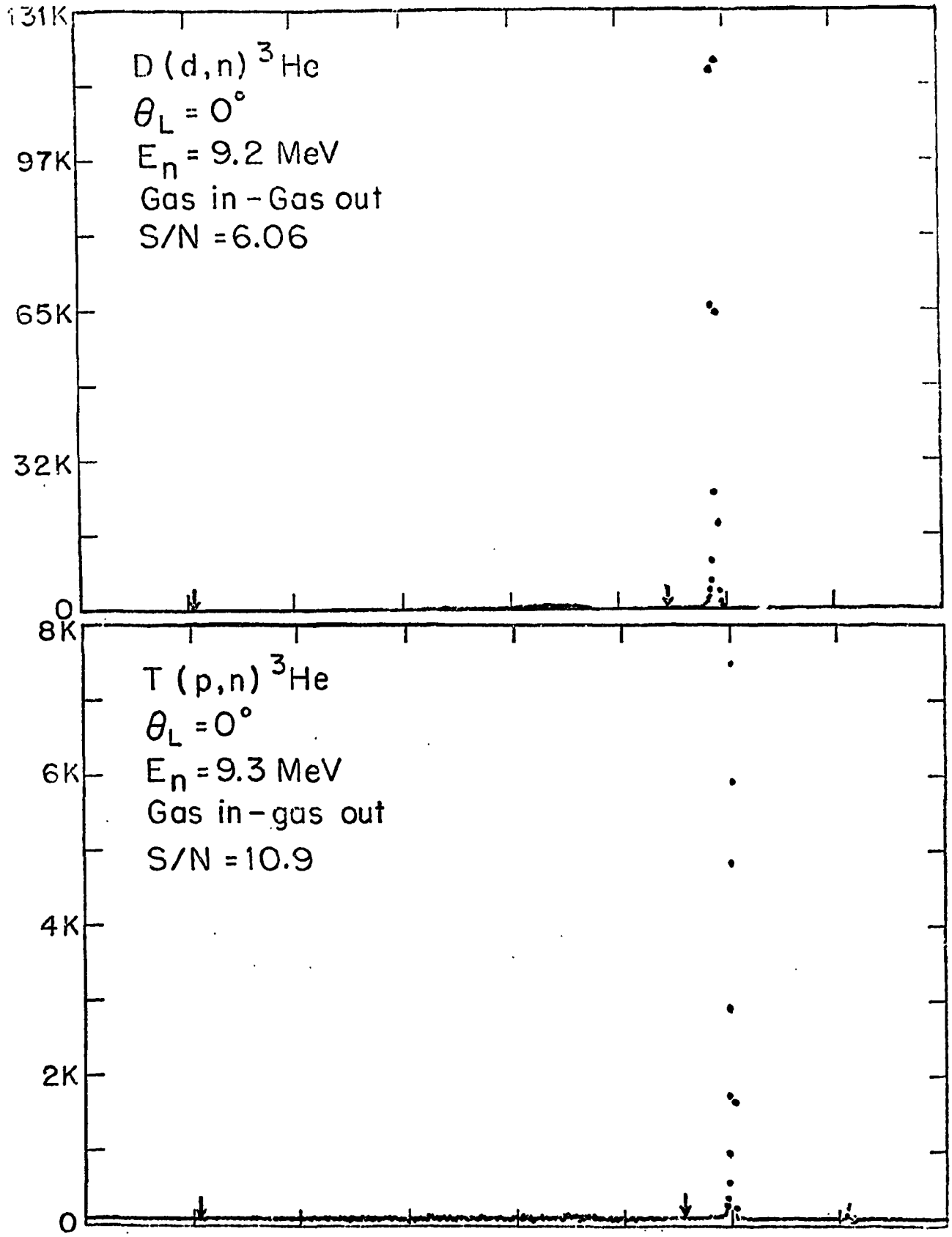

Fig. A1-3 Spectra at 0° for D(d,n) and T(p,n) reaction for 9.2 MeV neutron energy.

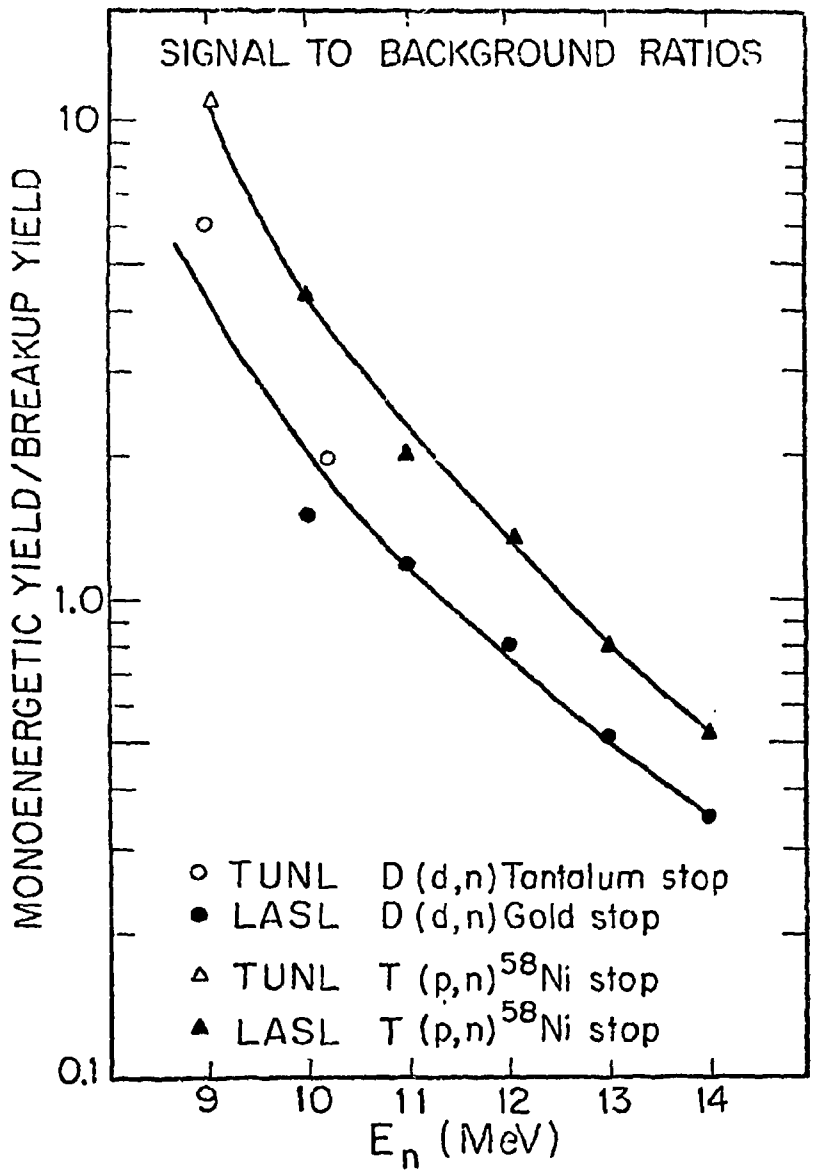

Fig. A1-4 Signal-to-noise ratio data obtained at TUNL and LASL.

Inside the shields, in both the 4-meter detector and the 6-meter detector, a lead shielded ^{241}Am source has been mounted a few inches from the liquid scintillator. By means of 180° rotation of a shaft attached to an externally mounted 72 rpm synchronous motor, the portion of the shield between the source and the scintillator is removed so the 60 keV gamma rays from the ^{241}Am can be used for bias checks. After the check, a reverse 180° rotation reshields the source. At present, these rotations are done by control room application of either -6 volt or 0 volt level signals to the relay-and-switch control of the motor. In the future, these levels will be programmed so that bias check spectra will be accumulated continuously and automatically in the computer during the time intervals between the actual time of flight runs.

In the past, our "in" scattering samples and our "out" samples had to be placed, one at a time by hand in the proper position. The horizontal location was determined by a 16-mil steel aircraft cable stretching under tension between two points which were co-axial with the pivot axis of the angular carts. A new system has been developed where five samples, six inches apart, form a portion of the cable system. The top of the cable now goes over a precisely located pulley to a one-kg weight. The bottom of the cable goes under another precisely located pulley, on to a spiral groove in a cylinder attached to the shaft of a stepping motor. The cable is fastened to the cylinder. Another cable fastened to the cylinder goes around another spiral groove and then down to a one-kg counterweight. At present, controllable frequency pulses are fed to the stepping motor until the desired sample is positioned correctly vertically as determined by the optical level. In the future, a computer program will cause the proper number of pulses to be sent to the proper winding in the stepping motor to correctly locate the desired sample automatically. The optical level will be used for any chain of five samples to determine initial positioning, operation thereafter will be computer controlled.

b. Computer Program Development for Neutron Data Correction
(H. Hogue, A. Beyerle, S. El Kadi, G. Glendinning)

Considerable work has been done during the report period on Monte Carlo data corrections programming for the neutron time-of-flight group. This activity proceeded toward three main objectives: (1) A general capability for correcting data for multi-element samples was desired. (2) An extension of the methods in use for correcting elastic and discrete inelastic scattering data to the problem of correcting continuum scattering was necessary. (3) The iterative correction procedure required reorganization to make it more straightforward, and some coding improvements were needed in preparation for publication. Two codes, dubbed EFFIGY and EFFIGYC, came about as a result of the work.

Program EFFIGY is a reorganized version of program MC, described in a previous report. Its purpose is to calculate attenuation, finite geometry, and multiple scattering effects for cylindrical samples of one or more elements. In process of obtaining these corrections, differential cross section libraries are input and time-of-flight spectra, analogous to the experimental spectra, are

calculated and summed over the time windows used in the experiment. A facility for subtracting previously calculated "out-count" spectra from the calculated spectra before window summation has been included. Thus, secondary effects of truncation of the timing tails in summing experimental spectra and over- or under-subtraction of the "out-count" spectra are corrected.

Program EFFIGYC is a companion program for EFFIGY, using most of the same subroutines but designed to correct "continuum" scattering data. The program takes as input differential cross section libraries for scattering to states at excitations low enough to give distinct groups in the time-of-flight spectra. It thus determines the energy distribution resulting from all other scattering processes, which (after correction for attenuation, finite geometry, and multiple scattering effects), gives the observed time-of-flight spectra. The removal from the scattering spectra of scattered gas breakup neutrons from the target cell has also been included in EFFIGYC.

c. CTR Related Measurements

(1) Lithium 6 and Lithium 7

A paper reporting the results of this measurement has been accepted for publication in Nuclear Science and Engineering.

(2) Boron 10

Eight angular distributions of elastic and inelastic scattering have been measured for incident neutron energies from 8.0 to 14.0 MeV. At the higher energies inelastic scattering to the 0.717 MeV state was not resolved from the elastic group.

Data were taken with a 92.41% enriched ^{10}B sample. Corrections for the 7.59% admixture of ^{11}B will be incorporated in the data analysis using our two-element Monte Carlo code and a combination of the ^{11}B ENDF4 library and ^{11}B elastic and inelastic cross sections previously measured at TUNL. The data is in the analysis stage.

(3) Boron 11

Eight angular distributions for elastic scattering and for inelastic scattering resulting from the 2.14, 4.46 and 5.04 MeV states have been measured for incident neutron energies from 8.0 to 14.0 MeV. Analysis has been completed on these data which will be transmitted to NNDC as a package with the ^{11}B data.

(4) Oxygen 16

Internal consistency checks prior to final release revealed discrepancies in three of the angular distributions for this isotope reported previously.

All of the data in question were acquired during a single experimental run. These angular distributions at 10.75, 11.5 and 12.5 MeV have been remeasured and the entire data set recorrected for finite size and multiple scattering effects using our improved Monte Carlo code EFFIGY. They are again in the process of final formatting for release to NNDC. The revised data are shown in Figure A1-5.

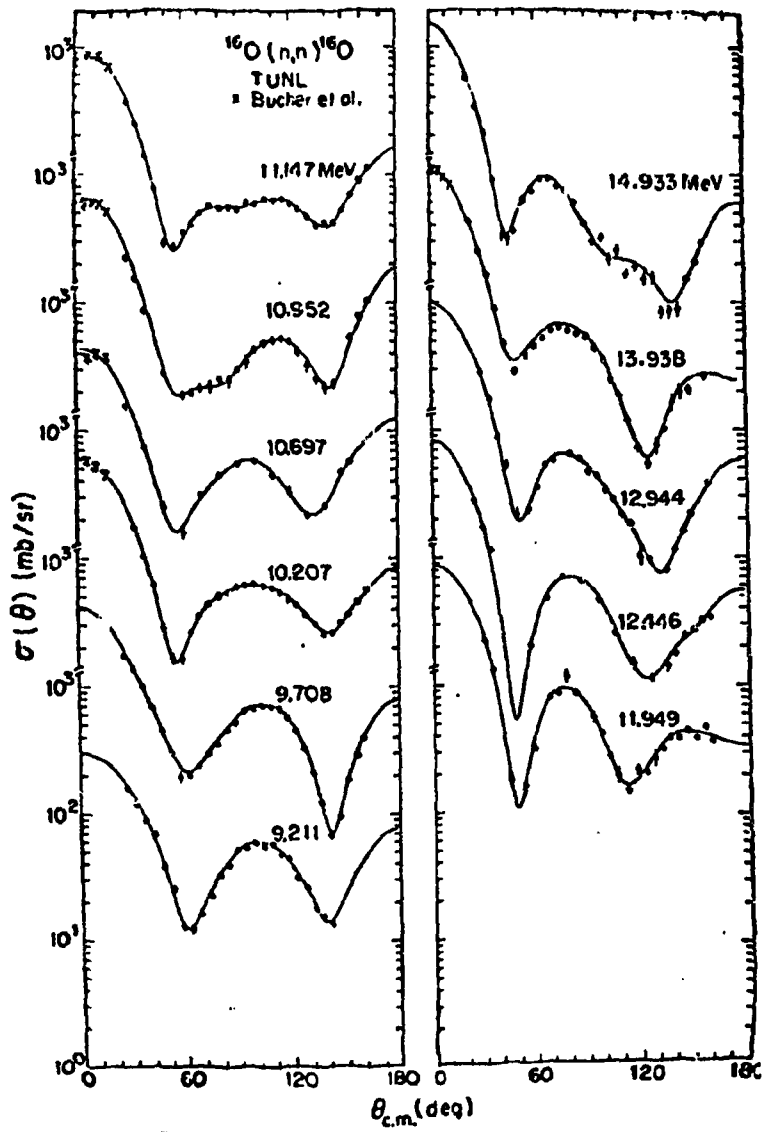

Fig. A1-5 Differential cross sections for $^{16}O(n,n)^{16}O$.

(5) ^{54}Fe and ^{56}Fe

Neutron scattering measurements with isotopic samples of ^{54}Fe and ^{56}Fe are presently underway. Two types of measurement are being made:

i) Elastic and first excited state inelastic scattering angular distributions at angles from 30 to 155 in 5° increments using the D(d,n) source reaction.

ii) Continuum neutron spectrum studies at a few angles with the T(p,n) source reaction.

For the elastic scattering angular distributions the maximum flight paths of 4m and 6m are employed for the detectors, and data have been obtained at 10 and 12 MeV bombarding energy. For the continuum measurements we are primarily interested in the lower energy neutrons and reduced flight paths of 2.7 and 3.7 m are employed. The detectors are biased at ~300 keV equivalent neutron energy and the T(p,n) source reaction is used because of the reduced background of breakup neutrons from the gas compared to the D(d,n) reaction. Low bias measurements have been made at 40°, 80°, 125° and 160° at 5.9 MeV; 35°, 65°, 95°, 125° and 155° at 9.1 MeV; and 80° and 125° at 10.1 MeV. Fig. A1-6 shows a difference time-of-flight spectrum obtained at 40° and 5.9 MeV bombarding energy with a flight path of 3.7 m. Here four spectra (gas in, sample in; gas in, sample out; gas out, sample in; gas out, sample out) have been normalized and subtracted to obtain the final $^{56}Fe(n,n')$ time-of-flight spectrum. At this energy, 11 discrete inelastic scattering groups are seen in the spectrum down to ~700 keV neutron energy. Analysis of the data is proceeding.

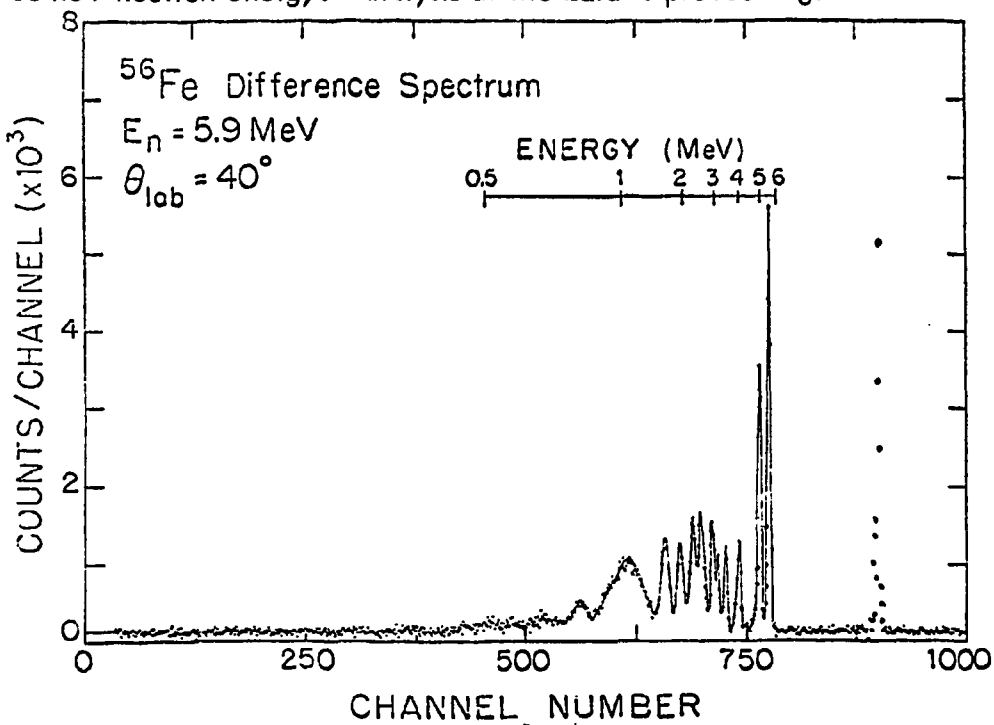

Fig. A1-6 A difference time-of-flight spectra for ^{56}Fe + n.

d. Theoretical Analysis of Neutron Scattering Data

(1) R-Matrix Analysis and Code Development (C.E. Nelson)

The neutron inelastic differential cross section measurements for ^{6}Li recently completed at TUNL show some indication of a state in ^{7}Li at approximately 17 MeV in excitation energy (E_n = 11 MeV). Evidence for a state near this energy is also seen in ^{7}Li(γ,n)^{6}Li photoneutron cross section measurements.[1] To determine the spin and parity of this state requires a multi-level, multi-channel R-matrix analysis of the ^{6}Li + n → ^{7}Li* compound nucleus system. The TUNL R-matrix code MULTI has been modified to accomplish this analysis.

The TUNL ^{6}Li + n data consist of detailed elastic and inelastic angular distributions at approximately 1 MeV intervals from 7 MeV to 14 MeV. Since many partial waves can contribute to the cross section at such neutron energies, the method of analyzing the excitation function data at several angles (which MULTI provided) was not deemed appropriate. It was decided to compute and plot the Legendre polynomial coefficients versus neutron energy for both the elastic and inelastic differential cross sections. These coefficients are then compared to the coefficients of each distribution determined by least squares fitting the differential cross section data to a sum of Legendre polynomials.

The coefficients calculated by MULTI and those experimentally determined are plotted by the computer for fitting purposes.

Calculations are proceeding to determine the R-matrix parameters that will best reproduce both the elastic and inelastic neutron differential cross section data for ^{6}Li + n. The non-zero spin of both the ground state (1^+) and first excited state (3^+) of ^{6}Li lead to a total of two channels that must be considered for each compound state included. This adds considerable complexity to the problem of determining a value of J^π for this state which best fits all the data available. A tentative conclusion arrived at thus far is that a state of positive parity fits the data better than a state of negative parity of the same J^π. If this conclusion is born out by further calculations, it will be the first experimental evidence for the existence of a positive parity state in the ^{7}Li compound system.

(2) Optical Model Analysis (G.G. Glendinning, F.O. Purser R.Y. Cusson, C.E. Nelson)

The last systematic optical model study of 1-p shell nuclei was published in 1969.[2] This study was dominated by proton scattering data due to the scarcity of precision neutron data at that time. With the completion of our measurements on ^{10}B and ^{11}B a body of data for neutron scattering now exists for all the 1-p shell nuclei. Data for ^{14}N, not measured at TUNL, are available from the work

---

[1] R.L. Bromdlett, et al., Paper 2B15S, Asilomar 1973
[2] B.A. Watson, et al., Phys. Rev. 182, 977 (1969)

of Bauer, et al.[1]

The optical model search code GENOA has been obtained from ORNL and adapted to our computer system. A global search for the 1-p shell region incorporating available neutron and proton scattering data for incident particle energies up to 15 MeV is planned. It is anticipated that a more precise determination of the energy dependent terms in the optical model parameterization will result.

2. Charged Particle Fission (D.H. Epperson, F.O. Purser, R.Y. Cusson, C. Kalbach)

Analysis of the more than 100 fragment mass and kinetic energy distributions measured for proton induced fission of ^{236}U, ^{235}U and ^{234}U is continuing. Inclusion of the effects of pre-equilibrium neutron emission has required refitting the entire excitation energy range covered, 0 to 30 MeV. Present preliminary results point to the necessity for modifying the level density formalism utilized to describe saddle point states in the statistical model used and the effects of such a modification will be tested next.

Since the original data analysis indicated the possible existence, at very low excitation energies, of mass divisions based on the magic 78 shell, a preliminary experiment was undertaken to investigate the possibility of a direct measurement to confirm the existence of such a break up. Calculations by Greiner predict such a structure in the fission of ^{238}U.[2] A measurement of $^{238}U(p,p'f)$ with appropriate excitation energy windows could test the existence of this structure in the fragment mass yield. Results of a test run for E_p = 14.0 MeV indicate such a measurement may be feasible at Cyclo-Graaff energies. This will be undertaken when the injector cyclotron is placed back in service.

3. Energy Spectra from (p,p') and (p,n) Reactions and The Griffin Preequilibrium Model (C. Kalbach, S.M. Grimes,* C. Wong,* I. D. Proctor,* D. Heikkinen*)

Investigations of the validity of preequilibrium reaction models are facilitated greatly by measuring the energy spectra of both the emitted protons and the emitted neutrons from a single reaction. The most recent measurements of this sort in an on-going collaboration were made last year at the LLL cyclograaff facility using beams of 18 and 25 MeV protons. The neutron and proton data are being analyzed at Livermore and at TUNL, respectively. The majority of the theoretical model calculations are being done at TUNL with the Griffin model code PRECO. Although comparisons with other codes will probably be carried out.

Recent evidence indicates that previous methods for making background corrections to the (p,p') data are inadequate and all the proton spectra from this collaboration are being reanalyzed. The phenomena being studied are (a) pairing effects

[1] R.W. Bauer, et al., Nucl. Phys. A93, 637 (1967)

* Lawrence Livermore Laboratory, Livermore, California

and (b) shell corrections in preequilibrium reactions. (See A.4 in Annual Report TUNL XVI ((1977)).

B. NEUTRON POLARIZATION STUDIES

1. General

A progress report on neutron polarization studies entitled "Recent Advances in Neutron Polarization Studies" was given by R. L. Walter in an invited talk at the Washington American Physical Society meeting in April, 1978. The abstract follows:

> "Because of the relative ease of detection of protons compared to neutrons, the quantity and accuracy of proton polarization information has greatly exceeded that for neutrons. In fact, in the past decade the production of intense beams of protons produced directly in the ion source has permitted this separation to widen. One result of this circumstance is that theoretical predictions are often compared to scattering and reaction data obtained with charged particles, leaving the neutron predictions to be inferred from these calculations. In reality, steady progress also has occurred in the measurements involving neutron polarization quantities, and the types of experiments and their accuracy are becoming significant for testing models for neutron interactions. The purpose of the present talk is to review several aspects of neutron polarization phenomena which highlight the features of the current technique for production of polarized neutron beams and the standard method for measuring the polarization of neutron beams. Recent results for n-p, n-d, and n-^{4}He scattering and comparisons between the polarization $P(\theta)$ and the analyzing power $A(\theta)$ for (p,n) reactions will be described. The presentation also will include a brief description of results for polarization transfer studies in (d,n) and (p,n) reactions induced with polarized-proton or -deuteron beams. Although the talk will be restricted to beams of energies below 30 MeV, many of the concepts apply to higher energies as well."

2. Analyzing Power Measurements for n-p Scattering from 10 to 18 MeV

(W. Tornow,* P.W. Lisowski,** R.C. Byrd, R.L. Walter)

In the last report the details of an experiment to measure the analyzing power function $A_y(\theta)$ for neutron-proton scattering were given. The data obtained had an absolute accuracy of ± 0.002, the best ever achieved in any neutron polarization experiment. The data were of an accuracy sufficient to show that the current neutron-proton global phase shift solutions must be restudied. Our results and this latter finding were reported in Phys. Rev. Letters 39 (1977). Since our last report,

---

* Physikalishes Institut, Universität Tübingen, West Germany
** Los Alamos Scientific Laboratory, Los Alamos, New Mexico

we have not obtained any new data, although it would be valuable to show that a similar discrepancy exists in other nucleon-nucleon observables, or at energies other than 16.0 MeV. We have learned privately that verification of our results may be forthcoming from another laboratory in the immediate future.

A long report of the experiment is nearly ready for submission for publication. It was hoped that our data would have been fitted by the nucleon-nucleon theorists by the time the paper was submitted, but it appears that a complete revaluation of nucleon-nucleon data will be necessary before a satisfactory description will be possible. For instance, the group of Arndt at VPI is finding that it is necessary to adjust the p-p data in order to move their global nucleon-nucleon phase-shift predictions in the direction of our data. There are also several new potentials for describing nucleon-nucleon scattering which supersede the Reid-Soft-Core potential. We are awaiting calculations from the Paris group to see if their model, perhaps the best available, can be adjusted to describe our data.

3. Analyzing Power Measurements for n-d Scattering at 12 MeV (W. Tornow, P.W. Lisowski, R.C. Byrd, R.L. Walter)

At 12 MeV, we have shown that the analyzing power functions $A_y(\theta)$ for neutron-deuteron elastic scattering are identical to published results for proton-deuteron scattering. This finding proves that the Coulomb and/or charge asymmetry terms are not significant to the accuracy of the data ($\sim\pm$ 0.005) at this energy. Furthermore, it provokes doubts concerning measurements at higher energies where differences have been observed. Three-nucleon theorists are still not capable of accurately describing the data; however, the data are considered to be testing the accuracy of the theories (rather than the reverse possibility). The experimental findings have appeared in a lengthy report in Nuclear Physics A296, 23 (1978).

4. Analyzing Power for $^{12}C(n,n)^{12}C$ Scattering (W. Tornow, R.C. Byrd, R.L. Walter)

In the n-p scattering experiment of section B2, an organic scintillator served as the proton target. Multiple scattering corrections for neutron scattering processes which involve the ^{12}C in the matrix were calculated in a Monte Carlo code and were applied to the data to obtain final n-p values. It was necessary to make assumptions about the n-^{12}C analyzing functions in the 8- to 14-MeV region to perform these calculations. Because of the significance of accurate n-p scattering data, we have decided to obtain $A_y(\theta)$ data for n-^{12}C scattering in this region. The experiment will involve a collaboration with visitors from the University of Tübingen who have previously participated in neutron polarization experiments at TUNL. One of them (W. Tornow) has already conducted feasibility tests at our laboratory, and we have determined that the experiment can be completed accurately and cleanly using a pure ^{12}C (diamond) scintillator.

5. Similarities Between $A_y(\theta)$ and $P^y(\theta)$ for the $^3H(p,n)^3He$ Reaction (W. Tornow, P.W. Lisowski, R.C. Byrd, R.L. Walter, T.R. Donoghue*)

Results obtained at our laboratory approximately two years ago showed that polarization $P^y(\theta)$ data available in the literature for the $^3H(p,n)^3He$ reaction in the 3- to 4-MeV region were in error. In addition, another repeated measurement indicated that new data for the analyzing power $A_y(\theta)$ in this same reaction agreed with old data (the new data having been obtained by our collaborator T.R.D. from Ohio State University). In Phys. Rev. Letters 37 (1976) 981 we published these data for $A_y(\theta)$ and $P^y(\theta)$ and showed that identical curves could describe both sets of data. Since that publication no new experimental data have been obtained. A long paper describing the experiment and discussing possible errors in earlier work is being prepared. This paper will accompany the report of the $A_y(\theta)$ results obtained at OSU. The data for both parameters will be compared to recent calculations of G. Hale of LASL for the 5-nucleon system. These calculations use an R-matrix formulation to describe all the mass-5 reaction data in this energy range. The agreement with our $P^y(\theta)$ data is good.

6. Neutron Polarization Produced by the Breakup of Vector Polarized Deuterons on ^2H and ^4He (P.W. Lisowski, R.C. Byrd, T.B. Clegg, R.L. Walter)

The $K_y^y(0°)$ data for the reaction $^2H(\vec{d},\vec{n})$ and $^4He(\vec{d},\vec{n})$ are now in final form. No new data will be obtained in the near future. The publication of these data is still receiving low priority.

7. Elastic Scattering of Nucleons from ^4He (P.W. Lisowski, R.L. Walter, T.B. Clegg)

The data on the analyzing power $A_y(\theta)$ for $^4He(n,n)^4He$ scattering have been incorporated into the analysis at LASL by G. Hale for the mass-5 system. Our R-matrix analysis of $^4He(n,n)^4He$ and $^4He(p,p)^4He$ has been terminated. The data have never been written up for final publication, but this will be done, perhaps taking precedence over initiating new projects.

8. Polarization Transfer Studies in The $^2H(\vec{p},\vec{n})p+p$ Reaction from 10 to 15 MeV (P.W. Lisowski, G. Mack,** T.B. Clegg, R.L. Walter)

Calculations of $K_y^y(0°)$ for the three body reaction $^2H(\vec{p},\vec{n})p+p$ have been made at LASL by one of us (P.W.L.) using the code of Jain (now at LASL, also). The data have been compared to this calculation, and the results are fairly well described. A draft of a publication describing this work has been prepared.

---

* Ohio State University

** Physikaliches Institut der Universitaet, Tuebingen, West Germany

9. Comparison of $P^y(\theta)$ and $A_y(\theta)$ in Analogue (p,n) Reactions on ^{15}N (R.C. Byrd, P.W. Lisowski, G. Mack, W. Tornow, T.B. Clegg, R.L. Walter)

The results for the comparison of the polarization $P^y(\theta)$ and the analyzing power $A_y(\theta)$ in the analogue reaction $^{15}N(p,n)^{15}O_{g.s.}$ were given in the last report. These data showed that, to within approximately ± 0.05, i.e., the accuracy of most of the data, $A_y(\theta)$ and $P^y(\theta)$ for this reaction are identical at a number of energies over the energy range of our experiment, that is, from 5 to 11 MeV. At some energies, e.g., 5.65 and 7.2 MeV, the two functions exhibit large differences at some angles. These results were verified by performing a number of tests. The interpretation of the results will proceed along two avenues: first, an analysis using the Lane optical model in the highest energy region, i.e., at 10.3 and 11.3 where $A_y(\theta) \cong P^y(\theta)$; second, a study of the spectroscopy of the $^{15}N(p,n)^{15}O_{g.s.}$ reaction to determine what unique information becomes available when one observes that $A_y(\theta)$ does not equal $P^y(\theta)$ in a reaction to an analogue state. Some early steps related to the first approach have been taken and will be described in this report in the Theory Section (M-22) on the Lane analysis. The second interpretation will involve theoreticians from outside TUNL. Our own involvement in this latter study is undetermined at the present. The information on $P^y(\theta)$ and $A_y(\theta)$ was presented most recently by one of us (R.L.W.) at the (p,n) workshop on 31 October at Lawrence Livermore Laboratory. A Ph.D. thesis by R.C. Byrd on this experiment (and a Lane model analysis of the $^{9}Be(p,n)^{9}B_{g.s.}$ reaction) was accepted in January 1978. A portion of the abstract follows:

> In order to supplement polarization studies of (p,n) reactions between mirror nuclei, absolute (p,n) cross sections for ^{9}Be and ^{15}N have been obtained in energy regions where it was felt that direct reaction calculations would be helpful in interpreting the observed polarization phenomena. The $^{9}Be(p,n_0)^{9}B$ data were measured every 10° from 0° to 100° (c.m.) at 11.0, 12.0, 13.5, and 15.0 MeV and are intended to extend the lower energy results of Walker et al. (1965). A 0° excitation function from 8 to 15 MeV suggests a broad resonance below about 11 MeV. Relative errors of about 3% and absolute normalization errors of 5-10% were assigned. For $^{15}N(p,n_0)^{15}O$, the data also allowed evaluation of the usefulness of the TUNL (n,n) time-of-flight cross-section facility for (p,n) measurements. Supplementary data to that of Wong et al. (1961) were obtained in the form of 0° to 170° (c.m.) angular distributions at 9.05, 10.3, 11.0, and 11.3 MeV in 10° increments, with a 0° excitation function in 200 keV steps from 8.45 to 11.65 MeV. Relative errors were about 3%, and absolute normalization should be good to 5%.
>
> A computer program TWAVE3 was written which is capable of simultaneously fitting cross-section and polarization data for (p,p) and (n,n) elastic and (p,n) quasielastic scattering.

The calculation solves exactly the coupled equations resulting from application of isospin conservation to the systems of proton-target, neutron-target, and neutron-analog optical model potentials. An important feature is the ability to use any of the various different potential representations, e.g., (U_0, U_1) or (U_p, U_n), and combinations of volume or surface-peaked form factors, all without compromising Lane model consistency. Particular attention has been paid to the inclusion of the isospin symmetry-breaking coulomb effects for target-analog coulomb displacement energies Δ_C and the proton coulomb correction energy, nominally the $\Delta V_C = 0.4Z/A^{1/3}$ term. Finally, a non-linear least-squares search can be carried out for up to twenty-two parameters to simultaneously fit angular distributions of the cross section and polarization for both elastic and quasielastic scattering.

As an application of this program, we have attempted to describe ^{9}Be data from 11 to 15 MeV for the elastic scattering cross section and polarization and the quasielastic (p,n) cross section--all using a single Lane potential. The predictions for this data were excellent, but no simultaneous fit to the charge-exchange analyzing power could be obtained. This work yields four conclusions. First, a careful application of the Lane model formalism is capable of impressive correlation of results for the three related elastic and charge-exchange reactions. Second, careful attention is needed to transformations of potential representations and form factors, e.g., surface versus volume potentials, and all potentials are not equivalent. Third, inclusion of significant isospin symmetry-breaking coulomb corrections must be handled in a reasonable and self-consistent manner--in other analyses this may have been a serious error. Finally, the failure to describe the charge-exchange analyzing power provides strong evidence for the need for the inclusion of an $(\ell \cdot s)(t \cdot T)$ isospin-dependent spin-orbit term to provide a direct spin and isospin flip, e.g., spin-up proton to spin-down neutron.

Comparisons of the polarization observables PY and A_y for (p,n) reactions between mirror nuclei are expected to provide information about isospin symmetry breaking effects (Conzett, 1974) and spin-flip mechanisms (Arnold, 1977) in nuclear reactions. We have therefore obtained a considerable amount of PY and A_y data on (p,n_0) reactions between the light mirror nuclei ^{3}H - ^{3}He, ^{9}Be - ^{9}B, and ^{15}N - ^{15}O. Specifically, PY data were obtained for ^{3}H as an excitation function from 2.0 to 3.75 MeV and angular distributions at 2.26 and 2.46 MeV. The data set for ^{9}Be includes angular distributions of A_y and PY

from 10°-100° (c.m.) for 8.1, 9.1, and 10.0 MeV, forward angle A_y angular distributions at 2.7 MeV (25° to 60°, c.m.) and 2.9 MeV (25° to 90°, c.m.) for comparison to the P^y data of Rohrer and Brown (1976), and A_y data from 0° to 100° (c.m.) at 11.0, 12.0, 13.5, and 15.0 MeV. Three-angle (30°, 50°, and 70°; lab) excitation functions of P^y and A_y have been obtained in at most 0.5 MeV steps through the energy region from 2.9 to 10.0 MeV. Uncertainties of most data are in the range of 2-5%. As with the previous $T(p,n_0)^3He$ data, all results indicate good to excellent agreement between the two quantities. In particular, there is impressive agreement between A_y data of Rohrer and Brown and the present P^y and A_y data at very low energies, where coulomb symmetry-breaking was initially expected to be most important. For ^{15}N, angular distributions of P^y and A_y from 10° to 110° (c.m.) (at 10.3 and 11.3 MeV) also indicate good agreement between the two quantities. This comparison was further checked by angular distributions of P^y and A_y at 5.65 and 6.28 MeV, and of A_y at 5.17, 7.9, 8.5, and 9.2 MeV. Excitation functions at 20°, 50° and 100° (lab) for both P^y and A_y were obtained from 4.5 to 9.2 MeV. In strong contrast to the earlier 10.3 and 11.3 MeV results, below about 9 MeV there are widespread differences in the magnitudes and even the signs of the two quantities.

We have attempted to understand the appearance of $P \neq A$ results for the $^{15}N(p,n_0)^{15}O$ reaction only in terms of the symmetry arguments of Conzett's Theorem (Conzett, 1974) and the constraints relating polarization observables (Arnold, 1977). Our results indicate that there is good evidence for the existence of isospin and configuration mixing effects in the ^{16}O intermediate state which could lead to $P \neq A$."

10. Comparison Between $A_y(\theta)$ and $P^y(\theta)$ for the $^9Be(p,n)^9B_{g.s.}$ Reaction
(R.C. Byrd, P.W. Lisowski, G. Mack, W. Tornow, T.B. Clegg, R.L. Walter)

As a counter-example to the ^{15}N case, last year we reported that $A_y(\theta)$ and $P^y(\theta)$ for the $^9Be(p,n)^9B$ reaction are identical to within the ±0.05 accuracy of the experiments. This is true over the entire range investigated, from 2.7 to 10 MeV. Therefore, no effects of isospin-breaking are evident in the comparison of P^y and A_y for this reaction. The analysis of these data has been part of the global Lane model described in this report in the Theory section (M-22). Our Lane model computer program does not allow for target spin; therefore, it always calculates $P^y \equiv A_y$. Fortunately, therefore, the $^9Be(p,n)^9B$ reaction provides an ideal situation for testing the applicability of this model and/or code from the fact that we have shown $P^y \equiv A_y$ experimentally.

11. Cross-Section Measurements for $^{9}Be(p,n)^{9}B$, $^{15}N(p,n)^{15}O$ and $^{13}C(p,n)^{13}N$ (R.C. Byrd, K. Murphy, P. Guss, C. Floyd, R.L. Walter)

In order to interpret the (p,n) polarization information discussed above, it is necessary to have information about the (p,n) reaction cross-section. In the previous report we described measurements of differential cross sections for $^{9}Be(p,n)$ and $^{15}N(p,n)$ which were obtained with the pulsed beam, time-of-flight system operating in the neutron polarization target area. With the recent installation of a second detector (at 6 meters) in the neutron scattering target area, we switched to this system to repeat some of the earlier measurements and to extend the measurements to higher energies and to another target, ^{13}C.

The first set of measurements utilized only the 4-meter detector and the normal time-of-flight target apparatus, which was not ideally designed for (p,n) differential cross-section measurements. The second set of measurements utilized a new, low-mass target arrangement. The first runs used the $^{2}H(d,n)^{3}He_{g.s.}$ reaction to obtain the absolute efficiency of the 4-meter detector system. (These calibration measurements were forerunners to the determinations of the absolute efficiency measurements of both the 4-meter and 6-meter detectors later obtained by the neutron time-of-flight group.) The third set of measurements were of (p,n) cross sections using the new, low-mass target arrangement to check earlier data and to obtain additional measurements. We now believe the system is capable of delivering (p,n) neutron measurements with an accuracy better than ±5%.

For reaction cross-section measurements the system is not beam limited, but count rate limited. Better data can be obtained in the future if the overall timing of the system can be reduced from the (typically) optimal 1.8 ns neutron peak width. One can sacrifice beam to improve the timing, but the present beam pickoff unit which provides the timing pulses becomes marginally operational. These problems will be addressed in the next year along with the project to improve the overall efficiency of the time-of-flight chopper/buncher system.

Improvements had to be made in the present computer for analyzing time-of-flight spectra. For the spectrum manipulation code, the major modification involved the error analysis procedures. In addition, a new code has been constructed to handle the attenuation in the target apparatus, the detector efficiency, monitor normalization procedures, and subsequent error propagation.

The results of the measurements below were presented at the American Physical Society meeting at Asilomar.

a. $^{9}Be(p,n)^{9}B_{g.s.}$ Reaction

Seven angular distributions were obtained for proton energies in the range between 11.0 and 15.7 MeV and usually for the angular region from 0° to 130°. In addition, an excitation function was measured over the same energy range for $\theta = 0°$. The analyzed results for the center-of-mass cross section are plotted in Fig. B11-1. The primary source of error is caused by background subtraction uncer-

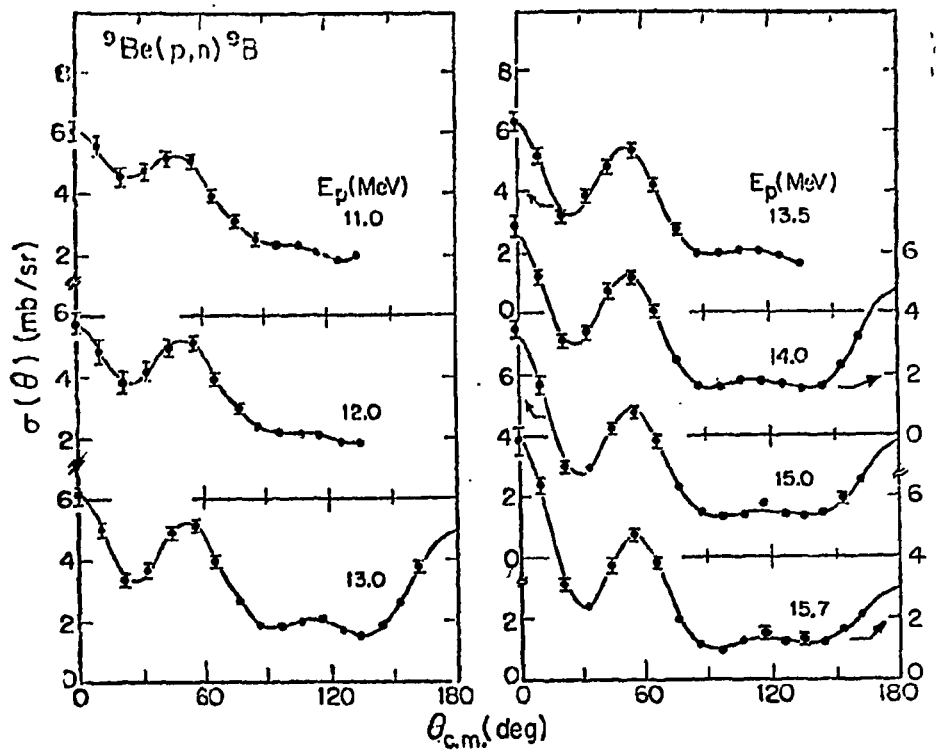

Fig. B11-1 Center-of-mass differential cross sections for the ^{9}Be(p,n)^{9}B reaction. The error bars represent the absolute uncertainties associated with the measurements.

tainties; there is a large component of neutron background from three body breakup reactions in the process ^{9}Be + p. The 11.0 MeV data compare favorably with earlier results reported by Walker et al.[1] The data exhibit little change with energy, one of the criteria desired before undertaking an optical model analysis. The data have been employed in the global Lane model analysis described in the theoretical section of this report.

b. ^{13}C(p,n)^{13}N$_{g.s.}$ Reaction

Using enriched CH_4 gas as a target, data were obtained for the ^{13}C(p,n)^{13}N reaction between 12.5 and 16.75 MeV. The cross-section results are shown in Fig. B11-2. Except for the distribution at 14.5 MeV, only a gradual change occurs as the proton energy is varied. The results at 13.3 MeV compare favorably with data recorded by Wong et al.[2] at the same energy, considering that the energy resolution of the two experiments were 150 and 600 keV, respectively. We have not measured A_y or P^y values for this reaction yet, nor have these $\sigma(\theta)$ data been employed in a Lane model analysis yet.

[1] B.D. Walker et al., Phys. Rev. 137B, 1504 (1965)
[2] C. Wong et al., Phys. Rev. 123, 598 (1961)

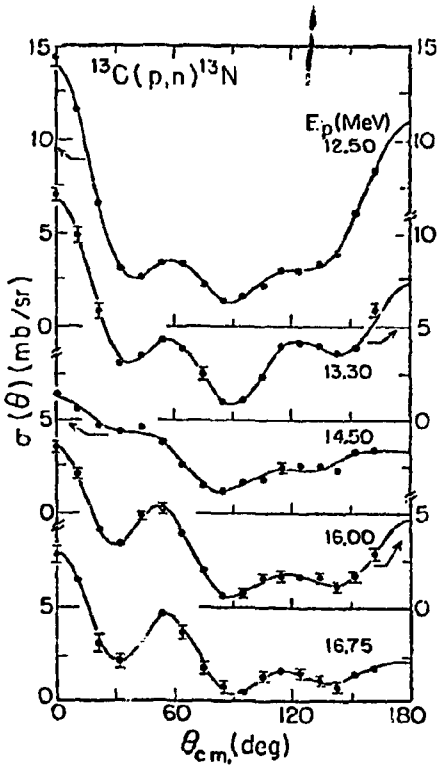

Fig. B11-2 Center-of-mass differential cross sections for the $^{13}C(p,n)^{13}N_{g.s.}$ reaction. The error bars represent the absolute uncertainties associated with the measurements.

c. $^{15}N(p,n)^{15}O_{g.s.}$ Reaction

The $^{15}N(p,n)^{15}O$ reaction exhibits much resonance structure below 11 MeV, the region where we have observed large differences between A_y and P^y. Above this energy, the structure is broader and less pronounced.[1] In order to study the similarities between the angular distributions at 10.3 and 11.3 (energies where we have observed that $P^y \simeq A_y$) and angular distributions at higher energies, we have measured ten angular distributions between 10.3 and 15.6 MeV. The data are plotted in Fig. B11-3. It is clear that a distinct pattern persists at all but one energy above 11.3 MeV, and also that the 10.3 and 11.3 MeV shapes are considerably different from this pattern. From the Lane model point of view it is unfortunate that we did not measure P^y and A_y above 11.3 MeV. Based on the successes we are having with the Lane model, these polarization data would permit an extension of our tests of the model to another nucleus. We may conduct these measurements during the next twelve months.

d. Summary

One asks if there is any similarity between the (p,n) reactions on light nuclei in this energy range. It is noteworthy that both the ^{13}C and ^{15}N reactions exhibit, in some of the energy regions, features that are shown over the entire range for $^{9}Be(p,n)$. This similarity, which is illustrated in Fig. B11-4, stimulates us to continue with our tests of the Lane model's application to light nuclei.

---

[1] S.H. Chew et al., Nucl. Phys. A298, 19 (1978)

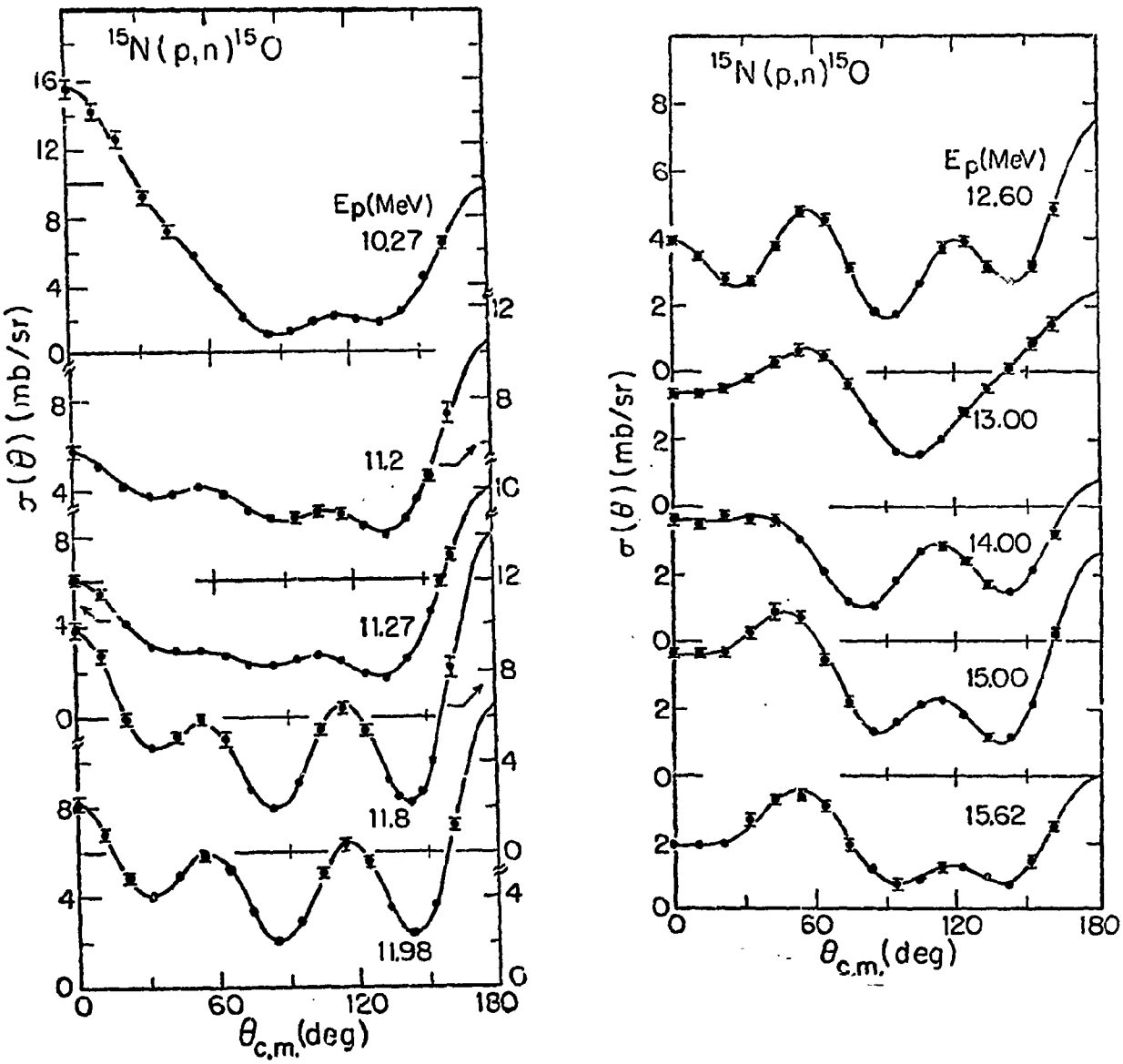

Fig. B11-3 Center-of-mass differential cross sections for the $^{15}N(p,n)^{15}O_{g.s.}$ reaction. The error bars represent the absolute uncertainties associated with the measurements.

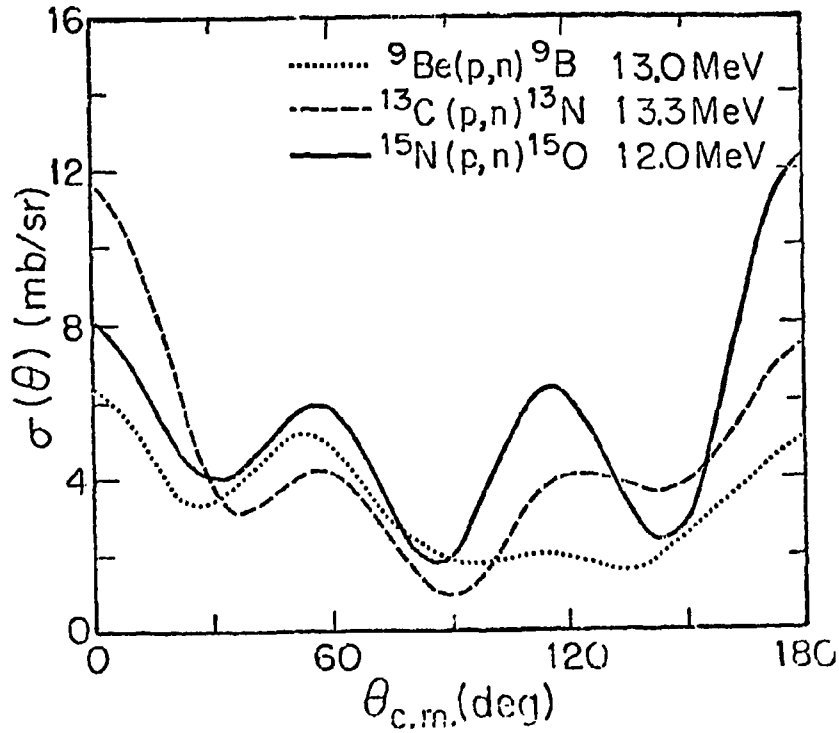

Fig. B11-4 A comparison of the typical cross section for $^{9}B(p,n)^{9}B$ reaction to the pattern observed for the $^{13}C(p,n)^{13}O$ at most energies and to the shape observed for the $^{15}N(p,n)^{15}O$ near 12 MeV.

12. Pulsed-Polarized Beams (R.L. Walter, S.A. Wender, P.W. Lisowski, T.B. Clegg)

Additional work on this project will be conducted during next year. The description appears in the Ion Source Development section (J-1e) of this report. The paper on the beam-pickoff for low beam intensities appeared in Nucl. Instr. and Meth. 146, 477 (1977).

13. Polarization Transfer Studies in $(\vec{d},\vec{n})$ Reactions (P.W. Lisowski, R.C. Byrd, G. Mack, W. Tornow, T.B. Clegg, R.L. Walter)

Additional changes have been made in the manuscript describing the results for the $K_{y'}(0°)$ parameter for $(\vec{d},\vec{n})$ reactions on ^{12}C, ^{14}N, ^{16}O, and ^{28}Si. The paper is now nearly ready for submission.

C. HIGH RESOLUTION STUDIES

1. High Resolution Elastic Scattering (E.G. Bilpuch, G.E. Mitchell, M.E. Bleck,* K.B. Sales, W.A. Watson, W.K. Wells,** C.R. Westerfeldt, K.M. Whatley)

The primary interests in elastic scattering concern the proton strength function and highly fragmented analogues. To obtain more information on the proton strength function we have extended our measurements on both the low mass end (^{26}Mg) and the high mass end (Zn). Our analogue state emphasis has been on ^{90}Zr.

a. ^{26}Mg

A paper has been published on this work: "High Resolution Study of the ^{26}Mg(p,p) Reaction", C.R. Westerfeldt, G.E. Mitchell, E.G. Bilpuch, and D.A. Outlaw, Nucl. Phys. A303, 111 (1978). The following is the abstract of that paper:

> "The differential cross section for ^{26}Mg(p,p) was measured from E_p = 1.54 to 3.06 MeV at lab angles of 90°, 105°, 135° and 160° with an overall energy resolution of ≈400 eV. Resonance parameters were determined for 61 resonances. Strong analogues of the sixth ($1/2^+$), eigth ($3/2^-$) and ninth ($7/2^-$) excited states of ^{27}Mg were identified and tentative identifications suggested for analogues of the seventh ($3/2^+$) and tenth ($3/2^+$) excited states. Spectroscopic factors and Coulomb energies were determined. One striking shift in the Coulomb energies was observed: the analogue of the eigth excited state of ^{27}Mg occurs below the analogues of the sixth and seventh excited states. The present values for Γ_p were combined with the results of previous capture measurements and total γ-ray widths determined for almost all of the resonances observed below E_p = 2.6 MeV."

These data also provide a showcase example of the success of the multilevel fitting procedure. In Fig. C1-1 is shown data and fit in an energy region with resonances of $J^\pi = 1/2^+$, $1/2^-$, $3/2^-$, $3/2^+$, $5/2^+$, $5/2^-$, $7/2^-$ and with widths ranging from 10 eV to 30,000 eV.

---

* Now at Sandia Laboratories

** Now at University of Pennsylvania

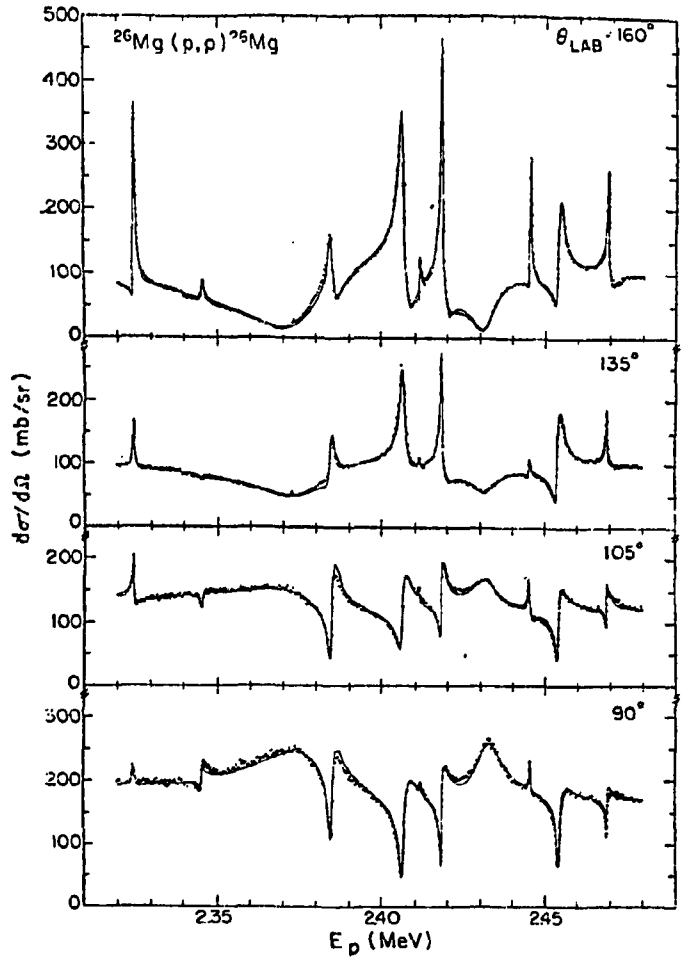

Fig. C1-1 The $^{26}Mg(p,p)^{26}Mg$ differential cross section from E_p = 2.32 to 2.48 MeV at four angles. The solid line is the multi-level R-Matrix fit to the data.

b. Zn

Our efforts on the Zn isotopes are primarily to obtain information concerning the s-wave strength function. This work has been delayed by difficulties in preparing Zn targets suitable for high resolution measurements. We have fabricated a glow-discharge system for preparing Zn targets, and expect to have more suitable targets in the near future. We then plan to study ^{66}Zn. Meanwhile, we have measured elastic scattering from ^{64}Zn from E_p = 2.50 to 3.24 MeV. Although the quality of the data is not as high as we would like, the data have been analyzed and the essential features of the results obtained. The s-wave strength function is $s_0 = 0.05$, consistent with all of our previous results and showing no sign of the 3s size resonance. In addition spectroscopic properties of three analogues ($1/2^-$, $3/2^-$ and $5/2^+$) were obtained. A preliminary report on this work was given at the Southeastern Section of the American Physical Society, October, 1978.

c. ^{90}Zr

The lowest s-wave analog state in ^{91}Nb was studied extensively with the FN tandem accelerator. Although the level density is so great that the fine structure was incompletely resolved, valuable information about both the experimental system and highly fragmented analog was obtained. The following is the abstract of a dissertation by M.E. Bleck:

> "Excitation functions for the reaction $^{90}Zr(p,p)$ were measured from 5.684 to 5.992 MeV at laboratory angles of 90°, 107°, 135° and 160°. Proton energy resolution varied between 425 and 450 eV. The data were fit to an R-matrix cross section containing 302 s-wave resonances. These levels comprise the fine structure of the lowest $1/2^+$ analogue state in ^{91}Nb.
>
> Excellent beam energy resolution was maintained through use of a three loop energy regulating system adapted for high resolution work at TUNL specifically for this experiment. This system includes an optical feedback path which permits high voltage modulation of the terminal stripper in order to null residual energy fluctuations.
>
> The fine structure distribution was incompletely resolved due to the extremely high compound nuclear level density. Nevertheless, a good fit to the theoretical distribution (Lane 1969) was obtained. The fine structure parameters extracted from the fit were found to be in mild disagreement with those obtained in an earlier, thick target experiment (Richard et al., 1971). Severe disagreement between the Robson estimate and the experimental value was obtained for the analogue spreading width.
>
> The statistical distributions of resonance widths and spacings were examined as a check on the R-matrix fitting procedure.
>
> The analogue proton spectroscopic factor was deduced and compared with spectroscopic factors for the parent and anti-analogue states obtained from the literature."

2. High Resolution Inelastic Scattering (G.E. Mitchell, E.G. Bilpuch, J.R. Chandler,* B.H. Chou, W.A. Watson, W.K. Wells,** C.R. Westerfeldt)

The program of high resolution inelastic scattering has developed rapidly during the past year. These measurements of magnitudes and relative phases (signs) of inelastic amplitudes provide a variety of new and interesting results for both doorway (analog) states and for statistical properties of widths. These multichannel studies of analog states provide subtle ways to test analog state theory, as well as more sensitive tests for non-statistical effects. The critical point is that the theories are formulated in terms of width amplitudes γ, but normal experiments measure the reduced widths γ^2. Since the measurement of amplitudes themselves are impossible, the best one can do is measure magnitudes and relative signs in multichannel processes.

The method involving inelastic scattering is very simple. Consider for isolated resonances the reaction $A(p,p')B^*$ followed by $B^* \rightarrow B+\gamma$. For our case $A= B= 0^+$, $B^* = 2^+$. For p-wave resonances, the p' and γ-ray angular distributions are both isotropic for $1/2^-$ resonances, but cannot be simultaneously isotropic for $3/2^-$ resonances. Thus we can uniquely distinguish between $1/2^-$ and $3/2^-$ resonances. If one can neglect $\ell' = 3$, then there are only 2 inelastic amplitudes ($j' = 1/2$ and $j' = 3/2$). The p' and γ-ray angular distributions suffice to determine the magnitudes $\gamma_{1/2}$, $\gamma_{3/2}$ and the sign of $\gamma_{1/2}\gamma_{3/2}$. Rephrased, the experiment determines the mixing ratio $\delta_j = \gamma_{3/2}/\gamma_{1/2}$. As in the electromagnetic case, it is often convenient to convert to $\phi = \tan^{-1}\delta$. Although similar measurements have been performed for isolated resonances, and for a very few cases the value δ_j was determined for a number of resonances, these are the first measurements of both the magnitude and sign of δ for many resonances.

We have generalized these results by extending the analysis to $d_{3/2}$, $d_{5/2}$, $f_{5/2}$, $f_{7/2}$, $g_{7/2}$, $g_{9/2}$ resonances and have also removed the restriction to one exit ℓ' value. For $p_{1/2}$ and $p_{3/2}$ states, the former can decay to a $2+$ state only by $j' = 3/2$, while the latter can decay by $j = 1/2$ and $3/2$. Thus, a $p_{1/2}$ resonance has a unique angular distribution, while a $p_{3/2}$ resonance has channel spin mixing. Except for d-wave resonances, this pattern carries through for other resonances--$f_{5/2}$ and $g_{7/2}$ states show mixing, while $f_{7/2}$ and $g_{9/2}$ resonances have unique distributions. Admixtures of higher ℓ'-values are expected to be small due to low penetrabilities, but must be included in general. A useful notation is

$$\delta(\text{lower}) = \frac{<(\ell'_{\text{lower}} + 1/2)>}{<(\ell'_{\text{lower}} - 1/2)>} \quad , \quad \delta(\text{higher}) = \frac{<\ell'_{\text{higher}} + 1/2>}{<\ell'_{\text{higher}} - 1/2>} \quad \text{and}$$

$\epsilon^2 \equiv (\ell_{\text{higher}}\ \text{strength})/(\text{total strength})$. The d-wave resonances are special. Since the lowest possible ℓ' value is $\ell' = 0$, there is no δ(lower), but δ(higher) and ϵ^2 can still be measured. In practice we have now measured many p-wave resonances, a number of d-wave resonances, a dozen f-wave resonances and one $g_{9/2}$ resonance.

---

* Now at Savannah River

** Now at University of Pennsylvania

The thrust of this work was summarized recently in an invited talk at the 1978 Small Accelerator Conference: "High Resolution Proton Scattering", G.E. Mitchell, Bull. Am. Phys. Soc. 23, 1023 (1978). The following is the abstract of that talk:

> "Results from the high resolution proton resonance studies at TUNL are presented. The thousands of resonances analyzed provide a body of data unique in charged particle resonance spectroscopy, with significant results in both statistical and non-statistical areas. One major area which has been explored in depth is the fine structure of analogue states. In another major area, detailed statistical analysis of spacing distributions confirm the existence of both short and long range correlations among level spacings. In addition to continuing work in these and related areas, recent emphasis has been placed on new experimental methods which permit the measurement of correlations between amplitudes in different channels. These results confirm predictions for common doorways, provide sensitive probes to search for non-statistical effects, and permit more detailed tests of certain statistical assumptions than hitherto possible. The experimental method for these latter measurements is described, and new data presented."

a. Off-Diagonal Strength Function

The reduced widths in these channels for an analog in ^{45}Sc are shown in Fig. C2-1, along with the product of the inelastic reduced width amplitudes.

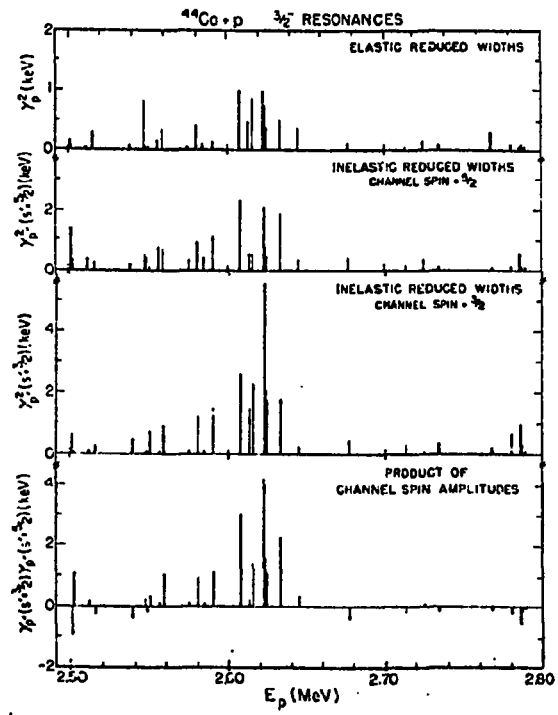

Fig. C2-1 (a) - (d). Plots of reduced width quantities $\gamma_{\nu o}^2$, $\gamma_{\nu 3}^2$, $\gamma_{\nu 5}^2$, $\gamma_{\nu 3}\gamma_{\nu 5}$ versus the energy of the $3/2^-$ resonances ν. $\gamma_{\nu o}^2$ are the widths of the elastic channel ^{44}Ca + p, while $\gamma_{\nu 3}^2$, $\gamma_{\nu 5}^2$ refer to channel spins $s' = 3/2, 5/2$ in the inelastic channel with ^{44}Ca in the 2^+ state at 1.57 MeV.

Standard theory gives for the form of $s_{cc'}$, near an analogue λ

$$s_{cc'} = A_{cc'} + \frac{1}{\pi} \text{Im.} \frac{\alpha_{\lambda c}\, \alpha_{\lambda c'}}{E_\lambda - E - (i/2)W_\lambda}$$

where $A_{cc'}$ is the "background" strength-function, E_λ and W_λ are the energy and width of the analogue, and $\alpha_{\lambda c}$ is the (complex) reduced width amplitude of the analogue in channel c. This may be rewritten:

$$s_{cc'} = A_{cc'} + \frac{B_{cc'}(E_\lambda - E) + C_{cc'}}{(E_\lambda - E)^2 + W_\lambda^2/4}$$

where:

$$\frac{2C_{cc'}}{W_\lambda} + iB_{cc'} = \frac{1}{\pi} \alpha_{\lambda c} \alpha_{\lambda c'}$$

The implication of this equation is that, apart from a sign, the diagonal quantities B_{cc}, C_{cc}, $B_{c'c'}$, $C_{c'c'}$ imply values of the off-diagonal quantities $B_{cc'}$, $C_{cc'}$:

$$(C_{cc'} + \frac{i}{2} W_\lambda B_{cc'})^2 = (C_{cc} + \frac{i}{2} W_\lambda B_{cc}) \, (C_{c'c'} + \frac{i}{2} W_\lambda B_{c'c'})$$

Thus, given the diagonal strength-functions, s_{cc} and $s_{c'c'}$, we may predict the energy-dependent part of the off-diagonal strength-function $s_{cc'}$. From fitting the diagonal data of Fig. C2-1 we obtain the values: $B_{33} = 1.82$, $C_{33} = 57.3$, $B_{55} = 1.52$, $C_{55} = 29.8$, where B, C values are in (keV), $(\text{keV})^2$, and the subscripts are twice the exit channel spin. This gives $B_{35} = 1.71$, $C_{35} = 41.4$ or $B_{35} = -1.71$, $C_{35} = -41.4$. The diagonal fits also give $E_\lambda = 2.624$ MeV, $W_\lambda = 15$ keV. In Fig. C2-2, we compare the predictions of s_{35} arising from both the positive choice of B_{35}, C_{35} (solid curve) and the negative choice of B_{35}, C_{35} (dashed curve) with the data. To remove fluctuations,

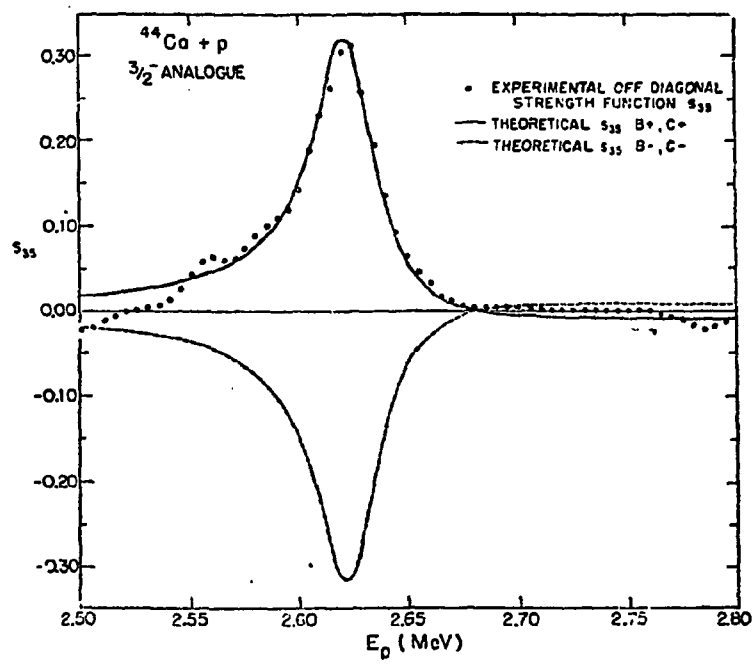

Fig. C2-2 Comparison of experiment and theory for the off-diagonal strength function s_{35}. (see text).

both quantities have been averaged over energy with a Lorentzian envelope of width 20 keV. The fit for the positive values of B_{35} and C_{35} is good.

This work was reported in a recent paper "New Probe of Line Broadening with Resolvable Fine Structure: The Off-Diagonal Strength Function", A.M. Lane, T.R. Dittrich, G.E. Mitchell, and E.G. Bilpuch, Phys. Rev. Letters 41, 454 (1978).

b. ^{44}Ca

Several papers have been published on our experimental results on $^{44}Ca(p,p'\gamma)$ in the vicinity of the analog resonance at $E_p = 2.62$ MeV. One Phys. Rev. Letters article on the off-diagonal strength function was described in the previous section. Another paper was presented at the "Third International Symposium of Neutron Capture Gamma-Ray Spectroscopy and Related Topics": "Experimental Demonstration of Phase Relation for Common-Doorway States", G.E. Mitchell, T.R. Dittrich, and E.G. Bilpuch. A more detailed paper has been accepted for publication by Zeitschrift für Physik: "Study of Inelastic Proton Amplitudes for a Fragmented Analog State in ^{45}Sc", G.E. Mitchell, T.R. Dittrich, and E.G. Bilpuch. The following is the abstract of that paper:

> "The relative sign of inelastic proton-channel amplitudes has been measured for 31 resonances in ^{45}Sc. These resonances include the fragmented $3/2^-$ analog state observed at $E_p = 2.62$ MeV in the $^{44}Ca(p,p)$ and $^{44}Ca(p,p')$ reactions. The analog fine structure is analyzed for the elastic and two inelastic channels; the Robson asymmetry is displayed clearly in the inelastic channels. The relative sign of the mixing ratio remains the same for the 15 fine structure resonances of the analogue. The mixing ratios enable the determination of the amplitude correlation of the widths in the inelastic channels. The recently introduced "off-diagonal strength function" is constructed from these data and compared with the theory of analog state broadening."

c. ^{46}Ti

Results on the $^{46}Ti(p,p')$ reaction provided another example of the constancy of the relative sign for amplitudes in a common doorway. The following is the abstract of the dissertation of John R. Chandler:

> "The $^{46}Ti(p,p'\gamma)^{46}Ti$ reaction was investigated between the proton bombarding energies 2.25 and 3.10 MeV using the high resolution system of the Triangle Universities Nuclear Laboratory 3 MV Van de Graaff accelerator. Both the proton and the de-

excitation gamma-ray angular distributions were measured for thirty-four p-wave and f-wave resonances. Expressions for the angular distributions are given for the inelastically scattered protons and for the de-excitation gamma-rays in two angular momentum coupling schemes for p-wave and f-wave resonances. Simple expressions are also derived for transformations between the two representations. The results of the two singles measurements unambiguously determine the spin of the compound state for each resonance, and the magnitudes and the relative sign between the inelastic amplitudes are obtained. In general the experimental results in the analogue state regions are nonstatistical. The off-analog data also suggest possible nonstatistical effects. In addition, properties of the observed analog states are obtained with emphasis on the fine structure of the analogue at $E_p = 2.87$ MeV."

A paper on these results will be prepared in the near future.

d. ^{48}Ti, ^{56}Fe

A large number of p-wave resonances have been investigated in ^{49}V and ^{57}Co. The $^{48}Ti(p,p'\gamma)$ data are particularly extensive and interesting. Analysis of these results is continuing. The following is the dissertation of W.K. Wells:

"Inelastic proton decay from p-wave resonances in ^{49}V and ^{47}Co were studied using the high resolution proton beam from the Triangle Universities Nuclear Laboratory's 3 MV Van de Graaff accelerator. The inelastically scattered proton and de-excitation gamma-ray angular distributions were measured at four angles for one hundred and twenty resonances in ^{49}V and thirty-six resonances in ^{57}Co. The results of the two singles measurements unambiguously determine the spin of the compound nuclear state for each resonance. The magnitudes and relative phase of the two inelastic decay channel amplitudes were measured for $3/2^-$ resonances.

Inelastic spectroscopic factors were determined for three isobaric analog states in ^{57}Co and for two isobaric analog states in ^{49}V. The strength functions for the elastic and inelastic scattering channels were calculated from the average spacing and reduced width data.

A sequence of 72 $3/2^-$ resonances in ^{49}V was used to test the statistical hypotheses for width distributions

in the orthogonal ensemble. Evidence is presented for non-statistical behavior indicative of two doorway states in ^{49}V."

e. ^{54}Fe

Angular distributions have been measured for ten f-wave resonances and 1 $g_{9/2}$ resonance in the $^{54}Fe(p,p'\gamma)$ reaction. Five of the f-wave resonances and the g-wave resonances were previously identified as analog states. All of the f resonances have $j = 5/2$. Contrary to previously published claims, the analog at $E_p = 3.80$ MeV has a very small $\ell' = 3$ component--only about 1%. The data are consistent with the $j = 9/2$ assignment for the g-state. A preliminary report on these data has been presented at the Southeastern Section Meeting of the American Physical Society, October, 1978.

f. ^{45}Ti - d-wave Resonances

Since $\ell = 0,1,2$ resonances predominate in the 1f-2p shell, and since $\ell = 0$ resonances are not suitable for these inelastic measurements, our emphasis is on p- and d-wave resonances. Our first study on d-wave resonances is the $^{48}Ti(p,p'\gamma)$ reaction. There are no $\ell = 2$ analogs in the region under study. We have studied 70 resonances in the energy region $E_p = 2.7 - 3.1$ MeV. Empirically the $\ell = 2$ admixture appears to be large enough to study and the data enable a distinction between $d_{3/2}$ and $d_{5/2}$ resonances. Analysis of these data is in progress.

3. Isospin Forbidden T = 3/2 Resonances (J.F. Wilkerson, E.J. Ludwig, T.B. Clegg, W.J. Thompson)

The program of measuring properties of isospin-forbidden resonances observed in σ and A_y excitation functions of proton elastic and inelastic scattering from self conjugate (N = Z) target nuclei is continuing. The calculated proton reduced widths for these isospin forbidden states indicates the extent of isospin mixing in the nuclei involved.

For these high-resolution resonance experiments, an accurate calibration of the momentum-analyzing system and a stable incident beam of known resolution (~700 eV) are necessary. A preliminary magnet calibration and studies of the beam resolution at higher tandem energies have been made and are discussed elsewhere in this report. (See Section K.)

The results of these two studies have facilitated our searches for these narrow T=3/2 states, by reducing the time required to find these resonances by at least 50% and by improving the beam resolution at higher energies. Our studies of ^{16}O and ^{32}S targets are continuing, particularly the ^{17}F T=3/2 ground state reached by $^{16}O(p,p)^{16}O$.

The new computer programs HRSYC and PRET32 allow quick data analysis of the yield curve and prepare the data for the computer program T32GRD which ob-

tains the proton partial widths. T32GRD is being improved in speed by about two orders of magnitude, allowing much faster data analysis.

D. GAMMA RAY SPECTROSCOPY

1. Spin Assignment of The 11.86 MeV Level in ^{24}Mg (S.A. Wender, C.R. Gould, D.R. Tilley, D.G. Rickel,* R.W. Zurmühle ((Univ. of Pennsylvania)))

This work has been published in Physical Review C17 (1978) 1365. The abstract follows:

"Linear polarizations of γ rays from the 11.86 → 8.12 → 4.12 MeV decay in ^{24}Mg have been studied with a NaI polarimeter. The 11.86 MeV level was populated via the $^{12}C(^{16}O,a\gamma)^{24}Mg$ reaction. The results are consistent with $J^{\pi} = 8^{+}$ for the 11.86 MeV level and in agreement with earlier work, rule against a 6^{+} assignment with 85% confidence."

2. Internal Conversion Measurement of Isomeric Transition in ^{100}Tc (S.A. Wender ((with D.J. Martin, Queen's Univ. Kingston, Ontario)))

This work has been published in Journal of Physics G: Nuclear Physics 4 (1978) 1347. The abstract follows:

"Two isomeric γ rays have been observed in ^{100}Tc following the $^{100}Mo(p,n)^{100}Tc$ reaction at $E_p = 3.7$ MeV. An isomeric level is identified at an excitation energy of 200.83 ± 0.10 keV and its half-life is measured using a pulsed beam technique as 8.46 ± 0.05 μs. This isomeric state decays via a 28.6 ± 0.4 keV γ ray to the first excited state at 172.12 ± 0.06 keV. A comparison of the predicted and observed Tc K x-ray intensities suggests that the 28 keV transition is pure E2 radiation."

---

*E.G. and G., Los Alamos, N. M.

E. CHARGED PARTICLE REACTIONS WITH POLARIZED BEAMS

1. $^{78}Kr(\vec{d},t)^{77}Kr$ Reaction (R.R. Cadmus, T.B. Clegg, E.J. Ludwig, S.A. Wender)

The low-lying states of ^{77}Kr have been investigated using a beam of vector polarized deuterons incident on a gas cell containing krypton gas enriched to approximately 99% in ^{78}Kr. The outgoing tritons were mass-identified in a detector system and the resultant energy spectrum had an energy resolution of 60 keV. The cross section and vector analyzing power angular distributions were used to establish the spins and parities of the ground and first-excited states of ^{77}Kr. A paper has been submitted to Nuclear Physics with the following abstract.

> "The differential cross sections and vector analyzing powers for the $^{78}Kr(\vec{d},t)^{77}Kr$ reaction leading to low-lying states of ^{77}Kr have been measured at an incident deuteron energy of 15.95 MeV. These data have been compared with distorted-wave Born approximation calculations, as well as with measurements of cross sections and analyzing powers on neighboring nuclei, in order to determine the spins and parities of these states and the spectroscopic factors for the transitions populating them. The ground state of ^{77}Kr, which had been the object of several conflicting spin assignments, has been found to have $J^{\pi} = 5/2^{+}$."

2. A Polarized Beam $(\vec{d},p)$ Investigation of States in ^{79}Kr (B.L. Burk, T.B. Clegg, R.R. Cadmus, E.J. Ludwig)

States in ^{79}Kr have been investigated using an 11 MeV vector polarized deuteron beam to bombard a gas cell containing krypton gas enriched to 98% in ^{78}Kr. The energy resolution of the resultant proton spectrum was approximately 55 keV and the yields corresponding to several states were extracted using a peak-fitting program. Cross section and vector analyzing power (VAP) angular distributions have been obtained for the outgoing protons. The cross section angular distributions were used to establish the orbital angular momentum (ℓ_n) of the transferred neutrons and hence the parity of the final nuclear states. Comparisons of these data with DWBA predictions have verified the ℓ_n values for approximately 10 states in ^{79}Kr as assigned by Chao et al.[1] using the (d,p) reaction initiated by unpolarized deuterons.

The VAP distributions are indicative of the total angular momenta (j_n) transferred and hence the spin of the final nuclear states populated in this reaction. Previous assignments[1] have been made from arguments based on shell model predictions. The preliminary results for the present work indicate the following spin-parity

---

[1] J. Chao, D.K. Olsen, C. Newsom and P.J. Riley, Phys. Rev. C11, 1237 (1975)

assignments; 0.0 MeV - $1/2^-$, 0.147 MeV group - $7/2^+$, 0.383 MeV - $3/2^-$, 0.533 MeV - $1/2^+$, 0.639 MeV - $5/2^+$, 0.688 MeV - $3/2^+$, 0.810 MeV - $1/2^-$, 1.912 MeV - $1/2^+$, and 2.060 MeV - $(5/2)^+$. These preliminary results disagree with the work of Chao et al. for 4 of the states.

3. A Polarized Beam Study of The (d,^{6}Li) Reaction (W.W. Jacobs ((Indiana University)), E.J. Ludwig)

The (d,^{6}Li) reaction has been used in recent years to extract information about possible alpha-particle clustering in nuclei. Since the spectroscopic factors extracted by various groups for α-transfer have differed considerably in recent years, it should be useful to carry out some (d,^{6}Li) experiments with polarized beam in order to a) establish whether compound nucleus formation is an important factor at our maximum accelerator energy and b) select optical model potential sets useful in describing this reaction.

Cross section and vector analyzing power distributions at various energies show a non-direct component in reactions induced by deuterons in the energy range 15 to 17 MeV. Plans are underway to perform these studies on targets of ^{28}Si and ^{40}Ca at 40 MeV using the Lawrence Berkeley Laboratory accelerator. Calculations of the expected results have been completed.

4. Spectroscopic Factors for The ^{207}Pb(d,t)^{206}Pb Reaction From Analysis of Polarized Deuteron Data (J. Willis, E.J. Ludwig, W.J. Thompson)

A final analysis of cross section and vector analyzing power angular distribution for the ^{207}Pb(d,t)^{206}Pb reaction taken with a 15 MeV vector polarized deuteron beam was made. The cross section and analyzing powers for eight excited states in ^{206}Pb from 0.0 to 3.12 MeV for lab angles from 25 degrees to 110 degrees were compared with distorted wave calculations using the computer program TDWUCK. Many of the levels in ^{206}Pb may be reached by two different angular momentum transfers. A computer program, MIXNPLOT, was written to do least squares fitting to the data of one, two, or three TDWUCK predictions for the different angular momentum transfers. Fits to the 0.80 MeV state are shown in Figs. E4-1 and E4-2. The program has an option to plot the results, enabling the user to adjust the optical model parameters and inspect the fit. Spectroscopic factors have been extracted and compared with theory[1] and other experiments.[2,3] The results are shown in Table E4-1.

---

[1] J.B. McGrory and T.T.S. Kuo, Nuclear Physics, A247 (1975) 283-316
[2] Robert Tickle and John Barowick, Physical Review 166 (1968) 1167-1172
[3] W.A. Lanford and G.M. Crawley, Physical Review C9 (1974) 646-659

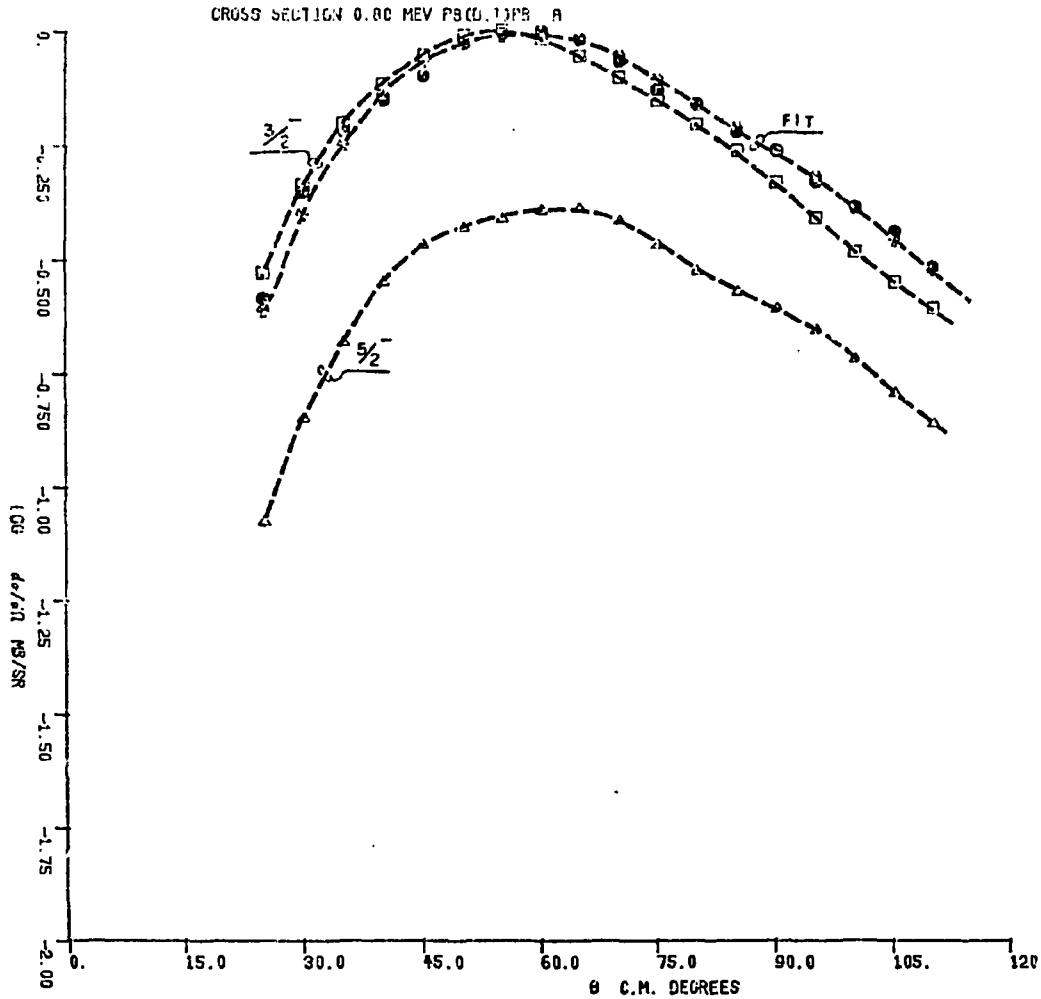

Fig. E4-1 Typical fit to the cross section for the 0.80 MeV state, fitting $p_{3/2}$ and $f_{5/2}$ theory to the experimental data.

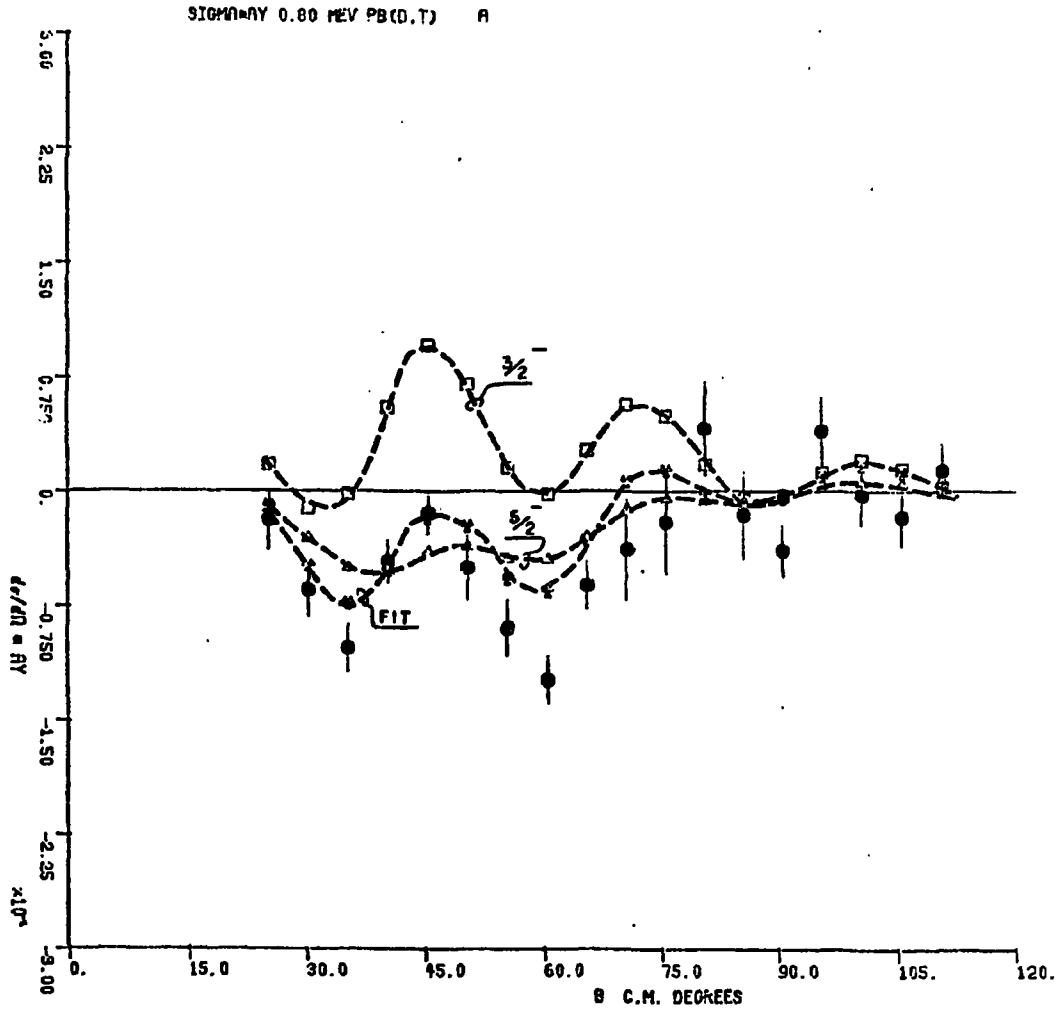

Fig. E4-2 Typical fit to the product of cross section times analyzing power for the 0.80 MeV state, fitting $p_{3/2}$ and $f_{5/2}$ theory to the experimental data. Optical model potentials were obtained by Hardekopf and Tonsfeldt.

TABLE E4-1

Spectroscopic Factors for $^{207}Pb(d,t)^{206}Pb$

Energy of State	Angular Momentum of State			
	1/2-	3/2-	5/2-	7/2-
0.0	0.46 ± 0.08	---	---	---
0.80	---	0.24 ± 0.08	1.62 ± 0.18	---
1.17	0.63 ± 0.13	---	---	---
1.34	---	---	2.20 ± 0.88	0.66 ± 0.07
1.47	---	1.90 ± 0.38	0.00 ± 0.20	---
1.70	0.00 ± 0.04	1.58 ± 0.36	---	---
Sum	1.09 ± 0.16	3.72 ± 0.53	3.82 ± 0.92	0.66 ± 0.07
Sum/2J+1	0.55 ± 0.08	0.93 ± 0.13	0.64 ± 0.10	0.08 ± 0.01
Theory:	McGrory-Kuo			
	0.50	0.98	0.95	0.00
Experiment:	Lanford-Crawley*			
	0.98	0.98	0.97	
Experiment:	Tickle-Bardwick			
	0.55	1.2	0.93	0.96

* ^{207}Pb Ground State Normalized to 1.

F. RADIATIVE CAPTURE REACTIONS

1. The Capture Program - General Status (N.R. Roberson, H.R. Weller, S.A. Wender, D.R. Tilley, M. Jensen, S. Manglos, L. Ward, M. Wright, C. Fitzpatrick)

The basic experimental set-up for radiative capture measurements remains the same as described in the previous report. The arrangement is shown in Fig. F1-1 below.

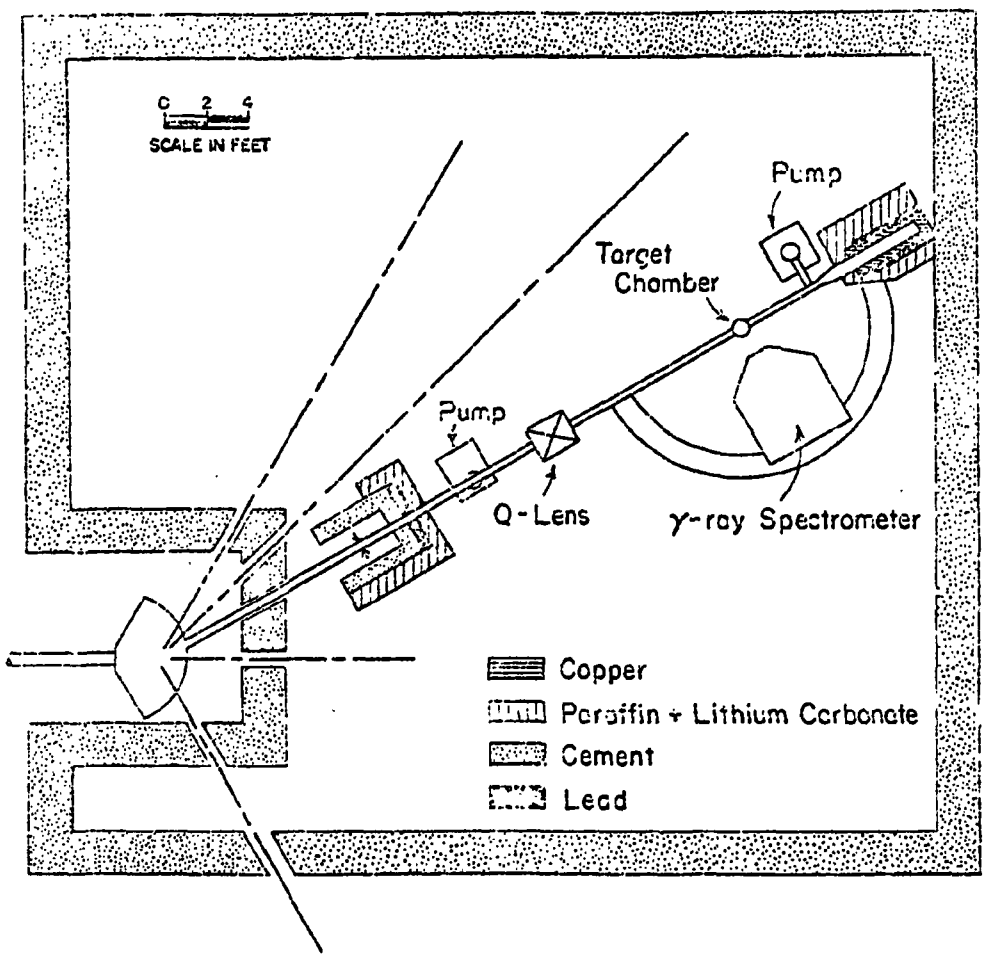

Fig. F1-1 Physical arrangement of the gamma-ray spectrometer in the target room.

A considerable effort has been made to document the spectrometer's efficiency--especially the energy dependent effects (e.g., attenuation and rejection effects). For our neutron capture studies we have been working to improve the shielding and reduce the background in general. We have found some improvement by increasing the deuterium gas cell pressure from 2 to 3 atmospheres, with a corresponding reduction in the beam intensity. Other changes, such as removing the beam dump material and the copper shielding which has been placed in front of the detector to attenuate high energy neutrons, appear to reduce the background count rate in the detector by about a factor of four. Our acquired experience with the positioning of the shadow bar has also made for more reliable results. In addition we have improved our neutron flux monitoring with the installation of a collimated zero degree monitor. A proton recoil counter has also been built and used to check our flux calibration.

The main emphasis of our capture program continues to be centered around the search for effects of the giant quadrupole resonances. The experiments involving polarized proton capture have been extensively analyzed by means of the direct-semidirect reaction theory. Our principle conclusions are:

1. A simple DSD model calculation of the E1 relative amplitudes and phases accounts for the general features observed in the experiment. Furthermore, this calculation provides a reliable means for choosing one of the two possible E1 solutions which are usually obtained from the experimental data.

2. Most of the E2 effects which we have been able to observe in proton capture are consistent with a calculation which assumes only direct E2 radiation. So it appears that this "background" E2 strength, along with the apparent weak strength of the isoscalar E2 resonance in the ground state proton channel, makes for an unfavorable situation vis a vis a study of the E2 isoscalar resonance.

3. The proton capture fore-aft asymmetry measurements which we have made in the energy region expected to contain the isovector E2 resonance have been carefully analyzed using the direct semidirect theory. These results are very encouraging and provide convincing evidence for a positive result in the case of $^{30}Si(p,\gamma_1)^{31}P$. Since the cyclotron is again operational, and since the direct semidirect theory seems to provide an effective tool for analyzing asymmetry data, we expect to begin a serious effort to investigate 20-30 MeV proton capture--especially directed towards observing the effects of the isovector GQR. This program should get underway this winter.

4. The neutron capture reaction appears to be a more favorable tool for studying the E2 resonances. This is primarily a result of the fact that the direct E2 strength is virtually eliminated as a result of the small quadrupole effective charge of the neutron. We have found that we observe a finite fore-aft asymmetry in the case of n capture by ^{40}Ca, which can be accounted for by including the (previously observed)[1] isoscalar E2 resonance in a direct-semidirect model calculation.

5. We have found that polarized neutron capture appears to be quite sensitive to non E1 radiation. Although we have just begun to perform these measurements, our results for the case of $^{40}Ca(\vec{n},\gamma)$ display rather large b_1 coefficients. Indeed the effects are much larger than the fore-aft asymmetry effects previously mentioned (typically 20% vs 5% effects). A detailed comparison with the predictions of the DSD theory is underway. It appears that these measurements may provide a viable technique for studying the giant quadrupole resonances. They will certainly provide a more stringent test of the DSD theory.

6. Our initial effort using polarized capture in the case of a few nucleon problem involved the $D(\vec{p},\gamma)^3He$ reaction (to be published). The results in this case were quite interesting. Recent continuum shell model calculations[2] have indicated that the analyzing power observed in certain few nucleon capture problems is related to the spin-orbit odd component of the effective nuclear force. This, plus our ability to measure both polarized neutron and polarized proton capture, suggests that we should perform experiments such as $^3He(\vec{n},\gamma)^4He$ and perhaps $D(\vec{n},\gamma)T$. Such experiments are being planned for the near future.

2. The $^2H(p,\gamma)^3He$ Reaction Using Polarized and Unpolarized Protons

(D.M. Skopik, H.R. Weller, N.R. Roberson, S.A. Wender)

This work has been prepared for and submitted for publication in Phys. Rev. C. The abstract of this paper follows:

"The 90° yield curve for the $^2H(p,\gamma)^3He$ reaction has been studied over the excitation region in ^3He of approximately 7 to 15 MeV. Both polarized and unpolarized proton beams were used to measure the angular distributions of cross section and analyzing power at E_x = 8.83, 9.83, and 10.83 MeV. If only the four non-spin flip E1 and E2 T-matrix elements are considered, their amplitudes and relative phases can be extracted. The E2 cross section obtained from this analysis is found to be (12 ± 5)% of the total cross section. The detailed balanced differential (θ_{lab} = 90°) and total cross sec-

---

[1] D.H. Youngblood, J.M. Moss, C.M. Rozsa, J.D. Bronson, A.D. Becker and D.R. Brown, Phys. Rev. C13, 994 (1976)

[2] D. Halderson and J. Philpott, Private Communication

tions at E_x = 10.83 MeV are found to be (117 ± 11)μb/sr and (1.07 ± 0.10 mb, respectively; the quoted errors represent the total uncertainties in the cross sections obtained in this experiment. The results are also compared with recent E1 and E2 calculations."

The principle results of this work were:

1. Of the two most recent Faddeev calculations, our absolute cross section measurements support the larger magnitude theoretical results.[1] These results are in good agreement with the early cloud chamber measurements of Fetisov et al.[2]

2. Our results indicate that the E2 integrated cross section near the peak of the total photoabsorption cross section in ^{3}He is approximately 120 ± 50 μb. This result, and all previous measurements of this E2 cross section indicate that the measured value is about three times larger than the calculated one.[3]

3. Our analysis in terms of S = 1/2 E1 and E2 amplitudes indicates that the two E1 matrix elements are equal to within their errors of about 5%, and the two E2 matrix elements are equal to within their errors of about 15% at the three measured energies (E_x = 8.83, 9.83 and 10.83 MeV in ^{3}He). Furthermore, while the relative phase between the two E1 and the two E2 matrix elements is small, The E1-E2 phase is approximately ±70 - 85°. Since the relative phase between the two E1 or the two E2 matrix elements is small (a few degrees), we can conclude that the assumption of a single E1 and a single E2 amplitude, with a relative phase of the order of 70 - 85°, is a good one.

The experimental technique employed in this work consisted of using a solid deuterated polyethylene target (CD_2). This limited us to a rather narrow energy window (E_p = 5 - 8 MeV) in which acceptable spectra could be obtained. In view of the results of this work, it would seem desirable to extend these measurements to other proton energies. The basic approach we have been considering to accomplish this is to detect the recoiling ^{3}He particles and then require a coincidence with the γ-rays, thus eliminating troublesome contaminants such as $^{12}C(p,\gamma)$. For the γ-ray angles of 30 - 150°, the recoils are all contained in a cone between ~2.3° and 5.1°. Three possible schemes are under consideration:

1. Use a thin annular detector collimated so as to accept the recoils in the proper azimuthal angular region. Count rate and pile-up considerations are presently being estimated.

---

[1] I.M. Barbour and A.C. Phillips, Phys. Rev. C1, 165 (1970)
[2] V.N. Fetisov, A.N. Gorbunov and A.T. Varfolomeev, Nucl. Phys. 71, 305 (1965)
[3] I.M. Barbour and J.A. Hendry, Phys. Lett. 38B, 151 (1972)

2. Use a magnet at 0° to separate the recoils from the beam.

3. Use a plastic detector near 0° and employ time-of-flight to identify the recoiling ^{3}He particles.

A thorough mapping of the E2 cross section for proton energies between 5 and 18 MeV will be attempted when our studies of the above techniques are completed.

3. The $^{13}C(\vec{p},\gamma_{0,1})^{14}N$ Reaction (J.D. Turner, N.R. Roberson, S.A. Wender, S.H. Manglos, H.R. Weller, M.J. Jensen, D.R. Tilley)

The 90 degree yield curves for the $^{13}C(p,\gamma_0)^{14}N$ and $^{13}C(p,\gamma_1)^{14}N$ reactions have been measured in 200 keV steps for incident proton energies of 6.25 to 13.6 MeV and in 100 keV steps for E_p of 13.6 to 17.0 MeV. In addition, data were obtained at proton energies from 12.6 to 14.55 MeV in 50 keV steps. These data are shown in Figs. F3-1 and F3-2. The integrated yield for the ground state transi-

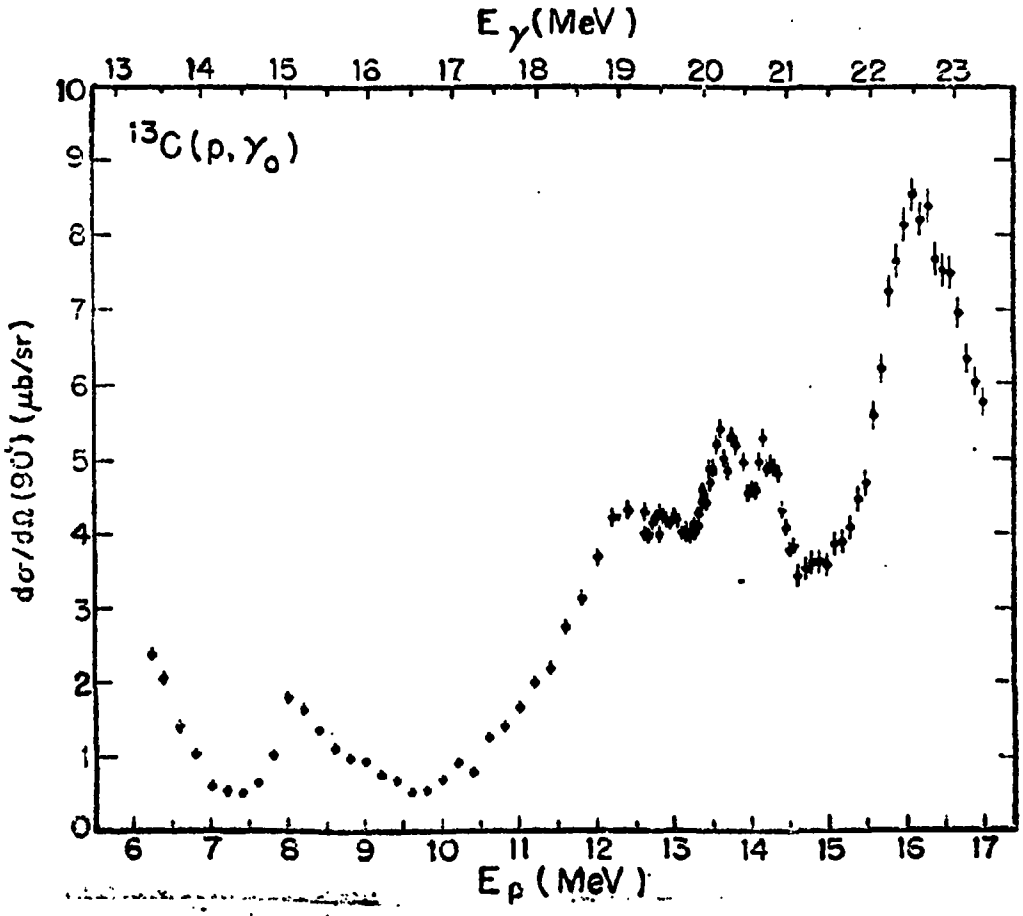

Fig. F3-1 The 90° yield curve obtained for the $^{13}C(p,\gamma_0)^{14}N$ reaction.

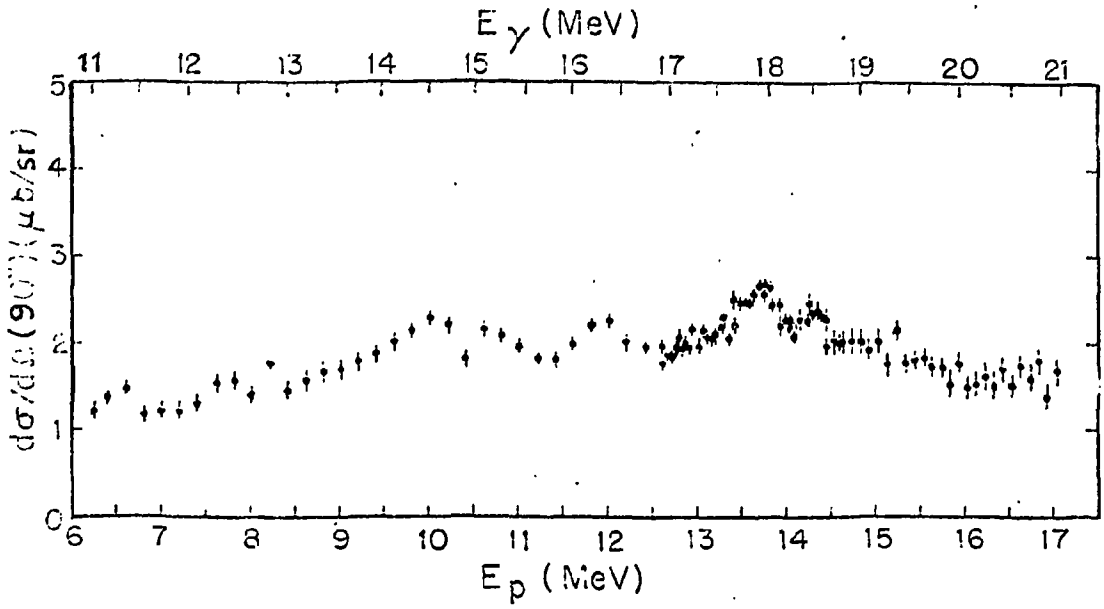

Fig. F3-2 The 90° yield curve for the $^{13}C(p,\gamma_1)^{14}N$ reaction.

tion exhausts approximately 6 percent of the classical dipole sum rule in the region of 13.3 to 23.3 MeV excitation. The transition to the first excited state exhausts about 9 percent of the classical dipole sum rule between 11.0 and 21.0 MeV excitation.

Angular distributions of both the cross section and the analyzing power were also obtained for these two reactions at twelve energies which span the giant dipole energy region. The cross section was measured at nine angles between 30° and 154°, while the analyzing power was measured at seven angles between 42° and 142°. These data were expanded in Legendre and Associated Legendre Polynomials as follows:

$$\sigma(\theta) = A_0 \left[1 + \sum_k A_k Q_k P_k (\cos\theta)\right]$$

and

$$\frac{A(\theta)\sigma(\theta)}{A_0} = \sum_{k=1}^{4} b_k Q_k P_k' (\cos\theta) \quad .$$

The resulting a_k and b_k coefficients are shown in Fig. F3-3 and Fig. F3-4.

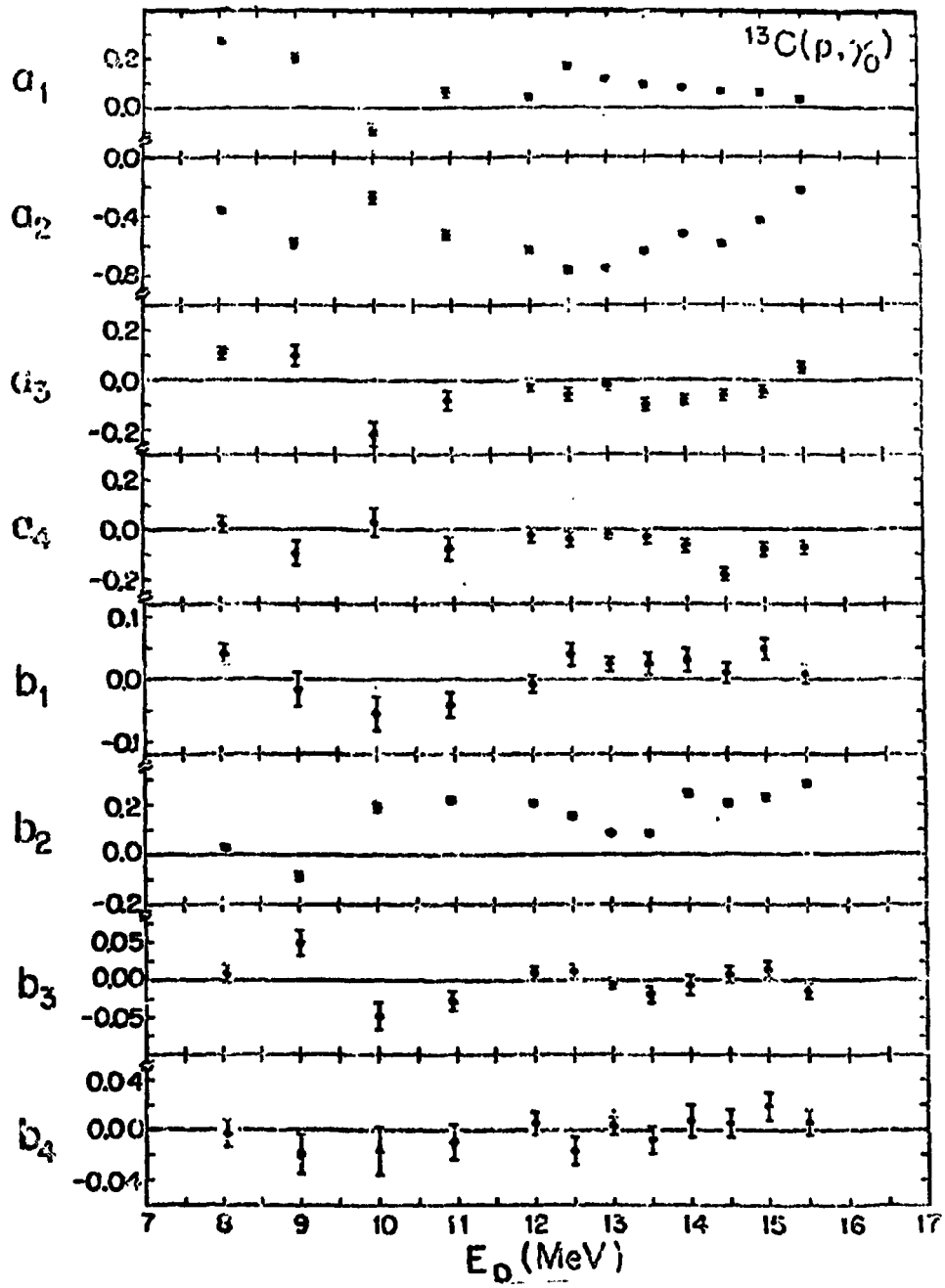

Fig. F3-3 Plots of the a_k and b_k coefficients obtained from fits to $^{13}C(p,\gamma_0)^{14}$ angular distribution data.

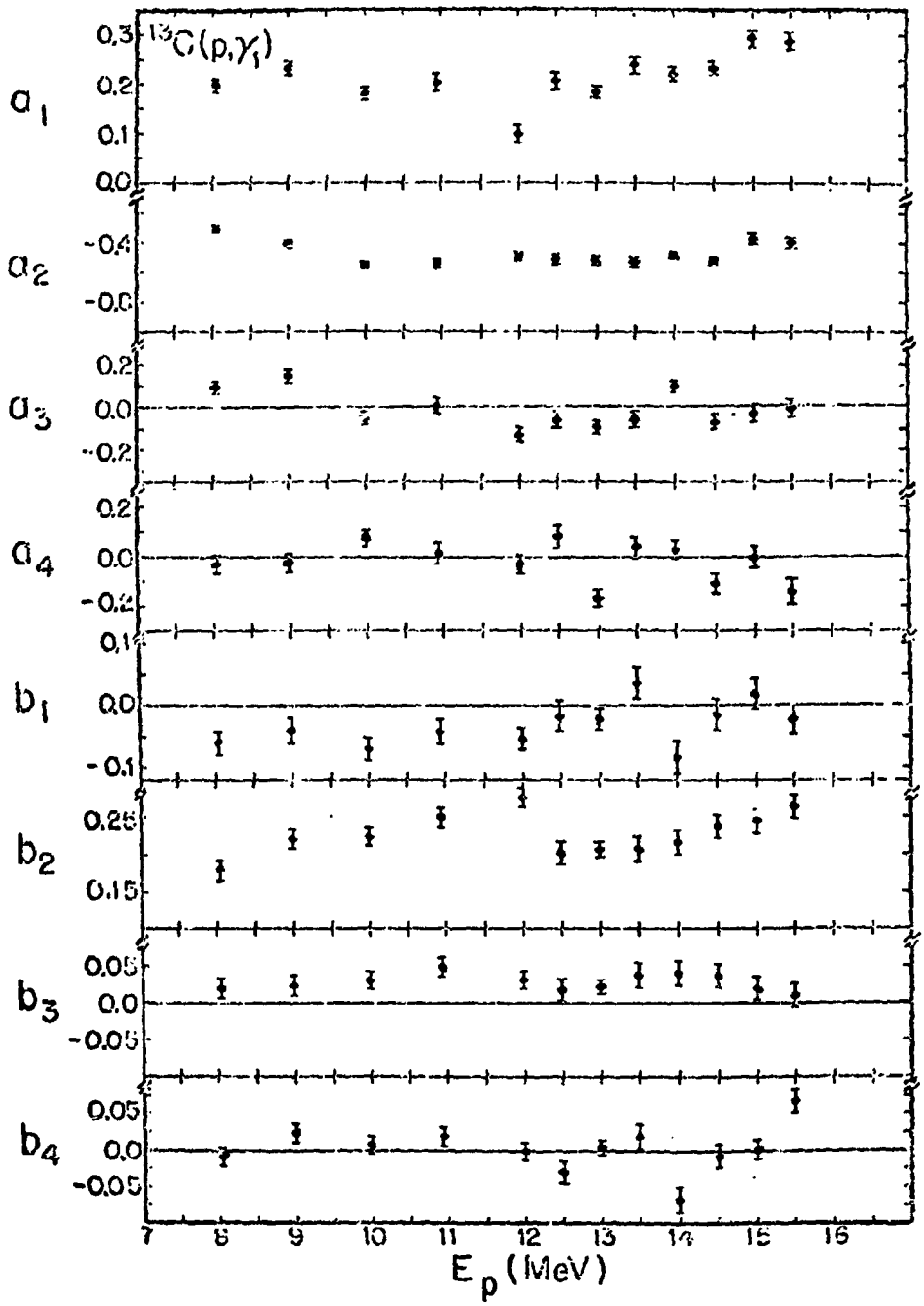

Fig. F3-4 Plots of the a_k and b_k coefficients obtained from fits to $^{13}C(p,\gamma_1)^{14}N$ angular distribution data.

Since the $^{13}C(p,\gamma_1)^{14}N$ reaction leads to a final state with spin zero, the analysis is more straightforward than for the $^{13}C(p,\gamma_0)^{14}N$ case. In the case of (p,γ_1), if we consider only E1 radiation we can express the relevant a_k and b_k coefficients in terms of the T-matrix amplitudes and phases as follows:

$$1.0 = 0.75(s_{1/2})^2 + 0.75(d_{3/2})^2$$

$$a_2 = 1.061(s_{1/2})\,(d_{3/2})\cos(\phi_s - \phi_d) - 0.375(d_{3/2})^2$$

$$b_2 = 0.5303(s_{1/2})\,(d_{3/2})\sin(\phi_s - \phi_d) \quad .$$

These equations were solved to determine the $s_{1/2}$ and $d_{3/2}$ amplitude and the relative phase from the experimental values of a_2 and b_2. The results are shown in Fig. F3-5. There are clearly two solutions, one of which is primarily $d_{3/2}$ strength

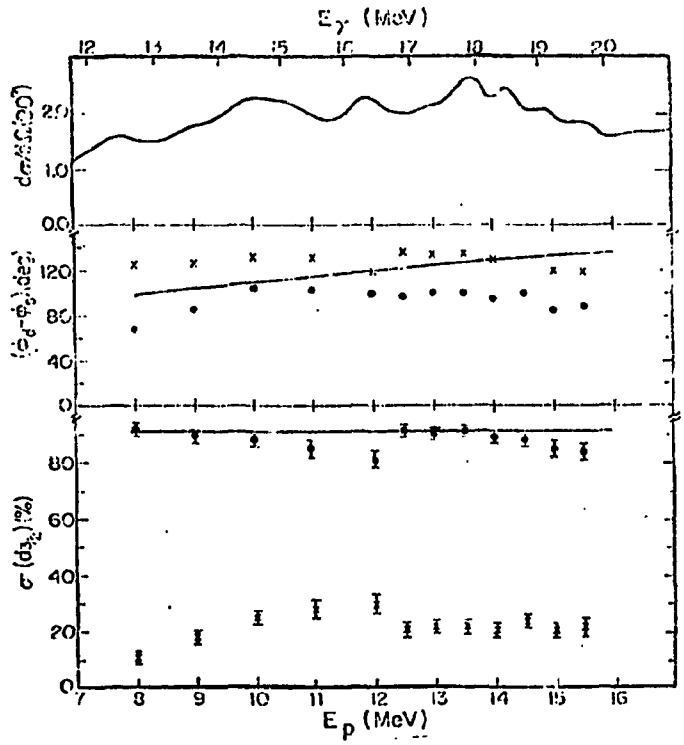

Fig. F3-5 Solutions obtained from a pure E1 analysis of the $^{13}C(p,\gamma_1)^{14}N$ data.

the other primarily $s_{1/2}$ strength.

A calculation using the simplified direct-semidirect model (form factor $\propto r$),[1] was performed for this case. The results are shown in Fig. 3-5. The calculation clearly favors the primarily $d_{3/2}$ solution and accounts for the relative amplitude and phase behavior rather well.

---

[1] Phys. Rev. C18 (1978) 65

Since the coefficients a_1, a_3, a_4, b_1, b_3, b_4 are non-zero, it is clear that radiation other than E1 is present. The most reasonable next step is to allow for the possibility of E2 radiation. This introduces--in this case of $^{13}C(p,\gamma_1)^{14}N$--two additional T-matrix elements: $p_{3/2}$ (E2) and $f_{5/2}$ (E2) with phases ϕ_p and ϕ_f, respectively. Equations for A_0, $a_1 - a_4$ and $b_1 - b_4$ can now be written down in terms of the four amplitudes (2E1's and 2E2's) and three relative phases. These four amplitudes and three relative phases were fitted directly to the experimental data through the minimization of chi-squared, calculated as follows:

$$\chi^2 = \sum_{\text{data}} \left(\frac{1}{\Delta\sigma_i}\right) \left[\sigma_i - \sum_k a_{k\,\text{calc}}\, Q_k\, P_k(\cos\theta)\right]^2$$

$$+ \sum_{\text{data}} \left(\frac{1}{\Delta\sigma_i A_i}\right) \left[\sigma_i A(\theta_i) - \sum_k b_{k\,\text{calc}}\, Q_k\, P_k'(\cos\theta)\right]^2$$

$$\text{where } \sigma_{exp}(\theta_i)/A_0 = \sigma_i$$

The quantities a_{calc} and b_{calc} are calculated from the equations for a_k and b_k written in terms of the complex T-matrix elements. The minimum of χ^2 is obtained with a gradient search routine, and the errors are derived from the error matrix.

Solutions were found at each energy with E1 amplitudes similar to the two pure E1 solutions previously described. Since the DSD calculation indicated that the physical solution was predominantly $d_{3/2}$ capture, the remaining discussion will consider only those solutions.

A search was conducted to determine if multiple solutions exist for the two E2 amplitudes. To do this, the $f_{5/2}$(E2) amplitude was held fixed and the remaining six parameters were varied for a minimum of χ^2. The cross section resulting from the $f_{5/2}$ amplitude was then varied from 0 to 20 percent of the total cross section in 1 percent steps. This was done at all measured energies. Fig. F3-6 shows a plot of

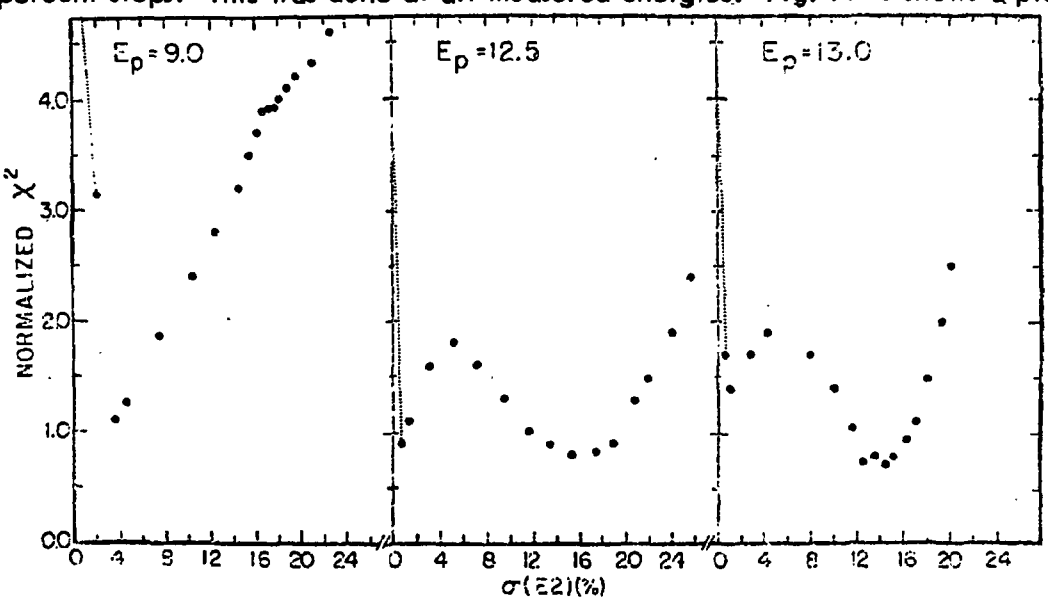

Fig. F3-6 Plots of Chi-Squared as a function of the E2 cross section obtained from an E1-E2 analysis of $^{13}C(p,\gamma_1)^{14}N$ data.

chi-squared per degree of freedom as a function of total E2 strength for three representative energies. The E2 strength is plotted as a percent of the total cross section.

Figure F3-7 shows a plot of the f amplitude and the f- to p-phase differ-

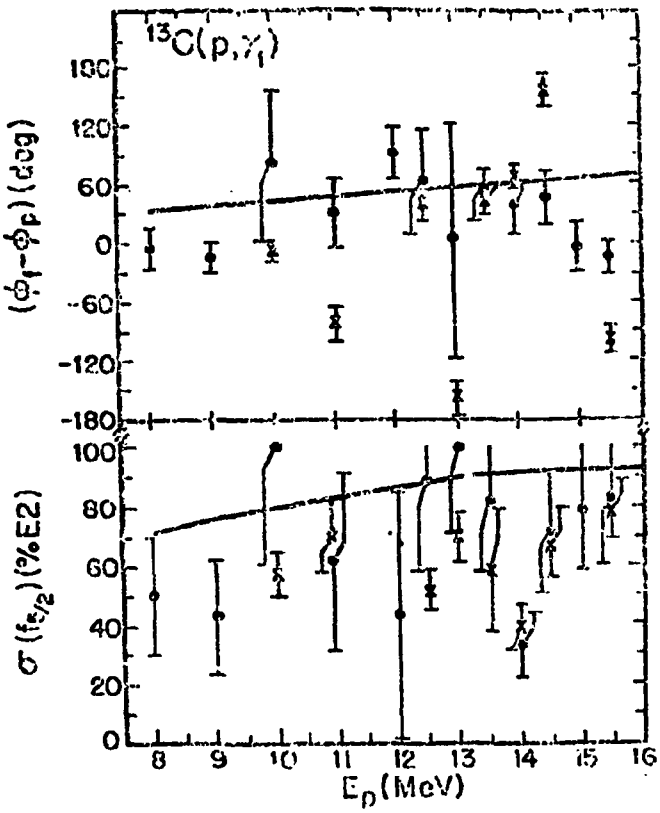

Fig. F3-7 Plots of the E2 amplitudes and relative phase extracted from $^{13}C(p,\gamma_1)^{14}N$ data.

ence as a function of energy. The f amplitude is plotted as a percent of the E2 cross section. The smaller E2 solutions are plotted as points while the larger ones are plotted as crosses. The results of the DSD calculation are shown as solid lines. There appears to be reasonably good agreement between the calculation and the smaller E2 solution.

The total E2 cross section found in our analysis is presented in Fig. F3-8. The solid line is the result of a calculation which assumes that only direct E2 radiation is present. It is apparent that the set of solutions with the smaller E2 cross section is in fair agreement with the pure direct E2 calculation. Although the experiment cannot rule out the larger E2 solutions, we find that they imply an exhaustion of over 100% of the E2 (ISEW) sum rule. We therefore conclude that the smaller E2 solution is preferred, and that if the isoscalar GQR has any strength in the ground state proton channel, its effects are too small to be observed in the present experiment above the E2 background which results from direct (non-collective) capture.

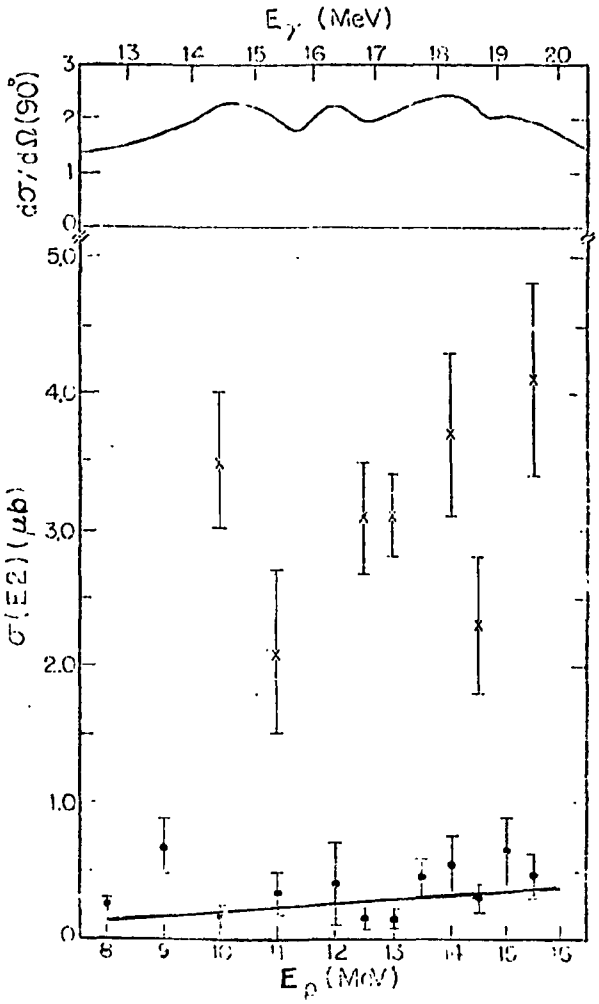

Fig. F3-8 The E2 cross section extracted from $^{13}C(p,\gamma_1)^{14}N$ data.

4. Measurements of The Reactions $^{15}N(\gamma,d_0)^{13}C$ And $^{13}C(\vec{d},\gamma_0)^{15}N$ in The Giant Resonance Region (D.M. Skopik, J.J. Murphy, II, H.R. Weller, R.A. Blue, N.R. Roberson, S.A. Wender, D.R. Tilley)

This work is the result of a collaborative effort between TUNL and the Saskatchewan Accelerator Laboratory. It has been prepared for publication. The abstract follows:

> "The reactions $^{15}N(\gamma,d_0)^{13}C$ and $^{13}C(\vec{d},\gamma_0)^{15}N$ have been measured and compared with previous results. A broad resonance was observed at $E_x \cong 21.9$ MeV in the (γ,d_0) channel. Vector polarized deuterons were used to measure the angular distribution of gamma rays at this resonance. The results were analyzed assuming that the two S = 1/2 E1 transition matrix elements are dominant."

The (γ,d_0) measurements, and the present (d,γ_0) measurements, give absolute cross sections which agree within their estimated errors of ± 12%. Furthermore, these results indicate that the original (d,γ_0) measurements[1] should be normalized up-

[1] H.R. Weller and R.A. Blue, Nucl. Phys. A211, 221 (1973)

wards by a factor of 2.5, in agreement with the conclusion of Ref. 2. (Note: the shape of the yield curve of Ref. 1 has been reproduced in Ref. 3.)

The polarized deuteron capture data were analyzed by assuming pure E1 radiation and by assuming that the dominant transition matrix elements would be those having $S = 1/2$: $(LS; J) = (1\ 1/2;\ 1/2)$ and $(1\ 1/2;\ 3/2)$. If the ground state of ^{15}N is pictured as $^{13}C + d$ with an $L = 0$ deuteron, this assumption should be reasonable. The results of our analysis produce two solutions at $E_x = 21.9$ MeV. They are presented in Table F3-1.

Table F3-1

	% Contribution		Relative Phase
Solution I	$(J = 1/2)$	6 ± 3	$\phi_{3/2} - \phi_{1/2} = 43° \pm 14°$
	$(J = 3/2)$	94 ± 4	
Solution II	$(J = 1/2)$	73 ± 7	$\phi_{3/2} - \phi_{1/2} = 22° \pm 6°$
	$(J = 3/2)$	27 ± 6	

5. Study of The Giant Dipole Resonance Region of ^{60}Ni (J.D. Turner,* C.P. Cameron,** N.R. Roberson, H.R. Weller, D.R. Tilley)

This work has been completed. It was published in Physical Review C 17 (1978) 1853, under the title "Polarized Proton Capture on ^{59}Co". The abstract follows:

"The angular distributions of cross section and of analyzing power for the $^{59}Co(\vec{p}, \gamma_0)^{60}Ni$ reaction have been measured throughout the giant dipole resonance region of ^{60}Ni. In addition, the 90° yield curve has been measured for E_p from 5.8 to 16.5 MeV. The data are analyzed to deduce the amplitudes and phases of the T matrix elements involved. Comparison of the results is made to both the dynamic collective model calculation of Ligensa and Greiner and to a direct-semidirect model calculation. The direct-semidirect calculation indicates that the reaction proceeds predominantly via the radiative capture of $d_{5/2}$ protons. Isospin splitting is also discussed."

---

* Now at Eastern Kentucky University, Richmond, Kentucky
** Now at Sandia Laboratories, Albuquerque, New Mexico

[2] W. Del Bianco, S. Kundu and J. Kim, Nucl. Phys. A270, 45 (1976)
[3] W. Del Bianco et al., Can. J. Phys. 56, 3 (1978)

6. Polarized Proton Capture in The Giant Dipole Resonance Region

(H.R. Weller, N.R. Roberson, S.R. Cotanch)

A paper has been published on this work; the abstract follows.

"Measurements of cross sections and analyzing powers are examined for polarized proton capture on ^{14}C, ^{30}Si, ^{54}Fe, ^{56}Fe, ^{58}Fe, ^{59}Co, and ^{88}Sr at energies which cover the giant dipole resonance region. These data are used to extract the relative amplitudes and phases of the contributing E1 T-matrix elements. A typical result exhibits two solutions. Calculations using the direct (or a direct-semidirect) capture model appear to provide a means for choosing the physical solution."

This paper describes the results of an analysis, which assumes pure E1 radiation, of the angular distributions of cross section and analyzing power obtained from polarized proton capture on the seven targets listed in the above abstract. For example, in the case of $^{14}C(p,\gamma_0)^{14}N$, the only angular distribution coefficient present are:

$$a_0 = 1.0 = (s_{1/2})^2 + 2.0\ (d_{3/2})^2 \ ,$$

$$a_2 = -(d_{3/2})^2 - 2.0\ (s_{1/2})\ (d_{3/2})\cos\ (\phi_s - \phi_d) \ ,$$

$$b_2 = (s_{1/2})\ (d_{3/2})\sin\ (\phi_s - \phi_d) \ ,$$

were $s_{1/2}(d_{3/2})$ represent the amplitude of the transition matrix elements for capture of an incoming $s_{1/2}(d_{3/2})$ proton, and $(\phi_s - \phi_d)$ is the relative phase between the two amplitudes. As a result of the quadratic nature of the above equations, the analysis always yields two solutions. For the case of $^{14}C + p$, we find one solution which indicates that approximately 90%(10%) of the cross section is due to $d_{3/2}(s_{1/2})$ capture and a second solution with approximately 20%(80%). Similar results were obtained for all cases, if spin-flip terms, when present, are ignored.

In the direct-semidirect (DSD) reaction model, the evaluation of the transition matrix elements requires the calculation of a radial matrix element having the form

$$\langle \phi_{n\ell j} | r + \frac{V(r)}{E_\gamma - E_d + i\Gamma_d/2} | \chi_{\ell' j'} \rangle$$

where $\chi_{\ell' j'}$ is the proton continuum wave function and $\phi_{n\ell j}$ is the wave function of the valence proton bound in the final state. Since we were interested in obtaining a reliable but simple method for extracting the correct relative amplitudes, we chose to utilize the pure direct model ($V_1(r) = 0$) for the E1 capture calculations.

There are two main conclusions from this work. First: these simple calculations do predict a result which is close to one of the possible solutions for a number of target nuclei. Even though there are discrepancies between the calculated

and experimentally determined phase differences at lower energies, it does appear that one can safely choose the physical solution on the basis of these calculations. Second: the surprising success of the pure direct model in predicting (to first order) the measured angular distributions (equivalently the relative amplitudes and phase of the T-matrix elements) indicate that we are observing the effects of the energy dependence of the proton continuum wave functions. So, although the GDR is essential in order to account for the magnitude of the cross sections, its presence does not show up very dramatically in the proton capture angular distributions.

7. Inelastic Alpha Cross Sections in The Region of The GQR for Nuclei Near Mass 60 (H.R. Weller, S. Manglos, S. Wender, N.R. Roberson, D.R. Tilley, M. Potokar)

A manuscript has been prepared for publication. The abstract follows:

> "Cross sections have been measured for the (α,α') reaction leading to the first excited (2^+) state for targets of ^{52}Cr, ^{54}Fe, ^{58}Fe and ^{60}Ni. Data were obtained at several angles as a function of E_α in the region of 8 to 18 MeV. These energies cover the isoscalar GQR of the composite nuclei--^{56}Fe, ^{58}Ni, ^{60}Ni and ^{64}Zn. It has recently been reported that this GQR of ^{58}Ni, ^{60}Ni and ^{62}Ni decays primarily by alpha emission. While the present data can be interpreted as being consistent with this result, alternative explanations cannot be ruled out."

A typical data set is shown in Fig. F7-1. These data show a peak which has a position, width and strength consistent with a GQR which decays primarily by α emission to the 2^+ state. Other interpretations are possible and are discussed in the manuscript.

8. Study of GDR of ^{89}Y via The Reaction $^{88}Sr(p,\gamma)^{89}Y$ (R.D. Ledford, C.P. Cameron, N.R. Roberson, D.G. Rickel, H.R. Weller, R.A. Blue, D.R. Tilley)

This work was described in Section F-6 of the previous report (TUNL XVI). It is being prepared for publication and should be ready for submission early in 1979.

9. A Search for The Isovector E2 Resonances in ^{31}P, ^{89}Y and ^{60}Ni (N.R. Roberson, H.R. Weller, R.A. Blue, C.P. Cameron, R.D. Ledford, J.D. Turner, S.A. Wender, S. Manglos, D.R. Tilley)

The injector cyclotron is scheduled to be in operation again in January 1979 following the long period necessary for replacement of the main coils (see Section K-1). We plan to resume work on the search for isovector E2 resonances at that time.

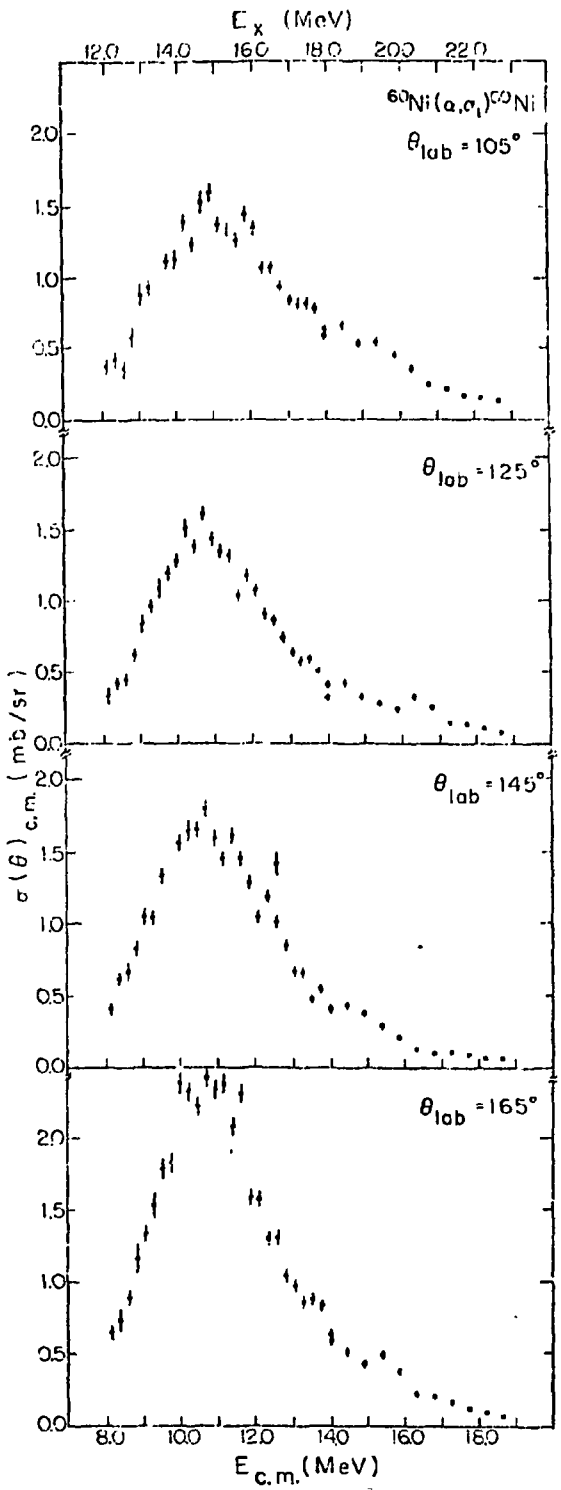

Fig. F7-1 Inelastic alpha cross section for ^{60}Ni in the region of the GOR.

10. Study of The Giant Dipole Resonance Region of ^{31}P (C.P. Cameron, R.D. Ledford, N.R. Roberson, D.G. Rickel,* H.R. Weller, D.R. Tilley)

The results of this study were described in Section F-4 of the previous report (TUNL XVI). A manuscript is being prepared for publication.

11. A Study of The GDR in ^{15}N Using Fast Neutron Capture (S.A. Wender, M. Jensen, M. Potokar, N.R. Roberson, D.R. Tilley, H.R. Weller)

As pointed out by Abert, George and Uberall,[1] no measurements have been reported for the $^{15}N(\gamma,n)^{14}N$ reaction. Such measurements may provide additional tests of shell model studies of the giant dipole resonance of ^{15}N. Furthermore, since the ground state of ^{14}N has T = 0, the $^{14}N(n,\gamma)^{15}N$ reaction should only populate T = 1/2 states of ^{15}N (whereas $^{14}C(p,\gamma)^{15}N$ can, in principle, populate both T = 1/2 and T = 3/2 states). Hence a study of the $^{14}N(n,\gamma)^{15}N$ reaction could help in sorting out the isospin makeup of the GDR of ^{15}N.

In order to obtain greater accuracy and to extend the measurements to lower energies, we have remeasured the excitation function of the $^{14}N(n,\gamma_0)^{15}N$ reaction over the GDR of ^{15}N. The results of these measurements are shown in Fig. F11-1, along with the previously reported measurements on $^{14}C(p,\gamma_0)$[2] and $^{14}N(p,\gamma_0)$.[3] The errors shown for the $^{14}N(n,\gamma_0)$ reaction on the plot do not include an overall 20% error in the absolute cross section. All data have been detailed, balanced and plotted as a function of excitation energy. It is clear from this figure that the $^{15}N(\gamma,p_0)^{14}C$ cross section (T = 1/2 and T = 3/2) is larger in magnitude and exhibits more structure than either the $^{15}N(\gamma,n)^{14}N$ or the $^{15}O(\gamma,p)^{14}N$ reactions. We also observe that the $^{15}O(\gamma,p)^{14}N$ and the $^{15}N(\gamma,n)^{14}N$ cross sections are very similar in magnitude and shape. In fact, if the $^{15}N(\gamma,n)$ data are shifted down by about 500 keV the positions of the minima and maxima line up quite well with the $^{15}O(\gamma,p)$ data. It is interesting to note here that if the energy difference between corresponding T = 1/2 levels in ^{15}N and ^{15}O is plotted as a function of excitation energy, a linear extrapolation suggests an energy difference of about 500 keV in the vicinity of E_x = 18 MeV. These observations support the notion that the $^{15}N(\gamma,n)$ and $^{15}O(\gamma,p_0)$ reactions are exhibiting the T = 1/2 strength of the GDR in the mirror nuclei ^{15}N and ^{15}O, while the $^{15}N(\gamma,p_0)^{14}C$ reaction displays both T = 1/2 and T = 3/2 strength.

In addition to these data we have obtained angular distributions at eight neutron energies between 6 and 13 MeV. These data, obtained at 7 angles, were fitted to an expansion in terms of Legendre polynomials. We are presently in the process of correcting the fits for the effects of finite target size. Satisfactory fits were obtained with the fits through order two. The resulting a_1 coefficients were quite small (typically $-.02 \pm .06$). This is in sharp contrast to the a_1 coefficients reported at corresponding excitation energies in the $^{15}O(\gamma,p_0)$ reaction (where a_1 ranged from .22 to .50 for E_x in the range of 14 to 24 MeV). This observation could be understood if the a_1 coefficient seen in the $^{15}O(\gamma,p)^{14}N$ reaction arose from interference between the dominant E1 radiation and a direct E2 contribution. If this occured one would expect a much smaller a_1 in the $^{15}N(\gamma,n_0)$ data due to the

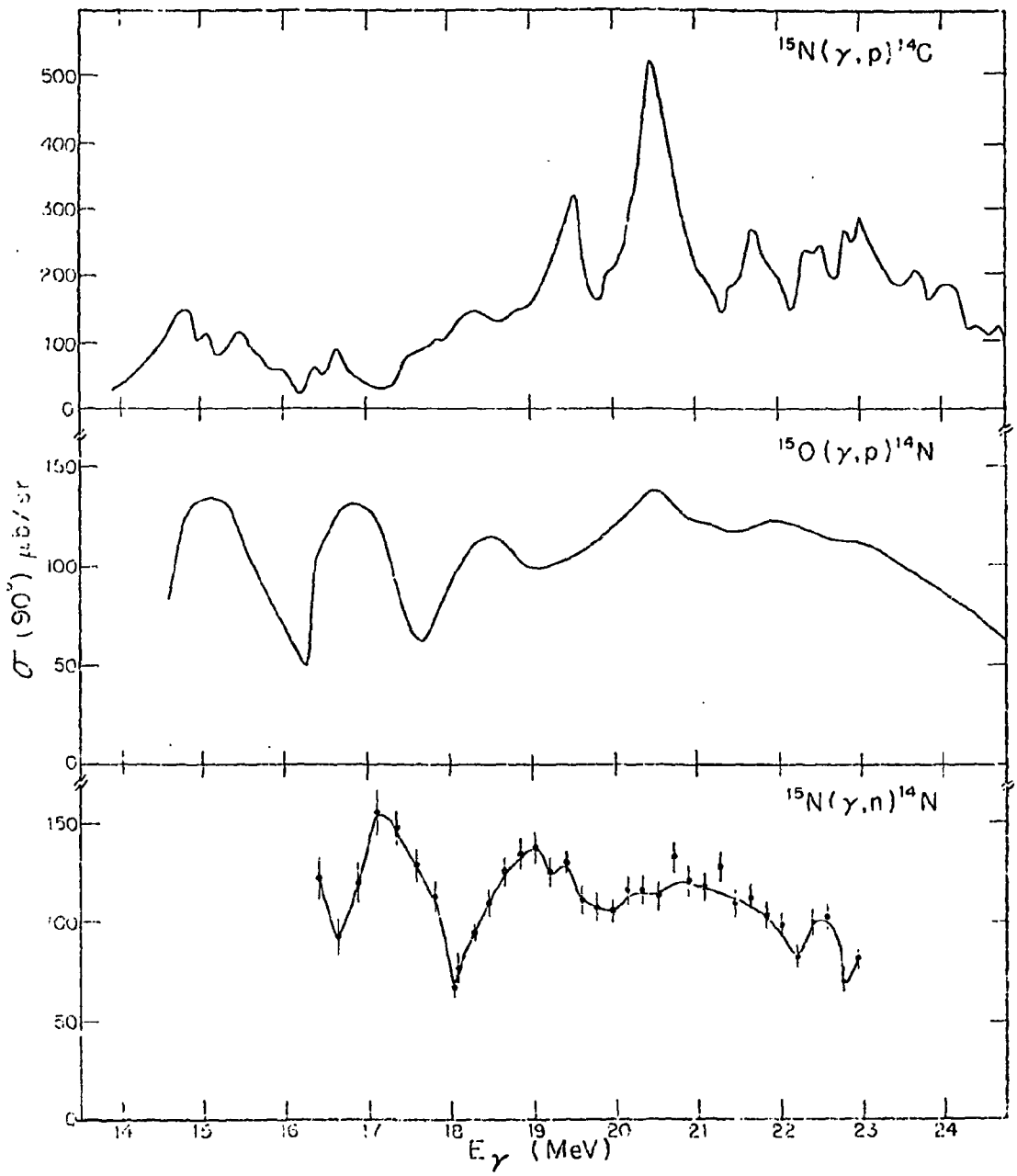

Fig. F11-1 Excitation function for $^{15}N(\gamma,p)^{14}C$, $^{15}O(\gamma,p)^{14}N$ and $^{15}N(\gamma,n)^{14}N$ obtained by detailed balance from the respective capture-reaction data.

fact that the direct E2 strength would be reduced by a factor of the order of Z/A^2, arising from the small quadrupole effective charge of the neutron. Calculations based on the DSD model are underway to further investigate this thesis.

The a_2 coefficients obtained from these data are shown in Fig. F11-2

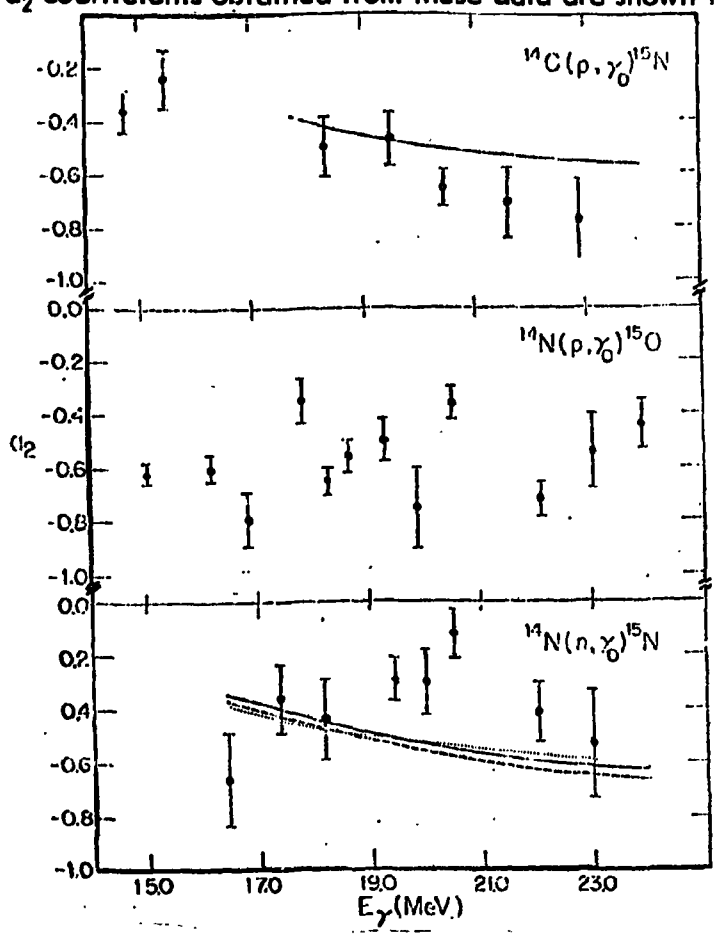

Fig. F11-2 Plots of a_2 coefficients obtained from $^{14}C(p,\gamma_0)^{15}N$, $^{14}N)p,\gamma_0)^{15}0$, and $^{14}N(n,\gamma_0)^{15}N$ data.

along with those obtained from the previously measured $^{14}N(p,\gamma_0)^{15}O$ reaction. Due to the spin-one target both the $^{14}N(p,\gamma_0)$ and the $^{14}N(n,\gamma_0)$ reactions have five E1 transition matrix elements. In a j-j coupling representation two of these correspond to projectiles having $s_{1/2}$ partial waves, two to $d_{3/2}$ partial waves and one to $d_{5/2}$. In a spherical DSD model the $d_{5/2}$ contribution will not contribute. The results of a direct calculation assuming a single $s_{1/2}$ and a single $d_{3/2}$ transition matrix element are shown as the solid lines in Fig. F11-2. Although the magnitude and general trend of a_2 is represented by this calculation, the data suggest an energy dependence in the region around 20 MeV which is not contained in this first order calculation.

Also shown in Fig. F11-2 are the results of a preliminary semi direct calculation using both a real and a complex form factor similar to those described in section F-6. This calculation includes an E1 resonance at 22.5 MeV with $\Gamma = 5.5$ MeV. The fraction of the E1 sum rule is taken from Bezic et al.[1] As shown in Fig. F11-2 this calculation also reproduces the general trend of the a_2 coefficients.

12. Quadrupole Radiation in ^{40}Ca Fast Neutron Capture (S.A. Wender, N.R. Roberson, M. Potokar, H.R. Weller, D.R. Tilley)

A paper on this work has been published (Physical Review Letters 41 (1978) 1217) and a talk presented during the Third International Symposium on Neutron Capture Gamma-rays Spectroscopy which was held at Brookhaven National Laboratory, September 1978. The following is the abstract of the paper.

> "Differential cross sections have been measured for the reaction $^{40}Ca(n,\gamma_0)^{41}Ca$ at seven angles in 1 MeV steps and at $\theta_{lab} = 90°$ in 200 keV steps for incident neutron energies of 6-13 MeV. The extracted a_2 coefficients and the fore-aft asymmetry are in good agreement with a direct-semidirect model calculation if the isoscalar giant quadrupole resonance is included."

The fast neutron capture facility used for this work was described in detail in a previous report (Annual Report - TUNL XVI, Section F-12). Briefly, the neutron source utilized the $^2H(d,n)^3He$ reaction with a pulsed beam incident upon a gas cell. The Ca target was a cylindrical, 3.8 x 3.8 cm ingot. The γ-ray spectrometer consists of our 25.4 x 25.4 cm NaI scintillator with an anticoincidence shield. Only events with proper time-of-flight were stored by the on-line computer, and this provided an effective discrimination against neutron induced background. The eight angular distributions obtained in this work are shown in Fig. F12-1. Each data point represents ~2.5 hours of running time. In Fig. F12-2, the 90° yield curve, the a_2 coefficients, and the fore-aft asymmetry coefficients, a_s, are presented. Assuming E1 and E2 radiation and neglecting a_4, we can write $a_s = 0.57a_1 - 0.39a_3$.

An extended DSD model[2] which includes quadrupole as well as dipole processes was used to calculate $\sigma(90°)$, a_2 and a_s. The results are shown as solid lines in Fig. F12-2. For the dipole term the coupling interaction of Ref. 3 was used and is proportional to $r\,U_1(r)$ where $U_1(r)$ is the complex optical-model symmetry potential. The quadrupole particle-vibration coupling had a surface-peaked shape proportional to $-r\,d\,U_0/dr$ where $U_0(r)$ is the real central potential. The curves labelled a and b in Fig. F12-2 are for $V_1/W_1/V_0 = 90/45/50$ and $75/37/50$ MeV, respectively. Also

---

[1] N. Bezic, D. Brojnik, D. Jomnek, and G. Kenee, Nucl. Phys. A128 (1969) 426
[2] A. Likar et al., Nucl. Phys. A298 (1978) 217
[3] M. Potokar, Phys. Lett. 46B (1973) 346

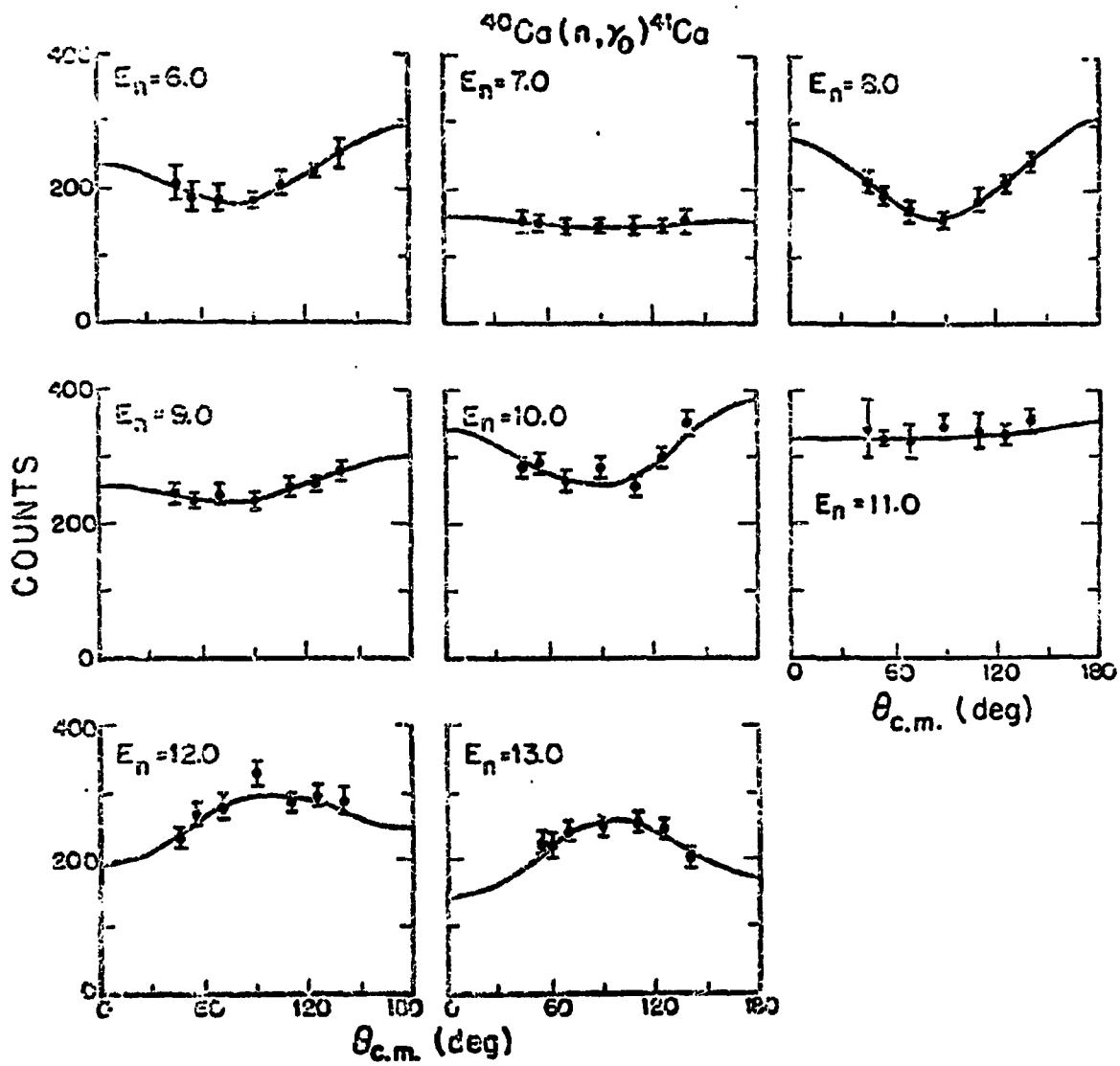

Fig. F12-1 Angular distributions obtained from the $^{40}Ca(n,\gamma_0)^{41}Ca$ reaction.

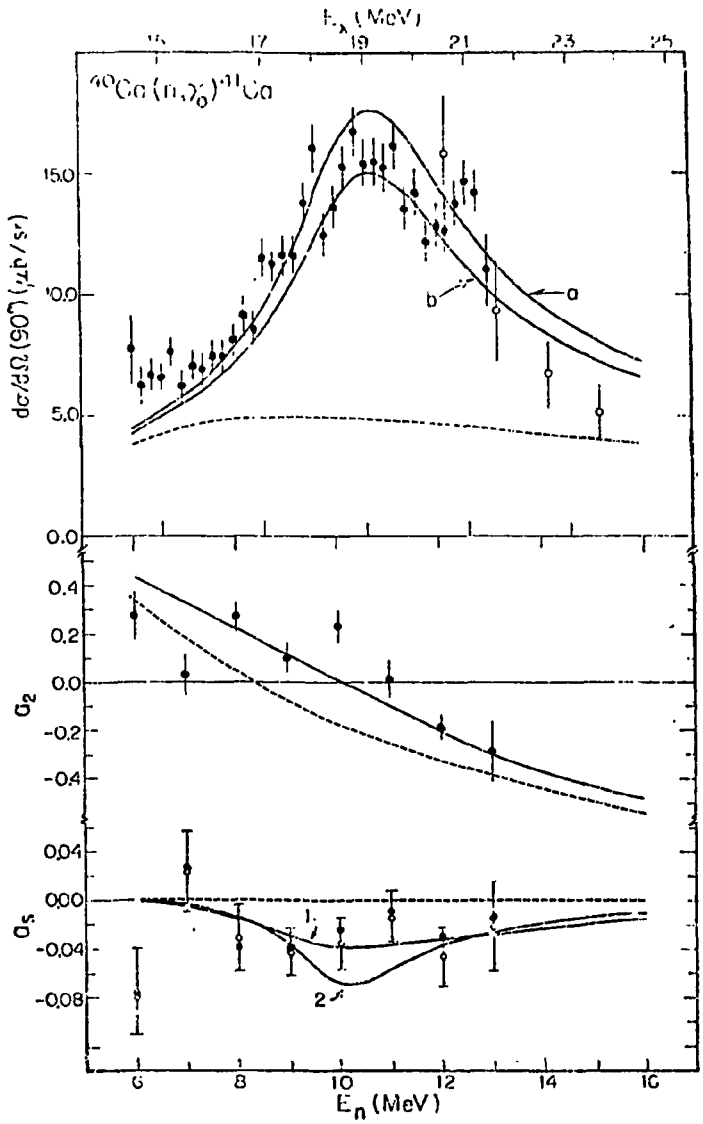

Fig. F12-2 Comparison of the a_2 coefficients, a_s coefficients and 90° yield curve with a DSD reaction-model calculation as described in the text.

$\Gamma_1 = 4.0$ and $E_1 = 18.4$ MeV. The values for E_{20}/Γ_{20} were obtained from inelastic α scattering[1] (curve 1) and from inelastic ^{3}He scattering[2] (curve 2) and are 18.0/4.0 and 18.2/2.2 MeV, respectively. The dashed curves shown for $\sigma(90°)$ and the a_2-coefficients are from a calculation assuming only a pure dipole term.

The results of a calculation of the fore-aft asymmetry, a_s, which include the DSD dipole terms and only a direct quadrupole term are shown as a dashed line in Fig. 12-2. The almost-zero values result from the small neutron quadrupole effective charge of Z/A^2. General agreement with the experimental values of a_s is obtained when the collective quadrupole resonance is included using either set of quadrupole parameters (case 1 and 2). It was, however,

[1] D. H. Youngblood et al., Phys. Rev. C13 (1976) 994
[2] T. Yamagata et al., Phys. Rev. Lett. 40 (1978) 1028

necessary to reduce the value of the collective quadrupole matrix element for case 1 from 43% to 30% of the EWSR. The reported value of 26% was used from case 2.

13. A Study of The $^{40}Ca(\vec{n},\gamma_0)^{41}Ca$ Reaction (M.J. Jensen, S.A. Wender, T.B. Clegg, M. Potokar, N.R. Roberson, D.R. Tilley, H.R. Weller)

To complement and extend our recent measurements of fast neutron capture on ^{40}Ca (Section F-12), we have initiated a program to produce a dc beam of polarized neutrons for use in studying the $^{40}Ca(\vec{n},\gamma)^{41}Ca$ reaction. Our first goal is to determine the b_1 and b_2 (and if possible, b_3) coefficients and search for evidence of the isoscalar E2 resonance in the b_1 (and b_3) coefficients. On the basis of the work reported in F-12 we expect b_1 to show a resonance shape with a peak near $E_n = 10.5$ MeV.

During the past two years we have obtained a detailed understanding of the neutron and gamma-ray induced background in our 25 x 25 cm NaI crystal. With a TOF system, we have determined that there is basically no difference in the spectrum in the region of the γ_0 peak with and without the time criterion. Consequently, for the $^{40}Ca(\vec{n},\gamma_0)$ reaction it is possible to use a dc polarized neutron beam and to correct for the background by fitting to the counts above the γ_0 peak. It should be noted that for $E_n \geq 8$ MeV, the background counts are about 5 - 10% of the γ_0 peak, and that for $E_n < 8$ MeV, they are about 10 - 30% with the larger value occuring at 55°.

The polarized neutron beam is obtained via the $^2H(d,n)^3He$ reaction with a gas cell (3 atm) and a polarized deuteron beam ($p_Z = p_{ZZ} = 0.7$). Recent improvements made to the TUNL Lamb shift polarized beam ion source have yielded increased beam current. We now are able to maintain 150 - 175 nA deuteron beams on target. The vector polarization, $p_{ny}(0°)$ of the neutrons produced by the $^2H + d$ reaction is given by[1]

$$p_{ny}(0°) = \frac{\pm(3/2)K_y^y(0°)\,p_Z}{1-(1/4)A_{zz}(0°)\,p_{ZZ}} \quad , \qquad (1)$$

where the ± sign applies for spin up/down and p_Z and p_{ZZ} are the vector and tensor polarization relative to the axis of symmetry of the polarized beam ion source. The zero-degree analyzing powers, $A_{zz}(0°)$, and polarization transfer coefficient, $K_y^y(0°)$, have been measured by P. W. Lisowski[1] and have a rather slowly varying energy dependence (typical values are $A_{zz}(0°) = -0.45$ and $K_y^y(0°) = 0.63$ near 8.5 MeV). The neutron vector polarization obtained by this method is from eqn. 1

$$p_{ny} \cong 0.6 \ .$$

Using the same experimental setup as discussed in Section F-12, two runs have been completed. Angular distributions of analyzing power, $A(\theta)$, were measured at 7.5, 8.0, 9.0, 10.0 and 11.0 MeV. Figure F13-1 shows our preliminary

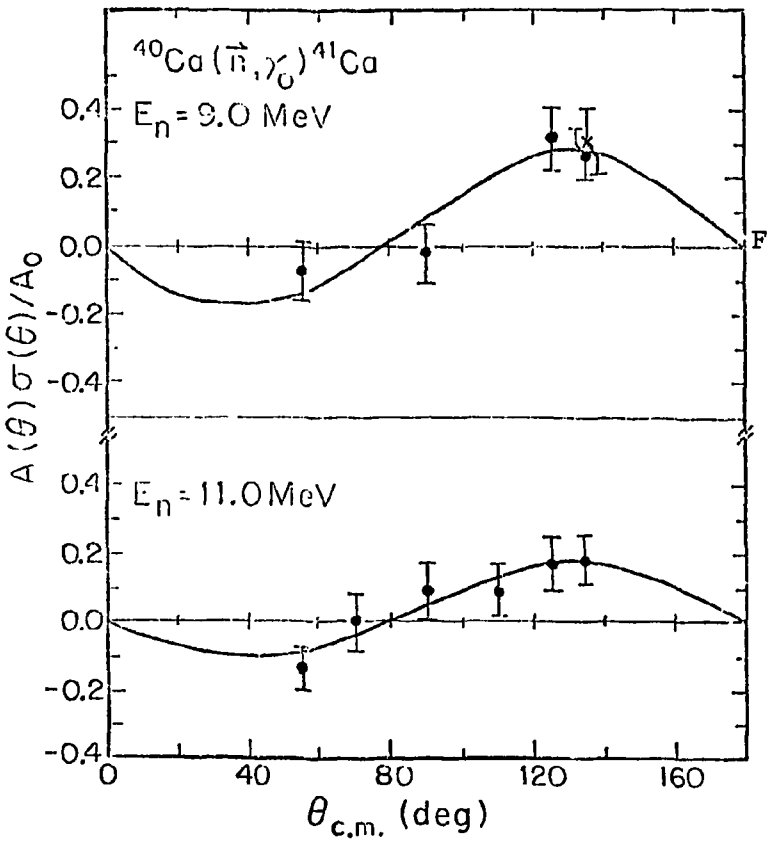

Fig. F13-1 Preliminary data from angular distribution of analyzing power measurements of polarized neutron capture by ^{40}Ca.

results at E_n = 9.0 and E_n = 11.0 MeV. It is emphasized that these are preliminary results, i.e., no corrections have been made for (1) asymmetries in the forward angle neutron yield due to the deuteron polarization, (2) target multiple scattering which includes polarization effects, and (3) other finite geometry effects.

An experimental estimate of the size of these correction factors was made by measuring A(θ) at 135° and at E_n = 9 MeV using a target 1/6 the volume of our standard target. The result of this measurement is shown as an (x) in Fig. F13-1. Clearly, this result indicates that the final corrections will be a reasonably small fraction of the analyzing powers shown here.

Preliminary values of b_2 are shown in Fig. F13-2 along with the results of a DSD calculation which uses the same parameter as the calculation discussed in Section F-12. A study of the $^{40}Ca(\vec{n},\gamma_0)$ reaction is clearly feasible and more experimental work is planned for the coming year. Besides providing a critical test of the DSD model calculations these measurements may provide confirmation of the isoscalar GQR in ^{41}Ca.

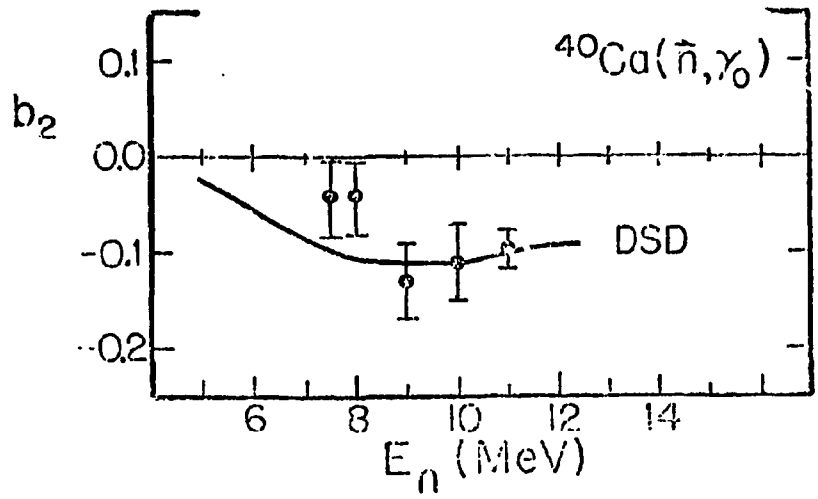

Fig. F13-2 Plots of the analyzing-power distribution coefficient b_2 from analysis of preliminary $^{40}Ca(\tilde{n},\gamma_0)^{41}Ca$ data.

14. On The Study of The $^{208}Pb(n,\gamma)$ Reaction (M. Potokar,* M. Jensen, D.R. Tilley, H.R. Weller, S.A. Wender, N.R. Roberson, S. Raman**)

The problem of neutron capture on ^{208}Pb has a long history in the study of the radiative capture process in the GDR region. Yet it seems still to be poorly understood. The observed excitation functions[1] for $^{208}Pb(n,\gamma)$, $^{208}Pb(n,\gamma_1)$, $^{208}Pb(n,\gamma_2+\gamma_3)$ and $^{208}Pb(n,\gamma_5+\gamma_i)$ helped to demonstrate that the physical idea of the DSD model for the nucleon capture dynamics in the GDR region is correct. However, the model calculations have shown also that the shape of the cross section is not reproduced in detail. The experimental excitation functions showed symmetric resonances, while the calculated ones showed higher cross sections on the high energy slope. The complex coupling, introduced to take into account other possible few-step processes in an average way,[3] was found to bring the theory and experiment into better agreement. However, the imaginary part of the coupling was much stronger than that deduced from other reaction data. While the complex nature of the coupling interaction has been justified[3] by deriving the DSD model in the doorway state approximation using Feshbach's unified reaction theory, very little has been done to demonstrate the degree of importance of the imaginary part of the coupling. More experimental data on the detailed shape of the excitation function and on the angular distribution a_2-coefficients are needed, since the nature of the coupling is most strongly reflected in these two quantities.

---

*

**Oak Ridge National Laboratory

1 I. Bergqvist, D.M. Drake, and D.J. McDaniels, Nucl. Phys. A231 (1974) 29
2 M. Potokar, et al., Nucl. Phys. A277 (1977) 29
3 M. Potokar, Phys. Lett 46B (1973) 346, and to be published

We have initiated measurements of the 90° yield curve for the $^{208}Pb(n,\gamma_0)$ reaction in the energy reaction $E_n = 7$ to 12 MeV in small energy steps. The excitation energies studied cover the high energy side of the GDR. A spectrum is shown in Fig. F14-1. At a few energies a_2 coefficients were obtained for the (n,γ_0) as well as the (n,γ_1) channel. Analysis is underway.

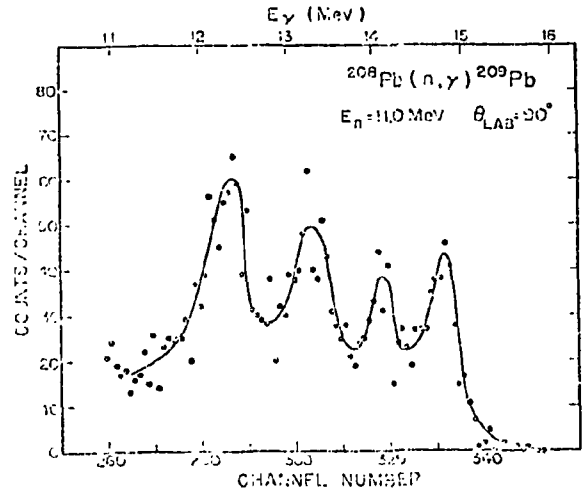

Fig. F14-1 Spectrum from the $^{208}Pb(n,\gamma)^{207}Pb$ reaction.

15. Gamma-ray Spectrometer Calibration (L. Ward, C. Fitzpatrick, M.J. Jensen, S. Manglos, D.R. Tilley, N.R. Roberson, H.R. Weller, S.A. Wender, M. Wright)

A drawing of our gamma-ray spectrometer (and TOF system) is shown in Fig. F15-1. During the past year we have removed 4" of lithium carbonate plus

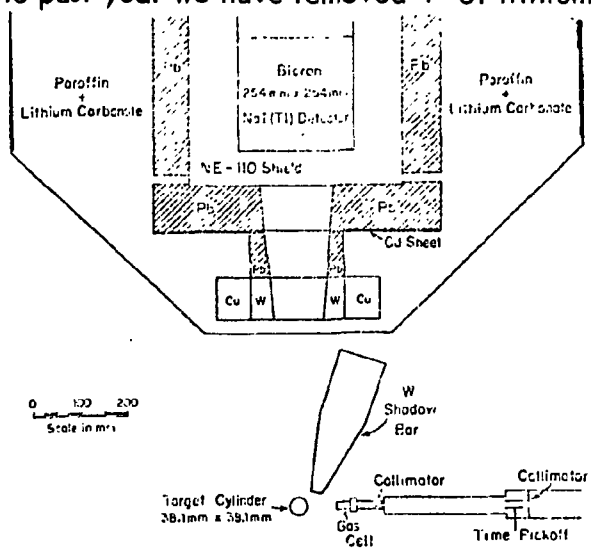

Fig. F15-1 A drawing of the gamma-ray spectrometer as used in neutron capture measurements.

paraffin from the collimator throat. We find that the remaining 8" of Li_2CO_3 plus paraffin gives adequate protection for the NaI crystal from fast neutrons that enter the collimator. For this new arrangement we have remeasured the efficiency (probability ϵ that a photon will be recorded if it reaches the spectrometer) of the detector system.

The thick target (50 keV for 14.2 MeV protons) yield was obtained for the $^{12}C(p,\gamma_0)$ reaction over the 15.07 MeV resonance in ^{13}N. This yield, when combined with the recent measurement[1] which determined that the step in the total thick-target yield corresponds to $(6.83 \pm 0.22) \times 10^{-9}$ γ-rays per incident proton, permits a determination of the product, $\Omega\epsilon$, of the detector solid angle and efficiency. Since it is somewhat more informative to discuss the efficiency alone, we have divided out the solid angle and will present our results in terms of ϵ. It should be kept in mind that the percentage error given for ϵ is in fact the percentage error in $\Omega\epsilon$.

The anticoincidence shield of the spectrometer is viewed by eight XP 1031 phototubes operated at 2000 volts. The anode signal of each tube is amplified by a factor of 4 before mixing. After the mixer circuit there is an additional gain which is variable from 4 to 112. The resulting signal is fed to a fast discriminator the output of which is used to reject all events that occur in both the NaI crystal and anti-coincidence shield. Fig. F15-2 shows the effi-

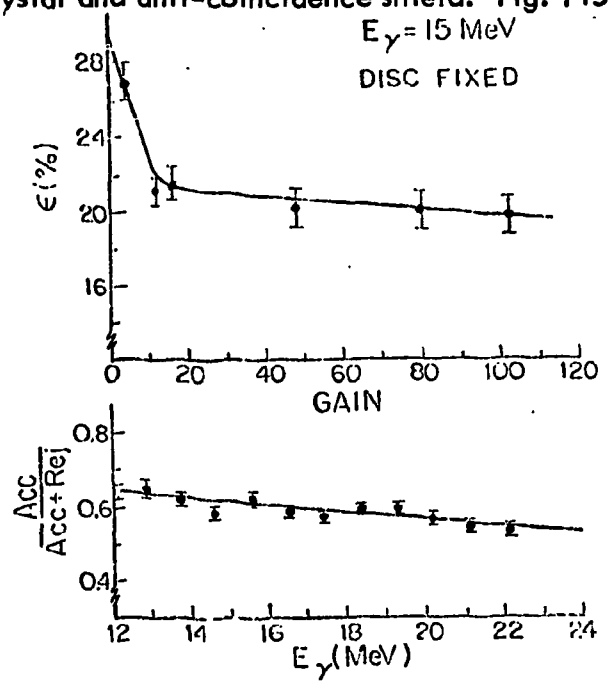

Fig. F15-2 Gamma-ray spectrometer efficiency vs. gain (upper portion) and acceptance ratio vs. gamma energy (lower portion) as discussed in the text.

ciency vs. gain for E_γ = 15.0 MeV when the peak was summed in the full energy region and the discriminator trigger level was kept fixed (EG and G TD101, disc = 023).

The spectrometer efficiencies at other energies have been obtained by correcting for the experimentally determined energy dependence of (1) the crystal response function, (2) the attenuation of the gamma rays by the shielding in front of the crystal, and (3) the rejection rate due to the anti-coincidence shield. The crystal response functions have been obtained from the work of Evans Hayward, W. R. Dodge and B. H. Patrick[1] who have measured γ-ray spectra in a 25 x 25 cm NaI crystal for mono-energetic gamma rays. The attenuation of the gamma rays as a function of energy was calculated using standard cross sections. An accurate measurement of the attenuation for our setup was made at 15 MeV and a small renormalization of the calculated attenuation coefficients was made. The rejection rates were determined for the γ_0 and γ_1 transitions obtained with the $^{13}C(p,\gamma)$ reaction (see Section F-3) and are shown in the lower part of Fig. F15-2. With small extrapolations at the lower and higher energies, we have obtained the spectrometer efficiencies for $10 \leq E_\gamma \leq 25$ MeV.

As a check on our procedures, we have calculated ϵ at E_γ = 15 MeV using item (1), (2) and (3) as discussed above and obtained $\approx$19.4% which compares well with the measured value of $\epsilon = (19.8 \pm 1.0)\%$. We have also compared cross sections obtained at TUNL for the $^{13}C(d,\gamma_0)^{15}N$ reaction with those of the $^{15}N(\gamma,d_0)$ reaction measured at the Saskatchewan Accelerator Laboratory.[2] For E_γ = 20 - 25 MeV, we find agreement to about 3% which is well within the stated accuracy of both experiments.

16. Computer Program Development for Neutron Capture Data Correction (M.J. Jensen, H.H. Hogue, S.A. Wender)

FIXER, a FORTRAN code, has been developed to correct the observed (n,γ) cross sections for finite geometry and neutron multiple scattering effects. These effects include deuteron beam spread and energy loss in the gas cell, $\sigma(\theta)$ for the $^2H(d,n)$ reaction, neutron and gamma ray absorption in the target, and solid angle corrections for both neutron and gamma ray fluxes. The neutron multiple scattering correction procedure takes account of single, double, etc., scatterings of the neutron before an (n,γ) reaction.

17. Direct-semidirect Model Analysis of $^{30}Si(p,\gamma_1)$ in The Region of The Isovector Giant Quadrupole Resonance (M. Potokar)

As previously reported,[3] the TUNL Cyclo-Graaff has been used to search for the effects of E2 resonances above the region of the GDR via the $^{30}Si(p,\gamma_1)^{31}P$ reaction. The fore-aft asymmetry coefficients, $a_s = 0.57a_1 - 0.39a_3$, were measured in 1 MeV steps up to an energy of E_p = 28 MeV ($E_x \approx 32$ MeV). (The yield

[1]Evans Hayward, W.R. Dodge, B.H. Patrick, to be published
[2]D.M. Skopik, SAL, private communication
[3]C.P. Cameron et al., 1976 Progress Report, TUNL XV, p. 43. C.P. Cameron, Ph.D. Thesis, Duke University 1976 (unpublished), H.R. Weller, et al., 1976 Progress Report, TUNL XV, p. 54

for the (p,γ_1) channel are shown in Fig. F17-1. These data have previously been

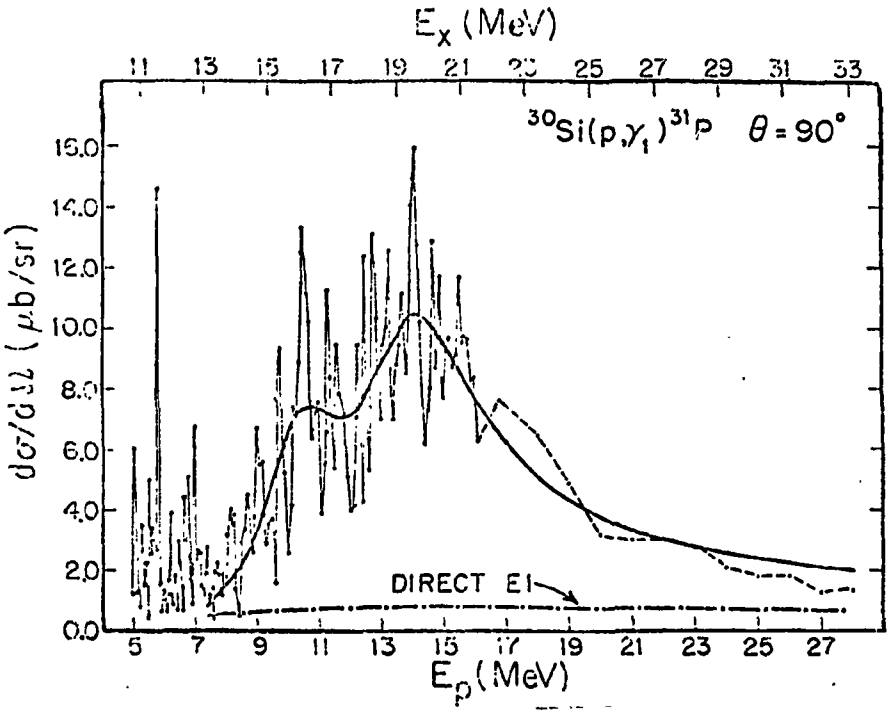

Fig. F17-1 Yield curve for the $^{30}Si(p,\gamma_1)^{31}P$ reaction.

interpreted[1,2] using a rather simple calculation, as showing evidence of the isovector E2 resonance. In this report, we present a more detailed theoretical analysis.

We used the generalized direct-semi-direct capture model[3] to analyze these data. Transition amplitudes of the following form were used to calculate the differential cross sections:

$$T_{p,\gamma} \propto \langle\langle \Psi_f | t \rangle | d(x) + \sum_T \frac{V_d^T(x)}{E-E_d+(i/2)\Gamma_d} + q(x)$$

$$+ \sum_{\tau=0,1} \frac{V_q^\tau(x)}{E-E_q^\tau+(i/2)\Gamma_q^\tau} | \langle t | \psi^{(+)} \rangle\rangle \ .$$

Here $\Psi_f\rangle$ is the final state of the nuclear system, $|t\rangle$ is the target nucleus ground

[1] C.P. Cameron et al., 1976 Progress Report, TUNL XV, p. 43
C.P. Cameron, Ph.D. Thesis, Duke University 1976 (unpublished)
H.R. Weller, et al., 1976 Progress Report, TUNL XV, p. 54
[2] C.P. Cameron, et al., Bull. Am. Phys. Soc. 21, 8 (1976) 996
[3] M. Potokar, Stanford Progress Report, 1977, page 99 and the references therein

state, d(x) and q(x) are the dipole and quadrupole single particle operators, respectively, $V_d(x)$ and $V_q(x)$, are dipole and quadrupole particle vibration coupling interactions and E_d, Γ_d and E_q, Γ_q the resonance parameters of the dipole and quadrupole collective state, respectively.

As the 90° excitation function for the $^{30}Si(p,\gamma_1)$ reaction clearly shows two resonances, we assumed that the process proceeds via two uncoupled collective dipole excitations (T = 1,2). Using a real dipole coupling interaction, the strengths of the two excitations were adjusted to fit the experimental excitation function averaged over the interval of 1.1 MeV. We found E_d/Γ_d = 15.8/3.4 and 19.1/4.0 MeV for the two peaks. In the isoscalar (τ = 0) quadrupole semi-direct term the coupling was assumed to be surface peaked (U_0 = -50 MeV) and the resonance parameters were taken as observed for ^{32}S from the (a,a') reaction.[1] For the isovector quadrupole the coupling was of the volume form, $\propto r^2 U_1(r)$ where $U_1(r)$ is the symmetry term of the optical model potential. Only the real part measured (V_1 = 75 MeV). The resonance parameters were treated as free and were adjusted until the best fit to the observed asymmetry coefficients was obtained.

The results, as shown in Fig. F17-2, reveal that the quadrupole collective excitation is located at ~ 30 MeV with the width of ~ 7 MeV. We found that the isovector quadrupole coupling interaction strength used corresponds to the EWSR depletion of ~ 75% in the target nucleus. In the particular channel, however, there is only about 4% of the total quadrupole EWSR in the energy interval between E_x = 13 to E_x = 33 MeV.

The data presented here are the first firm evidence of the isovector quadrupole resonance in this nuclear mass region.

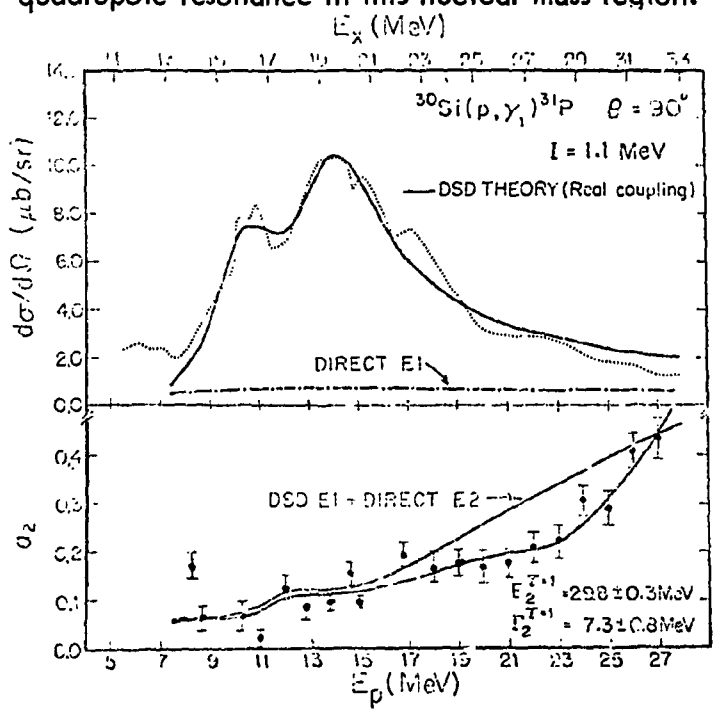

Fig. F17-2 Results of a direct-semidirect model analysis of $^{30}Si(p,\gamma_1)$ as described in the text.

[1] Compilation b, F.E. Bertrand, Ann. Rev. Nucl. Sci. 26 (957) 1976

18. On The Giant Dipole Resonance Built on The Ground And The First State of ^{31}P (M. Potokar)

Inherent to the direct-semidirect model for the dynamics of nucleon capture in the giant dipole resonance region is the use of the Brink hypothesis[1] for the single particle final states reached in the reaction and the assumption, that the giant dipole resonances of these states are well represented by the weak coupling model.

The case of proton capture on ^{30}Si seems to provide a useful example in which to consider the latter assumption in a slightly deformed γ nucleus. The excitation functions for two reaction channels are well known and there appears to be no difficulty in DSD model calculations, which would be related to the ambiguities in the optical model potentials used.

In the Fig. F18-1a we present the cross section for $^{30}Si(p,\gamma_1)$ energy averaged over the interval of 1.1 MeV. The calculation is described in Section F-17 of this report. The same dipole particle-vibration coupling and the same "target nucleus GDR parameters" were used to calculate the excitation function of $^{30}Si(p,\gamma_0)$. The result along with the energy-averaged experimental excitation function is shown in Fig. F18-1b. We observe that the calculated curve has to be shifted

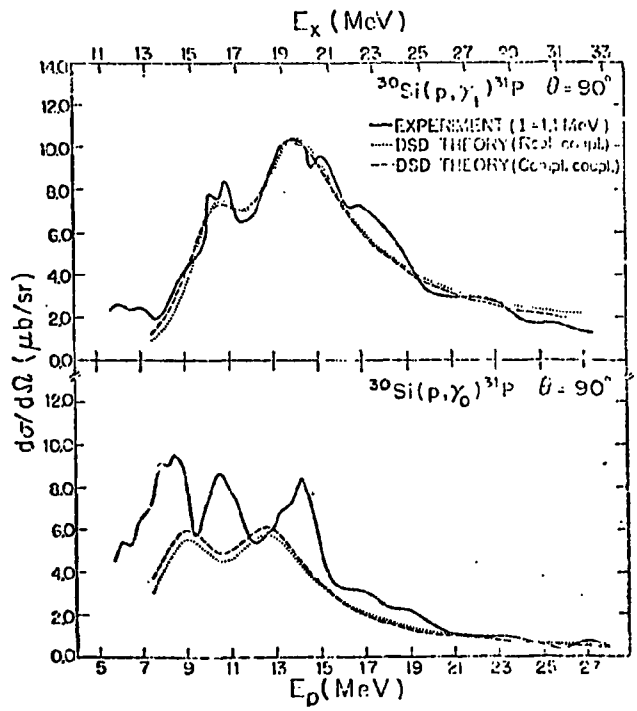

Fig. F18-1 The energy averaged cross section for $^{30}Si(p,\gamma_1)^{31}P$ (upper plot) and $^{30}Si(p,\gamma_0)^{31}P$ (lower plot). The calculated curves are discussed in the text.

[1] D.M. Brink, Thesis, Clarendon Laboratory, University of Oxford (May 1955)

toward either lower or higher energies to at least partially fit the experimental data. From the shape of the high energy tail and from the calculated angular distribution (Section F-19, this report) it appears that the shift toward higher energies is more likely ($\approx$ 1.4 MeV). In any case, it is shown that the use of weak coupling approximation in this problem is unfounded. It is not clear yet how to explain the observation. The most probable interpretation seems to be that one of the giant resonances is supported by a more deformed basic state than the other.

19. The Calculation of Angular Distribution Coefficients for $^{30}Si(p,\gamma_0)$ by The DSD Model (M. Potokar)

Previously reported[1] a_k and b_k coefficients are compared with those calculated by the DSD model. Parameters used in the calculation were the same as those found in fitting the $^{30}Si(p,\gamma_1)$ data (Section F-17, this report), except that the positions of the resonances of the collective states were shifted up in energy by 1.4 MeV, and the strength of the dipole particle-vibration coupling was slightly increased. While we have already commented on this shift in Section F-18 of this report, the need to increase dipole coupling strength relative to the (p,γ_1) channel is probably due to the poorly known spectroscopic factor[2] for the first excited state ($d_{3/2}$) in ^{31}P.

Our results are shown in Fig. F19-1. While the main trend of the data

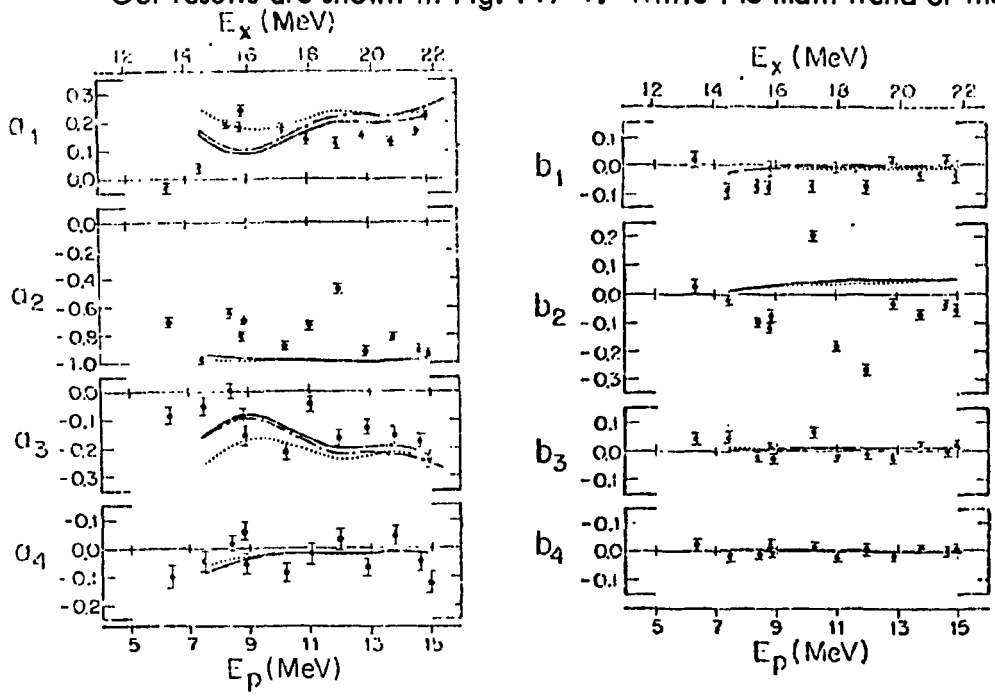

Fig. F19-1 A plot of experimentally-determined a_k and b_k coefficients for $^{30}Si(p,\gamma_0)^{31}P$. The calculated curves are discussed in the text.

[1] C.P. Cameron et al., 1976, Progress Report, TUNL XVI, p. 51
[2] P.M. Endt, Atomic Data and Nucl. Data Tables 19 (1977) 23 and references therein

is well reproduced, there are some discrepancies. One of the most probable reasons for the deviation of the experimental a_k coefficients from the calculated ones is the fact, that the measured angular distributions were often taken at the peaks of the intermediate structure appearing in the 90° cross section. This may also influence the agreement in the b_k coefficient. However, the calculation of the phases between the various reaction amplitudes may not be reliable, if the optical model potential used[1] is not an appropriate one for p + ^{30}Si system in this energy region.

20. Direct-semidirect Reaction Contributions in The GDR Region of The Isobaric Analogue States of The Reaction ^{88}Sr(p,γ_0) (M. Potokar*)

The giant dipole resonance of ^{89}Y as observed through the p_0 channel exhibits particularly strong intermediate structure below the excitation energy of ~ 18 MeV. Some of this structure is known to correspond to the analogue states excited in this energy region while the origin of the rest is uncertain. In order to initiate any studies of the intermediate structure it is necessary to establish what kind of reaction mechanisms are competing here. The aim of this report is to present the amount of the contributions which results from the excitation of the usual giant collective dipole state.

In our attempt we made use of the previously reported data[2] on ^{88}Si($\vec{p}$,γ_0) angular distributions and analyzing powers and the generalized DSD model. The 1/2 spin of the final state reached in the reaction guarantees that the dipole and quadrupole reaction amplitudes and the corresponding phases can be extracted in a model-independent way. Now, if we are able to reproduce those amplitudes or their linear combinations as they appear in the a_k and b_k coefficients on the high energy side where the direct semi-direct reaction mechanism is dominant, we can safely conclude how important this mechanism is on the low energy side.

The results are shown in the Fig. F20-1. It is obvious that the a_k and b_k coefficients are excellently reproduced on the high energy side of the calculated resonance. In fact, this example represents one of the best demonstrations of how well the simple DSD model actually works. It is important to know that in this calculation the parameters used were taken from other experiments--the spectroscopic factor from Ref. 3, the parameter for T< and T> GDR from Ref. 4, and the GQR parameter from Ref. 5. The exception was the dipole coupling interaction strength which was adjusted to get the fit in the tail. However, it turned out that also this strength is in accordance with the data obtained from other sources, which give the value V_1 between 60 and 110 MeV. The Becchetti Greenlees optical model potential was used. We observe that in the dominant, dipole contribution the $d_{3/2}$ reaction amplitude is about twice stronger than the $s_{1/2}$ amplitude at higher energies; but toward lower energies, the $s_{1/2}$ amplitude is increasing, rela-

---

[1] F.D. Becchetti, Jr. and G.W. Greenlees, Phys. Rev. 182, 1190 (1963)
[2] R.D. Ledford, et al., 1976 Progress Report, TUNL XVI, p. 58
R.D. Ledford, Ph.D. Thesis, 1976, Duke University (unpublished)
[3] J. Picard and G. Bissard, Nucl. Phys. A131 (1969) 636
[4] R. Pittham et al., Phys. Rev. C16 (1977) 970
[5] Compilation by F.E. Bertrand, Ann. Rev. Nucl. Sci. 26 (1976) 457

tively. At the low energy side of the resonance the two amplitudes are nearly of the same intensity. The result is, of course, in agreement with the experimental one above the resonance.

In the Fig. F20-1 we also present the calculated odd coefficients obtained if, in the model, the excitation of the collective quadrupole states is ignored. We note, that this difference can practically be attributed only to the isovector quadrupole model.

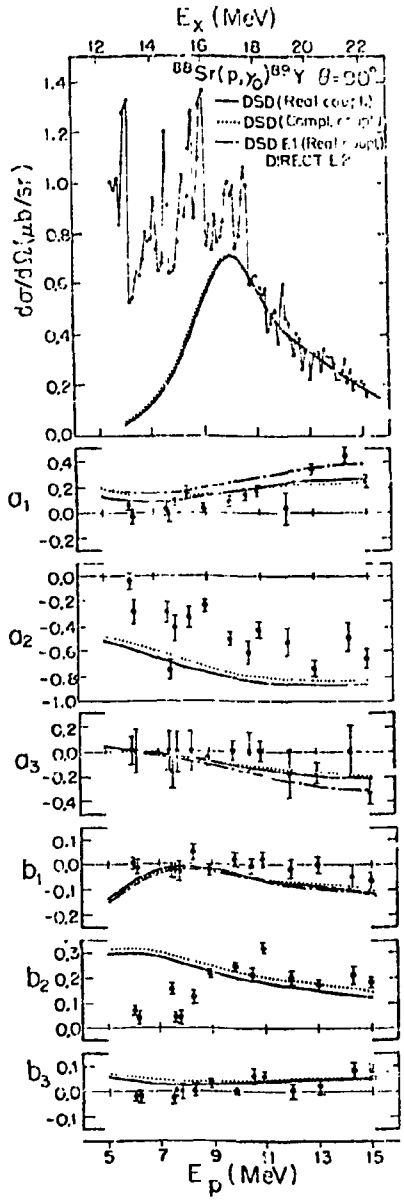

Fig. F20-1 Plots of 90° yield and a_k and b_k coefricients for $^{88}Sr(p,\gamma_0)^{99}Y$ and comparisons with calculations discussed in the text.

G. ATOMIC PHYSICS

1. Target Thickness Effects in Heavy Ion Collisions (M. Clark, J.M. Feagin, A. Kodre,* J. Swenson, S.M. Shafroth, J. Willis, J.A. Tanis, R. Mowat, A. Waltner)

During 1978 the major progress has been a further study of target thickness effects on both the projectile characteristic and REC x-rays as well as target characteristic x-rays. Using the model of Betz et al. (PRL 33, 807 (1974) to describe the passage of a heavy projectile such as Cl^{q+} through a thin film such as Cu, we have obtained sets of parameters for projectile energies of 20, 40, 60 and 80 MeV.

J.A. Tanis gave an invited talk on this work at the small accelerator conference in Denton, Texas, November 6 - 8, 1978. A written version has been accepted for publication in the IEE proceedings of the Fifth Small Accelerator Conference and will appear as a bound volume in 1979.

We plan to submit it for journal publication in the near future. S.M. Shafroth presented it at the International Conference on X-ray and XUV Spectroscopy, Sendai, Japan, August 28 - September 1, 1978. He was invited to give a more detailed presentation at Tohoko University on September 2, 1978. Journal articles (by J.A.T. and S.M.S.) describing two aspects of this work were published this year. The first of these was entitled "Target-Thickness Dependence of Radiative Electron Capture in Heavy-Ion Collisions" and appeared in Phys. Rev. Letters 40, 1174 (1978). The abstract follows:

> "We show how the target-thickness dependence of heavy-ion-induced x-ray production cross sections can be used to normalize the measured K REC (radiative electron capture) intensity to the fraction of incident ions with K vacancies. Experimental REC cross sections for Cl ions on Cu targets are in good agreement with the free-electron theory of Bethe and Salpeter if it is assumed that all of the M- and N-shell electrons in Cu contribute to the REC process."

The second article, entitled "Projectile Fluorescence Yields in Heavy Ion Collisions", was published in Physics Letters 67A, 124 (1978). The abstract follows:

> "Fluorescence yields of highly ionized projectiles entering thin solid foils are determined from a target-thickness analysis of projectile and target K X-ray cross sections. Values are obtained for 20-80 MeV Cl ions on Cu and compared with scaling calculations."

---

* Fulbright fellow from Ljubljana, Yugoslavia

The target thickness dependence of Cl^{10+} and Cl^{16+} K x-ray cross sections along with the calculated curves based on the parameters of the Betz model is shown here in Fig. G1-1.

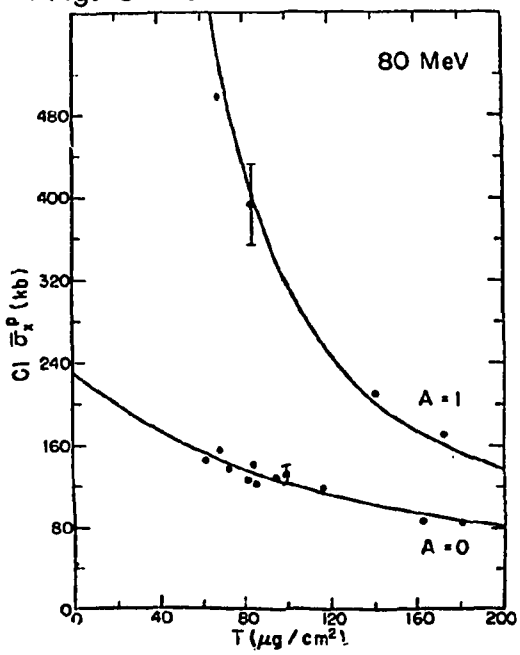

Fig. G1-1 Projectile K x-ray cross section vs. target thickness for 80 MeV Cl^{10+} (A = 0) and Cl^{16+} (A = 1) ions incident on thin Cu coils.

We have also studied Cl^{q+} projectile K_α x-rays under high resolution with a curved crystal vacuum x-ray spectrometer for thin C, Cu and KCl targets and incident energies of 20, 40, 60 and 80 MeV, as well as target Cl K x-rays when projectiles of Cl^{q+}, O^{q+} and protons were incident on KCl. Fig. G1-2 shows typical spectra. A 3-MeV proton beam incident on a KCl target was used

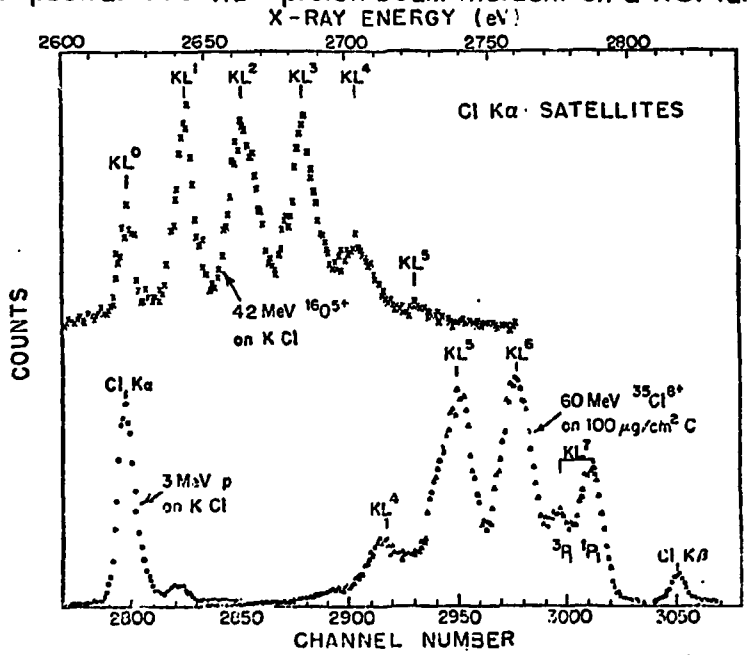

Fig. G1-3 Cl K_α satellites arising from 60 MeV Cl^{8+} ion bombardment of KCl.

to calibrate the spectra. The low energy Cl satellites are clearly seen in the O^{q+} on KCl spectra. These are transitions occurring in the presence of from 1 to 5 L-shell vacancies. The high energy satellites are seen in the spectrum obtained with 60 MeV Cl^{q+} on C. The energies for these peaks must be increased by ~0.2% to compensate for the energy loss due to transverse Doppler effect. A spectrum of Cl K x rays when 60 MeV Cl^{q+} impinges on KCl (Fig. G1-3) shows the full range of satellites - the high energy ones being due to the projectiles, and the low energy ones being due to the target x-rays.

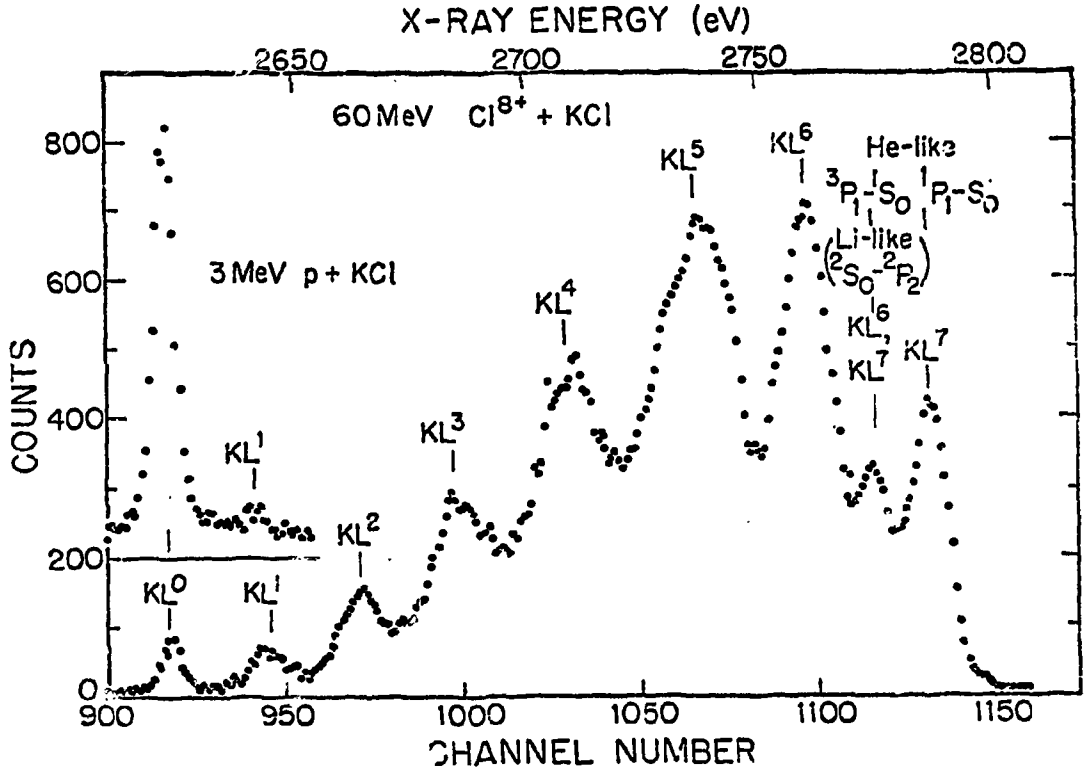

Fig. G1-2 Composite figure showing Cl K_α x-ray satellites. In the upper left is a spectrum of Cl target K_α satellites excited by 42 MeV O^{5+} ion bombardment of KCl. At the lower left and extreme lower right are Cl K_α and K_β spectra resulting from 3 MeV proton bombardment of KCl. The remaining spectrum is Cl K_α satellites from 60 MeV Cl^{8+} ions on Ca target.

The width of the peak labled $KL^7(^1P_1 - {}^1S_0)$ can also be understood in terms of Doppler broadening. A preliminary description of this work was given by S.M.S. at the Southeastern Section meeting of the American Physical Society in Blacksburg, Va., October 28, 1978. The lifetime of the forbidden $^3P_1 - {}^1S_0$ transition can be inferred by studying its intensity as a function of target thickness. So far we have data at 20 and 100 $\mu g/cm^2$.

A further interesting feature of these data is the energy dependence of $P_L(O)$, the probability of simultaneous K and L shell ionization at zero impact parameter.

It may be possible to understand theoretically the experimental values of $P_L(O)$ using non-perturbative calculations of Wu and Merzbacher, and this is being investigated.

2. Resonant Raman X-ray Scattering (A. Kodre, R. Mowat, J. Swenson, S.M. Shafroth)

As part of our effort to study x-ray processes we decided to investigate the recently discovered (1974) Resonant Raman x-ray scattering which can be more important than Compton scattering if the incident x-ray energy is slightly less than the K-shell binding energy of the scatterer.

This work was done with various x-ray tubes, a G. E. spectrogoniometer, a flat LiF crystal (2d = 4.028A), and Soller slits to obtain monochromatic x-rays with a spread of ~ 30 eV and with variable energy. Scattered x-rays were detected with a Si(Li) detector which has been converted from vertical to horizontal. The results of 120° scattering of near K- edge radiation on a thick Mo target are shown in Fig. G2-1 for incident x-ray energies varying between 2.5 keV and 40 eV below the Mo K

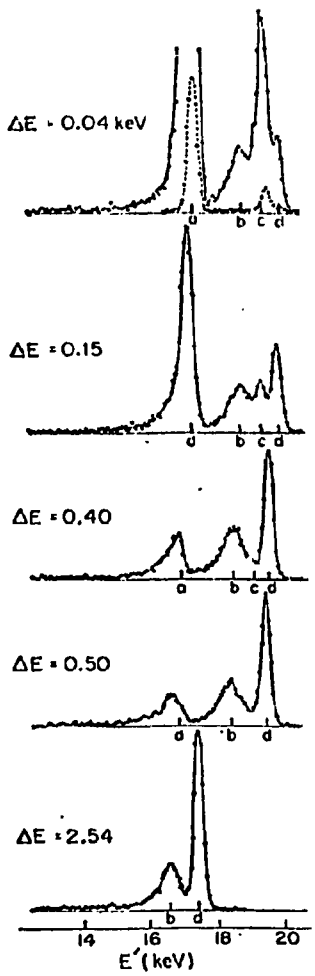

Fig. G2-1 Energy spectra of x-rays scattered at 120° from a thick Mo target in the order (from bottom to top) of increasing energy of the incident radiation shown by the labels $\Delta E = E_K - E$. Arrows a - d on the energy scale point to the calculated positions of the K-L RRS cutoff, the Compton peak, the K=M RRS cutoff, and the elastic peak, respectively. With the uppermost spectrum, a Mo fluorescence spectrum (dashed line - not to scale) is shown to provide a comparison for RRS peak positions. All spectra are normalized to the same incident beam intensity.

edge (19.999 keV). In addition to the previously known K-L Raman scattering where the scattered peak is found at about 17.4 keV (Mo K_α) - ΔE, we found a new peak corresponding to K - M scattering at 19.6 keV (Mo K β_{13}) - ΔE. This was the subject of a paper which has been accepted for publication in Physical Review A. It is entitled "Resonant Raman Scattering of X-rays: Evidence for K-M Scattering". The abstract follows:

> "Resonant Raman x-ray scattering on molybdenum was studied using a Mo-anode x-ray tube and a LiF crystal monochromator. Beside the usual resonant Raman peak corresponding to the fluorescent Kα lines another peak with a smaller energy loss was found. It is attributed to resonant Raman scattering with a final state M-shell vacancy corresponding to the fluorescent Kβ lines. Both contributions are shown to be independent of the scattering angle. Absolute cross sections have been determined and compared with theoretical predictions."

A second paper in which we deduce widths of K - vacancy excited states in a series of elements by comparing the resonant Raman scattering cross section with the above K edge fluorescent spectrum is ready to submit for journal publication. The contents of both of these papers were reported at the International Conference on X-Ray and XUV Spectroscopy at Sendai, Japan and the Small Accelerator Conference at Denton, Texas. The abstract follows:

> "The ratio of the cross section for X-ray fluorescence and the cross section for resonant Raman scattering depends on the width of the intermediate state involved. Thus, a method is developed to determine level widths in a low-resolution experiment. Widths of K-vacancy excited states in Zr, Mo, Rh, Ag, and Sn were determined as (4.0 ± 0.3) eV, (4.6 ± .3) eV, (6.4 ± .5) eV, (7.6 ± .7) eV and (12.0 ± 1.5) eV, respectively, with the apparatus of ~50 eV resolution."

Presently we are searching for shifted Auger electrons following below-edge irradiation of Co with a Ni anode x-ray tube. Photoelectrically ejected Auger electrons are detected with a parallel plate electron spectrometer. The incident x-rays are selectively filtered with a Co absorber so that Ni K_α is the major constituent of the x-ray beam incident on the Co target. Preliminary results appear promising.

A paper by B.L. Doyle and S.M. Shafroth has been submitted to Phys. Rev. A entitled "$L_1 - L_2\,M_{4,5}$ and $L_1 - L_3\,M_{4,5}$ Coster-Kroning transition thresholds in the Region $37 \leq Z \leq 56$". This paper describes the Ph.D. thesis work of B.L. Doyle. The abstract follows:

"The L_1-L_2 $M_{4,5}$ and L_1-L_3 $M_{4,5}$ Coster-Kronig transition thresholds in the atomic number region $37 \leq Z \leq 56$ are determined by bombardment of these elements with 2.5 MeV H^+ ions and detection of the resulting L X rays with a curved crystal spectrometer. The intensities of both the L_α, $L\beta_1$ and $L\beta_{3,4}$ x rays which are produced during these collisions are dependent on the energetic permissibility of these Coster-Kronig transitions. The discontinuous nature of these intensity ratios as functions of atomic number indicate that the L_1-L_2 $M_{4,5}$ and L_1-L_3 $M_{4,5}$ transitions are energetically allowed for the elements with atomic numbers in the regions $Z \leq 39$ or 40 and $Z \leq 49$ or 50, respectively."

H. HEAVY ION PHYSICS

1. Neutron Emission in Deep Inelastic Scattering Processes

Strongly damped collisions between heavy ions have been studied extensively in recent years. Measurements of neutron emission can determine the excitation energy carried away by each fragment, and determine the time scale of energy equilibration during the collision. Two such measurements have been performed at the UNILAC of GSI, Darmstadt; a feasibility study of the Xe-Au system with a relatively simple experimental setup, and a thorough study of the Kr-Er system with a kinematically complete charged particle identification system and in- and out-of-plane detection of neutrons.

a. Neutron Multiplicities in Inelastic Collisions of ^{132}Xe with ^{197}Au (C.R. Gould,* R. Bass, J. Czarnecki, V. Hartmann, K. Stelzer, R. Zitzmann and Y. Eyal,** ((Institut für Kernphysik, Frankfurt and GSI, Darmstadt)))

A preliminary account of this experiment has been published in Zeit. Phys. A284, 353 (1978). The abstract is given below.

> "The multiplicities of neutrons emitted from the light and heavy fragments, respectively, in the inelastic scattering of 7.5 MeV/amu ^{132}Xe ions from ^{197}Au have been studied as a function of total energy loss. The measured multiplicity ratios are close to the Au-Xe mass ratio for all Q-values, consistent with a rapid thermalization of the excitation energy. The absolute multiplicity values are lower than expected and suggest significant pre-equilibrium effects."

This measurement of multiplicity ratios equal to the Au-Xe mass ratio provided the first direct experimental evidence for a rapid equilibration of the excitation energy in a deep inelastic scattering process. That the absolute multiplicities were ~25% low was less firmly established because of the large experimental errors. We concluded that our results implied non statistical emission of neutrons in the early stages of the collision. The later, more accurate Kr-Er experiment found no evidence for pre-equilibrium effects, however.

To investigate the source of this discrepancy an experimental determination of the neutron attenuation of the chamber and detector material was made at Frankfurt using 5, 10 and 15 MeV neutrons from the $^{2}H(d,n)$ and $^{3}H(d,n)$ reactions. These results indicated that the neutron absorption was underestimated

---

* On leave from N.C. State University, work supported by A. Humboldt foundation, West Germany

** On leave from Weizmann Institute, Rehovot, Israel

by ~10% in our original work, and that the absolute neutron multiplicities should have been ~10% higher.

A more detailed version of the Xe-Au paper is being readied for publication. We believe now that, although the neutron multiplicities are somewhat low, the results are not inconsistent with statistical equilibrium subject to the large experimental uncertainties.

b. Neutron Emission in Strongly Damped Collisions of ^{86}Kr on ^{166}Er at 602 MeV (Y. Eyal, A. Gavron, I. Tserruya, Z. Fraenkel, Y. Eisen, S. Wald ((Weizmann Institute, Rehovot)), R. Bass, C.R. Gould, G. Kreyling, R. Renfordt, K. Stelzer, R. Zitzmann ((IKF, Frankfurt)), A. Gobbi, U. Lynen, H. Stelzer, I. Rode, R. Bock ((GSI, Darmstadt)))

This experiment was performed with a pair of two-dimensional position sensitive parallel plate avalanche counters and an array of eight in- and out-of-plane neutron counters. Using the 250 ps bunched beam facility of the UNILAC at GSI, a mass resolution of ~10 a.m.u. FWHM and an energy resolution of ~50 MeV FWHM were achieved for the outgoing heavy fragments. The results have been described in Phys. Rev. Letters 41, 625 (1978). The abstract appears below.

> "The neutron multiplicity in strongly damped collisions of ^{86}Kr on ^{166}Er was measured at 602 MeV beam energy. The measured ratio of the neutron multiplicities for the light and heavy fragments is in good agreement with the corresponding mass ratio, indicating a sharing of the excitation energy proportional to fragment mass. The results are consistent with predictions of a statistical model calculation assuming evaporation of neutrons from fully accelerated, unpolarized fragments."

Fig. H1-1 shows the neutron multiplicities, ν, as a function of the fragment mass, A, averaged over the c.m. kinetic energy interval $160 \leq Ecm \leq 260$ MeV. The quantity ν (A) is the total number of neutrons emitted from both fragments. The solid lines are the results of evaporation calculations. The upper right hand corner shows the experimental results and theoretical predictions for the heavy/light mass ratio. Fig. H1-2 shows the neutron energy spectra in the cm system for the heavy fragment (open circles) and light fragment (closed circles).

The observed angular- and energy-distributions are in agreement with the assumption of isotropic evaporation from fully accelerated fragments; no evidence for pre-equilibrium emission is found. The results indicate that, for the fully relaxed component of the strongly damped collisions, the system is close to thermal equilibrium at the end of the interaction.

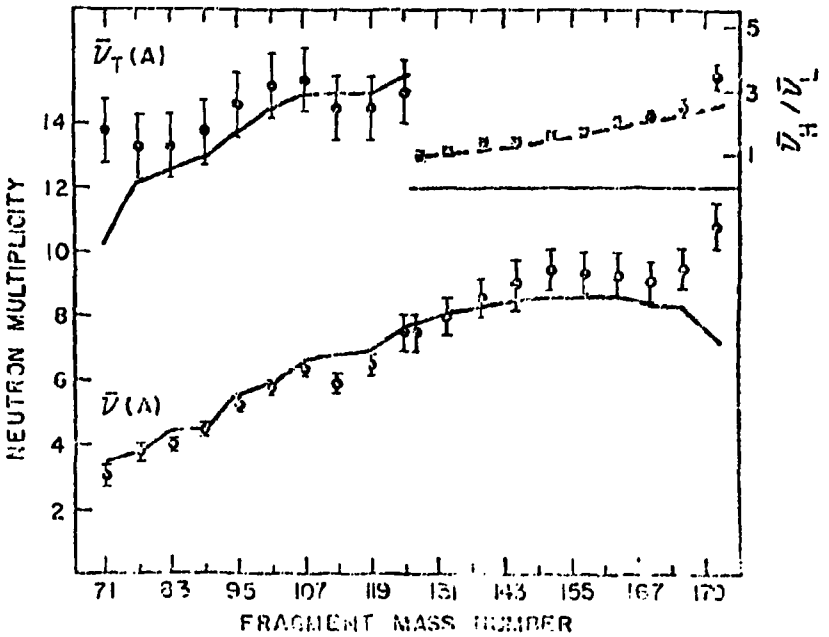

Fig. H1-1 Neutron multiplicities as a function of mass number for collisions between ^{86}Kr and ^{166}Er.

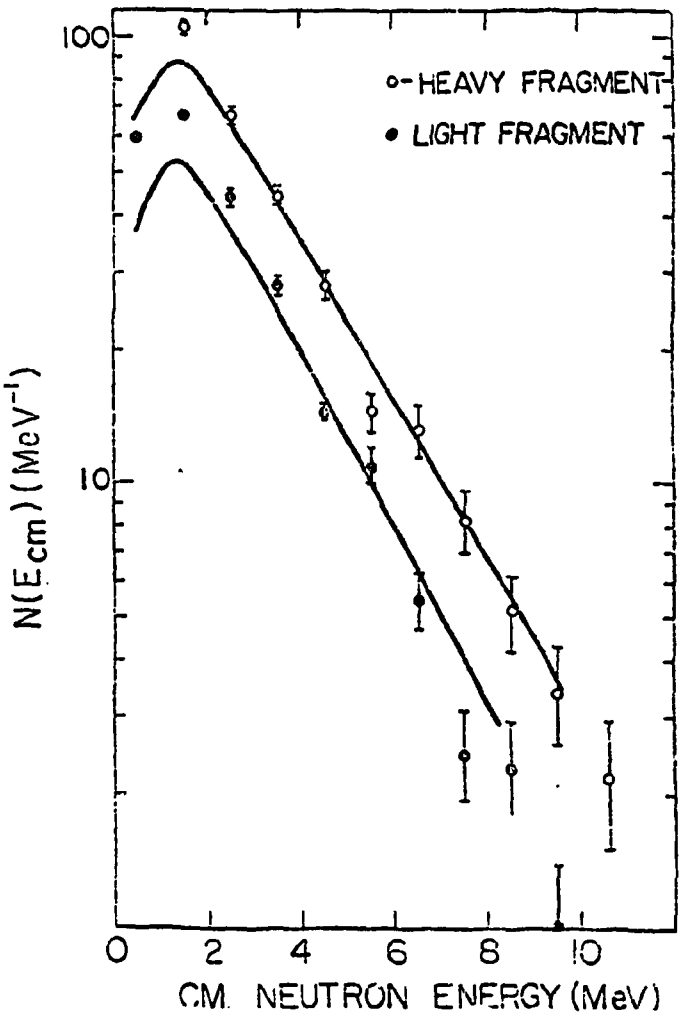

Fig. H1-2 Neutron c.m. energy spectra from the heavy and light fragments, emitted in reactions between ^{86}Kr and ^{166}Er.

I. APPLICATIONS

1. Production of Positrons Emitting Isotopes for PET: Positron Emission Emission Tomography (C.E. Nelson)

A facility for the production and transport of short-lived positrons emitting radioactive gases is under development in conjunction with the Department of Radiology of the Duke University Medical Center (DUMC). Present clinical interests are focused on the production of ^{15}O and ^{11}C.

The isotope ^{15}O can be used to label molecular oxygen, carbon dioxide, carbon monoxide and water. Common applications include regional pulmonary ventilation and blood flow studies, cardiac malfunction investigations, including the estimation of cardiac output and shunt determination, and myocardial, venal and cerebral blood flow. ^{15}O has been produced at the TUNL 4 MeV Van de Graaff accelerator via the $^{14}N(d,n)^{15}O$ reaction. Preliminary experimental work, completed in 1977, indicated a saturation activity of $A_0 \simeq 13mC/\mu A$.

^{11}C labeled carbon monoxide and carbon dioxide can be used for various studies including serial blood volume estimation, pulmonary investigations and red cell labeling with ^{11}C labeled carbon monoxide. It will be produced initially via the $^{10}B(d,n)^{11}C$ reaction using boric oxide as a solid target material (enriched in ^{10}B). The target output will be a mixture of ^{11}C labeled carbon monoxide and ^{11}C labeled carbon dioxide (formed when the ^{11}C produced chemically combines with the oxygen present on the basic oxide) and a sweep gas of helium.

Both of these radioactive gases will be transported to the DUMC hot lab through capillary tubing which will be installed in underground telephone cable conduits. A pressure difference of 4 atmospheres between the inlet and outlet of this tubing leads to a transit time of approximately 60 seconds between TUNL and DUMC. The simple chemistry required to produce $C^{15}O$, $C^{15}O_2$ and $H_2{}^{15}O$ requires no more than 60 seconds so that for ^{15}O, approximately one-half of the saturation activity can be made available for clinical use. The 20 minute half-life of ^{11}C allows for essentially all the saturation activity to be clinically available.

Funds for regular use of the TUNL 4 MeV Van de Graaff as a source of positron-emitting radionuclides in support of a positron-emission tomography camera have been included in a proposal submitted to the National Institute of Neurological and Communicative Diseases and Stroke. Further preliminary investigations of the ^{11}C yield at + MeV from several reactions is planned for the spring and summer of 1979, when the present investigator assumes a position in the Department of Radiology of DUMC.

2. Proton-Induced X-Ray Emission Analysis (B. Bacot, R.L. Walter)

The project to develop a Proton-Induced X-Ray Emission Analysis (PIXE) system for multielement determinations in bioenvironmental samples has been brought to a successful completion. Since the last report the project only operated during the summer months during which time the microscan capabilities were developed further and the evaporation studies were completed. Several hundred sections of animal tissue were provided by an NIH group who were performing heavy-metal toxicology experiments. The samples were either analyzed in bulk (as thick sections) or in a micro-scan method (as thick sections). Data for the toxic metal were cross-checked with standard atomic absorption techniques and both sets of abundances agreed favorably.

In summary, the developments in PIXE analysis at TUNL have provided considerable insight for this method for analyzing a wide range of samples. The PIXE method is either now in use, or has been used, in perhaps fifty laboratories with 2- to 10-MeV proton Van de Graaff accelerators. The method has been shown to compete favorably with other methods of analysis, and to have a unique role in some specific applications. As far as documentation of our contribution to the development of the PIXE technique, the TUNL work produced eighteen publications, one Ph.D. thesis, about ten lectures, and numerous scientific conclusions. The system is currently operational on the 4-MeV Van de Graaff and it would be easy to initiate another program of this type if the need and the resources are sufficiently great.

J. ION SOURCE DEVELOPMENT

1. Polarized Ion Source Development

Work has proceeded on the polarized ion source now installed at TUNL while design and construction of new components for the ion source have continued. Although we have been severely limited in manpower, significant progress has been made in nearly all portions of the development program. A detailed discussion follows.

a. Improved Source of Metastable Beam (T.B. Clegg, S.M. Mitchell, H.L. Manning, K. Murphy)

Extensive work on duoplasmatron and lens geometries has led to improvement in output polarized beam intensity. We have seen our "best accelerated polarized beam current increase from ~0.15 μA to ~0.37 μA during the year. Recently we were able to operate continuously with currents through the accelerator greater than ~0.2 μA for an experiment which lasted one week. Target currents of 0.20 to 0.24 μA were achieved.

In order to compare the beam from different duoplasmatron geometries, major effort has been put into trying to establish a reliable monitor of the metastable beam intensity emerging from the cesium charge exchange canal. For this purpose we have tried to build a device to scan the beam radially by quenching the metastable atoms in a well-localized, strong electric field and by observing the emitted Lyman-α photons in a commercial vacuum-ultraviolet photoionization chamber (Artech Corporation, Falls Church, Virginia). This chamber is furnished with an NO gas fill to 20 Torr and a thin MgF_2 window, and also with an accurate, unity-gain efficiency calibration of over 60%.

Over the six months we used one such device, its detection efficiency decreased by over an order of magnitude. We realized that for the photon flux being detected, if one assumes that each photon detected causes the ultimate dissociation of one NO molecule, we were dissociating approximately one-half the NO charge of the detector in one week of operation. We have recently sought to minimize this problem by reducing the detector solid angle and by collimating more tightly the metastable beam entering the detector. Up to now, however, this changing efficiency has made our comparison of metastable beam intensities from the various source geometries very difficult. Nevertheless, several tentative conclusions are possible from the extensive tests made to date.

For the same source geometry we have compared the intensity for $H_0(2S)$ and $D_0(2S)$ beams. We routinely observe more $D_0(2S)$ intensity than $H_0(2S)$ intensity. Measurements for the electric field quench region of the ionization chamber detector located 88 cm beyond the cesium charge-exchange canal (and beyond the spin filter) are shown in Fig. J1-1a. We observe, for our spin filter operating and selecting metastable atoms in a single hyperfine state, the radial metastable beam scans shown. Comparing the FWHM of the radial distributions, we observe that

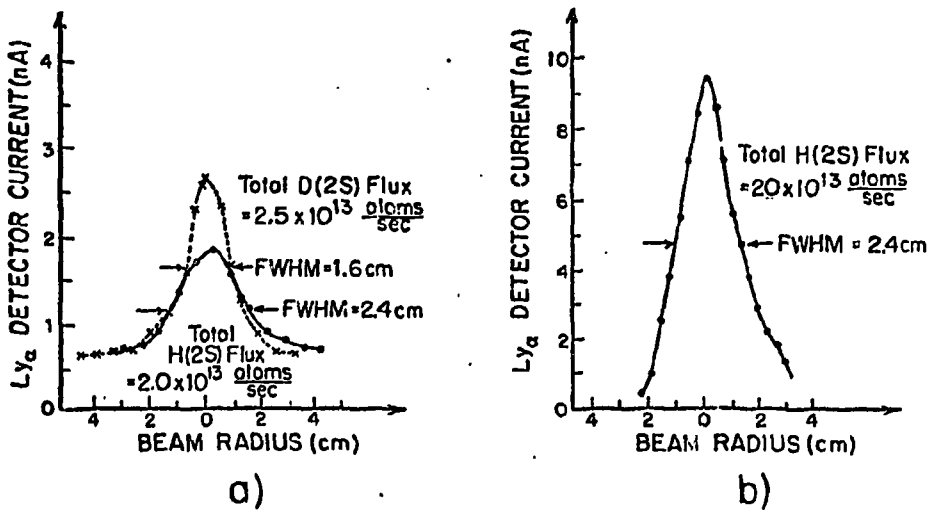

Fig. J1-1 Plots of metastable atomic beam flux versus beam radius for the duoplasmatron geometries described in the text.

the $D_0(2S)$ beam is not only more intense but is more peaked on axis. This narrower radial distribution can probably be attributed to the fact that the deuteron is heavier than the proton. A D^+ ion extracted from the duoplasmatron expansion-cup plasma with a given energy of radial motion will diverge less quickly than an H^+ ion with the same initial radial energy. As for the beam emittance for both $H_0(2S)$ and $D_0(2S)$ beams we can only state that 100% of the flux is included inside a phase space area of 5.5π mm-mrad-$(MeV)^{1/2}$.

Another conclusion from the metastable beam studies is that our spin filter can be tuned to operate with essentially 100% efficiency for selecting atoms in a single hyperfine state. Turning off the spin filter r.f. and d.c. electric fields and 575-G magnetic field increases the $H_0(2S)$ (or $D_0(2S)$) beam flux by a factor of 4 (or 6), as one would expect from the number of hyperfine states for atoms with nuclear spin 1/2 (or spin 1). Furthermore, this does not change the shape of the radial metastable beam distribution. Thus we are not quenching off-axis atoms in the metastable beam on entering and leaving the 575-G axial magnetic field.

We can also conclude from early measurements made with the detector, before its efficiency deteriorated, that in our ion source we can convert ~11% of our single-hyperfine state $H_0(2S)$ beam into accelerated, polarized H^- ion current measured on our Faraday cup immediately following the polarized source.

The measurements shown in Fig. J1-1a above were made using our

duoplasmatron followed by accel-decel beam extraction electrodes and a magnetic lens. This basic system has been described previously.[1] The largest improvement in output beam resulted from small changes in anode aperture geometry, following a suggestion of T.A. Trainor. The old and new anode apertures are shown in Fig. J1-2. Enlarging the maximum allowed angular divergence of the ions in the anode

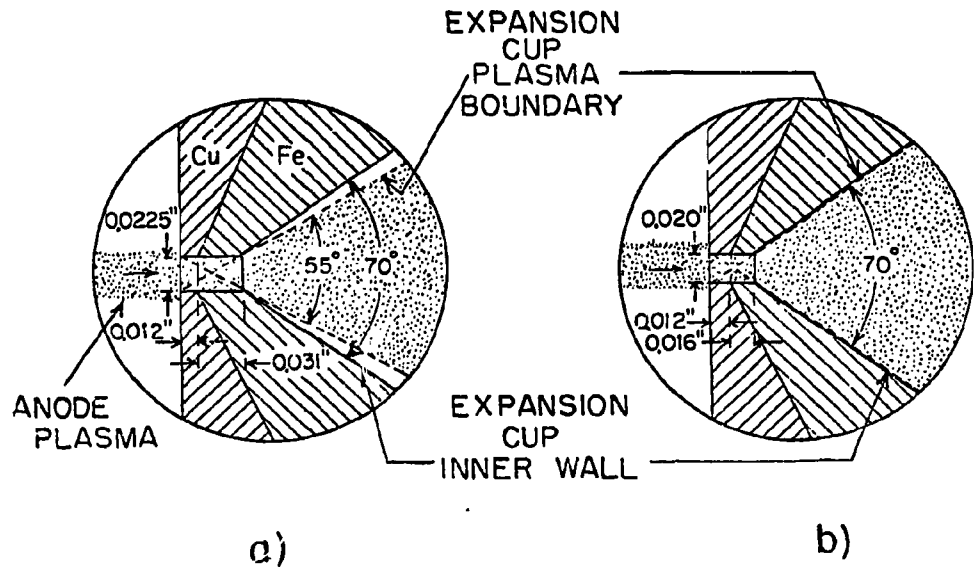

Fig. J1-2 The old (left) and new (right) anode aperture geometries tried with the polarized source. Improved filling of the expansion cup resulted in larger polarized beams.

aperture resulted in improved filling of the expansion cup and larger extracted ion beam.

Just prior to making the measurements shown in Fig. J1-1a, we made tests of the same duoplasmatron system with the magnetic lens removed. All H^+ ion focussing was accomplished by the electrostatic lens action of an accel-decel

[1] T.A. Trainor and T.B. Clegg, Proc. of 2nd Symp. on Ion Sources and Formation of Ion Beams, Berkeley, California, 22-24 October 1974, pg. IV-5-i.

electrode combination of slightly modified geometry. Figure J1-1b shows the $H_0(2S)$ beam measured on the same detector, this time with the spin filter off. Correcting for the fact that four hyperfine states were present in the beam, the measured $H_0(2S)$ flux in a single hyperfine state is still at least 2 times larger than that measured when using the magnetic lens system. This geometry was not used immediately to produce polarized beam because of beam instability when cesium vapor accumulates in the accel-decel region. Nevertheless, this measurement is very encouraging, and further tests are underway.

Because of the changing detector efficiency, the metastable intensities were inferred from frequent comparison of the negative polarized beam output with the Lyman-α detector current. Nevertheless, the relative normalization of the three data sets in Fig. J1-1 is no better than ±20% and the overall absolute normalization uncertainty is estimated to be ±50%. Work is continuing in an attempt to improve these results.

While these tests have been progressing at TUNL, tests have been made in Chapel Hill on other ion source geometries. The basic plan for one of these is to follow the duoplasmatron with an einzel lens with magnification greater than unity to produce a larger diameter (~1.27 cm) beam entering parallel or slightly converging into the cesium charge exchange canal to reduce unwanted space-charge effects. Here the best result has been an H^+ current at 550 eV of 17.1 μA in a 1.27 cm diam. Faraday cup 88 cm after the cesium charge exchange canal, but metastable beam measurements have not yet been successfully made. This positive current is greater than that observed with our "standard" source at TUNL, that for which the data in Fig. J1-1a were taken. Again, work is continuing.

Finally, we have constructed but not yet tested a multiaperture duopigatron source with magnetic cusp geometry to confine the source plasma. The geometry of the source is much like that developed at ORNL for injecting neutral beams into tokamak plasmas.[1] Discussions with J.A. Whealton at ORNL were initiated to learn how to use the ORNL-developed computer code[2] to determine the best beam extraction geometry for these low-energy, space-charge-dominated beams.

b. An Improved Interlock System for The Polarized Source (T.B. Clegg, W. Seward, M. Wright, N.R. Roberson, S.E. Edwards, A. Knott, J. Willis, R. Juelich)

A 6800 microprocessor-based interlock system has been completely designed and is now under construction. The design is basically very simple and will allow software rather than hardware changes to accomodate future interlock requirements.

---

[1] W.L. Stirling, C.C. Tsai, and P.M. Ryan, Rev. Sci. Instr. 48 (1977) 533
[2] J.H. Whealton, et al., Jour. Computational Physics 27 (1978) 32

Devices or systems to be monitored will be sensed by switches which open-circuit when a failure condition exists. Such an event then produces an optical signal to the microprocessor. Software logic determines the reaction required by this failure and other optical signals return to banks of relays which turn off systems in the necessary sequence.

c. Improved Control Links Between the Polarized Ion Source and The Computer (T.B. Clegg, W. Seward, M. Wright, N.R. Roberson, S.E. Edwards, A. Knott, J. Willis, R.E. Juelich)

The micro-processor will serve also as the communication channel through which control and readout of polarized source systems will be accomplished. The new readout capability will allow the user to monitor polarized source parameters during data collection through digital voltmeters mounted on the high-voltage frame of the polarized ion source or in the main accelerator control room. Multiplexed differential inputs for either voltmeter may be selected manually or under computer control. Control of devices (spin flip, quench, etc.) will be accomplished through optical signals to the relay banks mentioned in section 3b above. A faster control link, not yet designed, will accomodate other devices for which more rapid switching will be needed later.

A schematic of the overall microprocessor system is shown in Fig. J1-3.

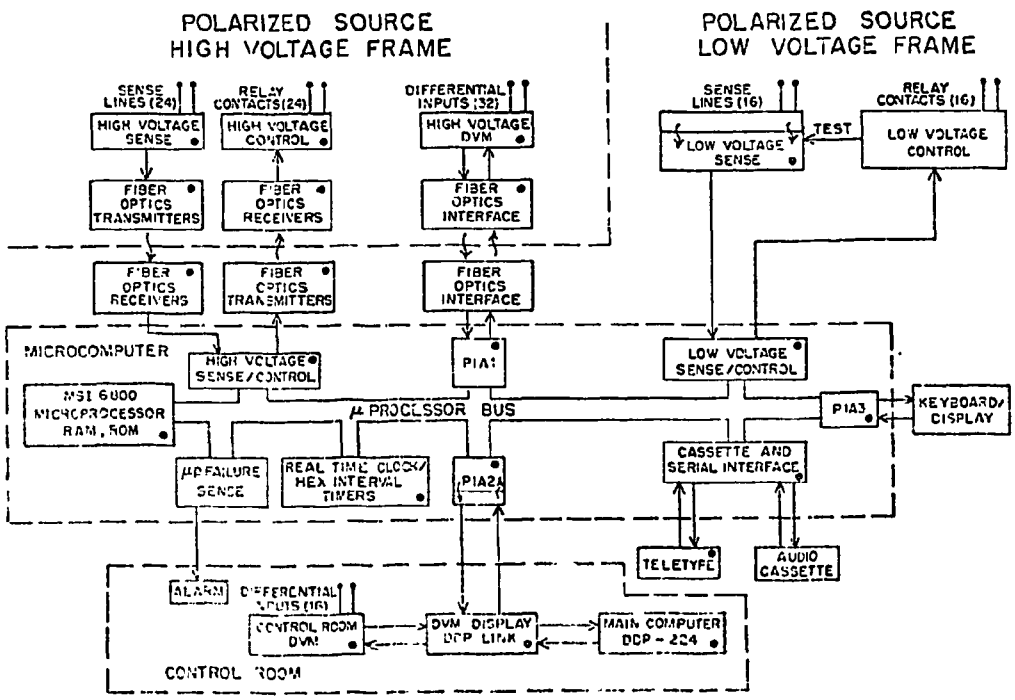

Fig. J1-3 The polarized source microprocessor system.

Devices for which hardware assembly is complete are indicated by a on this figure. Assembly and testing of the components shown in this figure should be complete during late 1978 and early 1979, and installation will begin immediately after that.

System software has not yet been developed but should proceed quickly when the hardware is constructed and ready for testing. To facilitate software development, we have acquired from Fairchild a 6800 - PL/1 Crossassembler and are working to get it running on the IBM 370 system at the Triangle Universities Computation Center.

d. Improved Systems for Separating Polarized Beam from Unpolarized Background (T.B. Clegg, R. Varner, G. O'Gorman, K. Murphy, S.E. Edwards, J.T. Harward)

Mechanical and electrical components are being designed and built for new cesium, spin filter, fast-slip, argon cryo-pumping, and lens systems. The combination of all these new systems is shown in Fig. J1-4 and will make the polarized source more reliable, versatile, and much easier for experimenters to use.

Design is complete for a wicked cesium canal, similar to that used at Los Alamos but with improved cooling of the ends of the cesium canal as suggested by Risler at the University of Washington. This will reduce our cesium consumption by approximately an order of magnitude. Valves are built to isolate the cesium region of the source from other source regions to prevent cesium contamination by air during maintenance.

A new spin filter system has been constructed which has all magnet coils which require cooling outside the vacuum system. This will eliminate all sources for cooling oil leaks into the vacuum system. These have plagued us in the past. We expect to achieve a base vacuum in this part of the ion source which is routinely $\sim 1 \times 10^{-7}$ torr. In addition to these mechanical changes, we have purchased a new solid-state oscillator for the spin filter cavity, and the new r.f. switching and control system containing this oscillator has been built and is ready to use. A new coil inside the vacuum system and around the actual spin-filter cavity will provide the possibility to add or subtract 10G from the magnetic field of the spin filter cavity. This will provide, for polarized deuteron operation, the capability of switching rapidly (up to 1 kH_z) between the three deuteron spin states.

A helium closed cycle refrigerator has been purchased and successfully bench-tested. It meets specifications and provides simultaneously 2.5 watts of cooling at 20° K and 5 watts of cooling at 77° K. A mechanical system for using this refrigerator to cryopump the argon charge-exchange region of the polarized source has been designed and construction has begun. This will provide better localization of the argon inside the source, reducing unnecessary beam scattering and quenching of the metastable beam from unwanted collisions.

The argon cryopumping will facilitate installation of rapid-spin-flip

fields in the source between the spin filter and argon charge exchange regions. This technique has been developed by McKibben at Los Alamos and provides the possibility to flip the spin direction for atoms in a pure hyperfine state rapidly (up to 1 kH_z) with very little associated change in spatial position of the beam on target. The same field can be adjusted to allow the source to operate using the Sona scheme to produce the nuclear polarization. For protons this offers the proven possibility of improving the beam intensity because the polarized beam results from two atomic hyperfine states instead of one. Coils to provide the spin-flip fields for our source are now being designed.

The negative, polarized beam emerging from the argon charge exchange region is best separated from the unpolarized background beam by focussing it immediately through a small (~2 mm diam.) aperture. Because of the magnification of the present lens system used to extract the beam at TUNL, this separation is impossible. A new lens system is designed which should allow this separation. This should raise our average beam polarization of ~75% for protons and ~65% for deuterons to the values of 85 to 90% and 75 to 80%, respectively, which have been obtained elsewhere.

e. New Bunching Systems for the Polarized Beam (S.A. Wender, T.B. Clegg)

We believe it should be possible to provide polarized beams on target, pulsed to $\lesssim 2$ nsec burst width, with an average beam intensity of perhaps 75% of the d.c. beam intensity obtained without bunching. Although no actual equipment has been built for this project during the past year, considerable attention has been given to understanding how the present bunching system operates, how well it transmits and bunches the polarized beam and how it might be improved. The design of a system to accomplish this efficient bunching is pointing to a two-step process.

A $5MH_z$ sawtooth voltage applied to the duoplasmatron will produce bunches at the argon charge-exchange canal ~50 nsec wide FWHM, with average intensity 90% of the d.c. beam intensity. The electronics to accomplish this were designed and tested successfully at Los Alamos in 1972. If this prebunched beam were presented to our existing two-gap buncher, only ~20% of the beam would be successfully bunched further and accelerated. This happens because the entire beam could not arrive at the two-gap buncher within the short time when the slope of the applied sinusoidal voltage is sufficiently linear, near the zero crossing, to bunch effectively. We believe that a two-gap bunching system, similar to that now in use, can be excited by a waveform more closely approximating a triangle wave than a sine wave, thereby extending the time to greater than 50 nsec over which this buncher can accept particles and bunch them effectively on target. The exact design of an electronics system to accomplish this is under study.

f. Improved Injection System Between Polarized Source and Tandem Accelerator (T.B. Clegg, R. Cadmus, F.O. Purser)

We have approached the problem of 30 to 50% beam-intensity-loss between the polarized ion source and the low-energy end of the accelerator on three fronts. First, exact ion optics calculations using the computer code TRANS were made for the present optical system used to accelerate and focus the polarized beam to the accelerator. Assuming an initial polarized beam emittance determined by the limiting apertures in the source and assuming no degradation in beam emittance in the charge-exchange processes or in the two electrostatic mirrors, calculations were made for actual ion optics parameters determined experimentally to yield maximum source-to-accelerator transmission. These calculations showed no reason to expect beam loss. Second, we decided to determine experimentally whether the smallest aperture in the beam transport system, the vertical gap in the inflection magnet, was causing the measured beam loss. We temporarily removed the magnet from the system and observed no significant improvement in beam transmission to the accelerator. Third, not really understanding these results, but in order to make more definitive tests, we have now decided to construct a beam-emittance measuring system which can be used routinely on the low energy end of the accelerator. Dr. Richard Blue of the University of Florida has cooperated in the design of this system and has agreed to construct and test the system at the University of Florida before bringing it to TUNL in the early summer 1979 for installation.

2. Sputter Ion Source (S.M. Shafroth, T.B. Clegg, J. Willis, F.O. Purser, R. Rummel)

The sputter ion source, which will allow us to produce beams of most atomic species suitable for injection in the TUNL tandem Van de Graaff is nearly ready for installation. An einzel lens which will be required before the sputter source can be used is now being built in the Duke Machine Shop. The lens should be completed and the source installed in early 1979.

K. ACCELERATOR DEVELOPMENT AND INSTRUMENTATION

1. Injector Cyclotron (F.O. Purser, R.L. Rummel, S. Manglos)

During this report period new main magnet coils were installed on the cyclotron, and the cyclotron was moved to a new location. The new coils are of hollow-core conductor construction and operate at a much lower temperature than the edgecooled aluminum ribbon coils which they replaced. The new coils have now been thoroughly tested and meet all specifications.

All components of the cyclotron have now been reassembled in its new position, and circulating and extracted beam have been obtained. Tests are currently under way to optimize extraction efficiency and accomplish final alignment prior to re-coupling the cyclotron to the tandem. Since the cyclotron shielding walls are as yet incomplete, these tests can be made only at night and thus have required a somewhat longer time than expected. However, it is now anticipated that the cyclotron will be in use as a component of the Cyclo-Graaff during January, 1979.

2. Deuteron Beam Polarization Monitor (S.A. Tonsfeldt, T.B. Clegg, E.J. Ludwig)

A deuteron vector and tensor polarimeter has been constructed which employs the $^3He(\vec{d},p)^4He$ reaction. The main components of the monitor are the following: (1) a split Faraday cup with a center hole which collimates the beam entering the ^3He gas cell and also provides feedback to steerers to keep the beam centered on target, (2) a gas cell with 6.4 μ Havar windows and ~3.7 atm. of ^3He gas, (3) a Ta foil deuteron beam stop, consisting of different foil thicknesses for use at different energies, (4) plastic scintillators viewed by phototubes at 0° and ±25° to detect the very energetic protons (Q ~ 18.35 MeV) that are only somewhat degraded in traversing the Ta foils. The large analyzing powers for the $^3He(\vec{d},p)$ reaction at these angles optimize measurement of the deuteron beam polarizations.

The angular resolution of the 0° detector has been improved to correspond to the geometry used at ETH[1] and TUNL[2] in measuring A_{zz} 0°, E_d and also to equalize detector counting rates. The vector analyzing power of the monitor has been calibrated from 5 to 16 MeV to an accuracy of ~2%. The beam polarization was determined by both the quench ratio technique and also by the accurate measurement of $^4He(\vec{d},d)$ scattering performed simultaneously in our main scattering chamber. Preliminary measurements of the tensor analyzing powers as functions of energy have been made, and analysis of the data is nearly complete.

---

[1] Nucl. Phys. A264 (1976) 45
[2] Nucl. Phys. A220 (1974) 533

3. Energy Stabilization of The Tandem Van de Graaff Accelerator for High Resolution Measurements (M.E. Bleck,* E.G. Bilpuch, G.E. Mitchell, W.A. Watson, W.K. Wells,** C.R. Westerfeldt)

Work is proceeding along several avenues to improve the performance and reliability of the high resolution system of the FN tandem Van de Graaff accelerator. This system was described in past reports. Recently a light pipe was fabricated and installed between the low energy baseplate and the terminal to carry the correction signal to the high voltage amplifier. This light pipe replaces a collimated light beam and should reduce the noise in the system due to light scattered off the accelerator rings. A new terminal amplifier with a higher current capacity has been constructed and is presently being bench tested. In addition, two new slit current pre-amplifiers have been constructed with several design changes to reduce noise, and are also being bench tested.

Another major avenue of development concerns the 90-90 analyzing magnet system. Some modifications to the present NMR magnetic field probe (used to "field lock" the magnets) which improve the signal to noise ratio of the detected resonance are being tested. These modifications should allow better control of the magnetic field and hence of the beam energy. Also under investigation is the use of other types of NMR probes. A microprocessor is being built which will step the programming voltage to the magnets on command from the computer; this task is presently handled by the computer itself. This programming voltage, in conjunction with a programmable frequency synthesizer serving as a reference for the NMR fluxmeter, allows the computer to stop the beam energy.

Finally, some testing has been performed (and is continuing) on the use of very thin stripping foils in place of gas stripping. Thus far the results are negative but designs for thinner and more durable foils will be tested in the near future.

4. Beam Resolution of The Tandem High-Resolution System at High Tandem Energies (8 - 15 MeV) (J.F. Wilkerson, E.J. Ludwig, T.B. Clegg)

High-resolution experiments require a stable beam with resolution of the order of or less than the natural width of the resonance in order to detect the resonance. In the theoretical analysis of the data the resolution of the beam in the target must be well understood in order to unfold the resolution function from the line shape. The two principal sources of spreading-out of the beam resolution are the energy straggling of the beam as it passes through the accelerator system and terminal voltage fluctuations.

---

* Now at Sandia Laboratories

** Now at the University of Pennsylvania

Studies have been made of the energy straggling of the beam as it passes through the tandem accelerator system. For practical purposes, three important areas must be considered: the accelerator low-energy end up to the terminal stripper, the terminal stripper (gas or foil), and the high-energy end from the end of the stripper to the target.

Experimentally it was found that reducing the pressure in the low-energy end of the accelerator by approximately a factor of two had no perceptible effect on the beam resolution, whereas, changes in the gas pressure in the stripper canal or use of carbon stripper foils had substantial effects on energy straggling, and thus beam resolution. To better understand the energy straggling, a computer program ESTRAG has been developed to calculate the energy straggling in materials of various thicknesses using Landsu, Vavilov, or Gaussian distributions as appropriate.[1] The program selects the proper distribution function from previously determined experimental parameters. Our analysis has pinpointed the critical region of energy straggling as the terminal stripper and shows that the beam in the low energy and high energy sections of the tandem accelerator should contribute negligibly to the energy straggling.

The terminal voltage fluctuations are controlled by the triple loop control system, which uses slit feedback signals. Under optimum operating conditions the triple loop system limits the terminal voltage fluctuations.[2] To achieve this regulation, it is necessary to have sufficient slit feedback current (25×10^{-9} A). In past high resolution experiments it was always customary to use gas stripping to reduce the energy straggling of the beam. However, at higher tandem energies the beam transmission efficiency through the tandem accelerator decreases drastically when gas stripping is used. At a terminal voltage of 6 MV, it is only about 10%. Thus, at high energies, using the gas stripper it has been difficult to maintain sufficient slit feedback current to regulate the triple loop system. Calculations using ESTRAG showed that at high tandem energies, it is feasible to use ^{12}C foils in the .1 - 4 $\mu g/cm^2$ thickness range, with acceptable energy straggling ($\sim$ 150 eV to 300 eV). Thus thin ^{12}C foils from .3 $\mu g/cm^2$ up to 5 $\mu g/cm^2$ were prepared using former or 97% transmission grids (and constructions) for initial support and placed in the tandem. Experimentally it was found that these foils have acceptable energy straggling and most importantly good transmission, which allows the triple loop system to maintain good regulation of the terminal voltage fluctuations.

Thus, at $E_p \cong 12$ MeV, good beam resolution ($\sim$700 - 800 eV) has been obtained through the use of thin ^{12}C foils to maximize transmission of the beam and yield sufficient slit feedback current to regulate the tandem, while also producing acceptable energy straggling.

---

[1] B. Schorr, Comp. Phys. Comm. 7 (1974) 215
[2] M. Bleck, TUNL Annual Report XVI (1978) XVI-93

5. Calibration of The High Resolution 90-90 Magnets Analyzing System (J.F. Wilkerson, E.J. Ludwig, T.B. Clegg)

A new calibration of the 90-90 magnets analyzing system is being performed for proton beams. The motivation behind the calibration is twofold. The first is the need to facilitate our searches for very narrow isospin forbidden resonances, especially at higher tandem energies (e.g., the $^{16}O(p,p)^{16}O$ $T^{3/2}$ ground state in ^{17}F found at 11.264 MeV)! The second reason is to allow a measurement of the mass energies of these resonant states which, in turn, will allow a determination of the isospin symmetry breaking forces' strength.

The initial calibration was performed using two absolute calibration points. The $^{19}F(p,p)^{19}Ne$ neutron threshold of an energy of 4.2343 ± .0008 MeV[2] and the $T^{3/2}$ isospin forbidden resonance, $^{12}C(p,p)^{12}C$, found at 14.23075 ± .0002 MeV.[3] Two other relative calibration points were measured. The $^{28}Si(p,p)^{28}Si$ $T^{3/2}$ isospin forbidden resonance at 5.834 ± .003 MeV and also the $^{16}O(p,p)^{16}O$ $T^{3/2}$ isospin forbidden resonance at 12.7077 ± .002 MeV, which has been measured relative to the $^{12}C(p,p)^{12}C$ resonance.[1]

Calibration data were taken on two separate runs, with several passes over both the $^{16}O(p,p)^{16}O$ and $^{12}C(p,p)^{12}C$ resonances. To insure accuracy, consistent tune through procedures were followed each time. Also, careful magnet recycling procedures were followed. Using the newly calculated calibration constant we are able to locate energies consistently to within 5 keV. Further studies, using additional calibration points, are planned.

6. Improvements in Pulsing and Bunching System (S.A. Wender, T.B. Clegg, R.L. Walter, F.O. Purser)

We are considering methods to improve the bunching efficiency of our present pulsed beam system. Such a system will try to satisfy the requirements of the various groups which utilize pulsed beams. The main design criteria are as follows: (1) The system must be compatible with and operate in conjunction with the pre-bunching system to be installed on the polarized ion source. A detailed description of the pre-bunching system is given in Section J-1e. (2) The pulse repetition rate must be on the order of 4 MHz to be useful for neutron time-of-flight experiments. (3) The system must be located after the second source box and the tandem so that it will be available for all the ion sources.

A system with a bunching efficiency of 75% has been developed at Argonne National Laboratory and operates at a frequency of approximately 50 MHz.

---

1 F. Hinterberger et al., Nucl. Phys. A263 (1976) 460
2 J. B. Marion, Rev. Mod. Phys. 38 (1966) 660
3 E. Huenges et al., Phys. Lett. 46B (1973) 361

This system involves the superposition of four harmonics applied to a single acceleration gap. This technique does not appear to be feasible for the low repetition rates we require. We are now investigating methods to drive a two-gap buncher system with additional frequencies to create a more linear wave form. Such a system will not have as high an efficiency as the Argonne system but will be more practical for repetition rates of 4 MH_z.

L. COMPUTER RELATED DEVELOPMENT

1. The Prime Computer System (J.R. Chandler,* B.H. Chou, K.B. Sales, C.R. Westerfeldt, S.E. Edwards)

During the past 12 months, the PRIME 300 computer system has been improved in several areas. Two BEEHIVE video terminals have been obtained to replace the two teletype terminals. This has greatly speeded up the I-O operations as the video units operate at 2400 BAUD instead of the 110 BAUD of the older teletypes. Secondly, this change has virtually eliminated down time as the result of I-O device failure. To provide hard copy output, we have purchased a DECWRITER III which is capable of output at 2400 BAUD, but is at present limited by software to 300 BAUD continuous output. The DECWRITER may also be substituted for either BEEHIVE terminal in case of failure.

The PRIME 300 computer itself has been upgraded by the addition of a 32K word board. This addition brings up the memory size to 64K words. With the 32K of memory, we were restricted in our data taking program to four charged particle or NaI spectra, plus a GeLi spectra. This had not been a problem in the past, but a new series of experiments required at least five spectra plus a GeLi spectra be stored in order to measure some more complex angular distributions.

With the 64K of memory installed and working, we have brought up the full PRIMOS II REV II operating system. This system has many advantages over the REV 10 system which we had been using. This revision seems to be the best for our single user system, and at this point we do not anticipate upgrading the system to higher revisions.

The new larger memory and operating system have allowed us to adapt several analysis programs from the old DDP-224 computer to the PRIME computer. This decreases our dependence on the DDP-224, and will greatly benefit programmers writing software for the proposed new computer system for the Tandem laboratory.

The CAMAC interface has been expanded with the addition of two quad input - 16 bit scalers, and one dual input - 16 bit preset scaler. The quad scalers will allow the data taking program to read in data such as the live time, total integrated charge, or data from single channel analyzers. The preset scaler will be used to count the integrated charge and initiate a sequence of events when the preset has been reached. This will be of great help in our elastic scattering experiments as it will free the experimenter of several operations previously required when preset was reached on the isolated preset scaler.

---

* Now at Savannah River

M. NUCLEAR THEORY AND PHENOMENOLOGY

1. Review of Physics with Polarized Nuclei (W.J. Thompson, T.B. Clegg)

A review of polarization in low-energy nuclear physics, written for the benefit of non-specialists, will be published in Physics Today in early 1979. The review includes concepts of polarization, polarized beam and target production, recent applications of polarization to basic symmetries, nuclear interactions, spectroscopy, NMR with unstable nuclei, and heavy-ion scattering. The examples are chosen to illustrate the wide variety of applications of polarization, and to emphasize the greater simplicity and detail obtained when polarization is employed.

2. Deuteron Scattering Potentials (W.J. Thompson)

A paper on non-locality effects in deuteron elastic scattering spin-orbit and tensor potentials has been submitted to Nuclear Physics. Currently, shell-closure effects in deuteron elastic scattering are being investigated for the A = 70-80 region in order to give guidance to TUNL polarized-beam experiments in this mass region.

3. Spin-Orbit Coupling in Heavy-Ion Scattering (W.J. Thompson)

Heavy-ion phenomena which are sensitive to spin-orbit coupling are being investigated. A survey paper on heavy-ion spin-orbit coupling potentials was presented at the University of Iowa - Iowa State University workshop "Double Folding Potentials for Heavy-Ion Interactions", at Iowa City on March 31 and April 1, 1978.

4. Compound-Nucleus Properties and Polarized Beams (W.J. Thompson)

Polarized-beam fluctuations of the Ericson type are being investigated theoretically, emphasizing the new information which can be obtained in the energy region of fluctuations by using such beams. The situation for elastic scattering of spin-1 beams has proved to be complicated by symmetry relations between the helicity amplitudes. Therefore the simpler spin-1/2 scattering problem is being investigated first.

Channel-channel correlation effects are being studied with the goal of designing polarized-beam, high-resolution experiments which will be sensitive to the presence of channel-channel correlations. Such experiments would supplement the previous $(p,p'\gamma)$ results at TUNL and would probably be more sensitive to resonance total J values.

5. Trion Spin-Orbit Potentials (W.J. Thompson, R.A. Hardekopf ((LASL)))

Trion (A = 3) elastic scattering optical-model potentials are important both to parameterize the scattering and to provide tests of the folding model for composite-projectile scattering. A paper describing the experiments and phenomenological optical-model analysis of the LASL 17-MeV polarized triton elastic scattering

data for 13 nuclei with $40 \leq A \leq 208$ is in final preparation.

We have determined that the spin-orbit potential has essentially the same geometric parameters and strength as for nucleon scattering. The result for the strength, parameterized in terms of the appropriate volume integrals of the spin-orbit potentials, is in strong disagreement with simple folding-model estimates of trion scattering, which claim volume integrals about 1/3 that for nucleons. This anomaly is being studied in terms of the trion structure, including D-state components.

There is no firm evidence from our analyses that the trion spin-orbit potential requires an imaginary component, contrary to recent suggestions that the deuteron spin-orbit potential has a significant imaginary part.

6. The Nucleon-Nucleus Spin-Spin Interaction (W.J. Thompson)

Detailed study of the spin-spin interaction V_{ss} in nucleon-nucleus scattering for target nuclei with spin $I = 1/2$ (which are the most favorable for interpretation of polarization data relating to V_{ss}) is underway. Recent consultation with experts in target polarization has suggested the feasibility of polarized-target experiments, scattering either polarized protons or neutrons. Such experiments may yield data very sensitive to V_{ss}. Theoretical difficulties encountered in calculating V_{ss} are the poorly-known spin-spin dependence of effective interactions in nuclei and the effects of core polarization. Compound-nucleus effects hinder the analysis at low energies, as summarized recently in a review of this author's work (P.E. Hodgson, New Scientist, 3 Feb. 1977, p. 16, and to be published).

7. Potential and Charge Deformations in Light Nuclei (W.J. Thompson, J.S. Eck ((Kansas State University)))

Our previous work on shape parameters of ^{12}C, ^{20}Ne, ^{24}Mg, and ^{28}Si has determined nuclear potential deformations from nuclear inelastic scattering and charge deformations from electromagnetic data. Our compilation is being extended to other light nuclei for which sufficiently accurate and diverse data are available, in order to understand the systematics of low-lying nuclear rotational states for $A < 40$. Tabulations of sources and results are being prepared for possible publication in Atomic and Nuclear Data Tables.

8. Scattering of ^{9}Be (W.J. Thompson, J.S. Eck ((Kansas State University and ANU, Canberra)))

We have tried to determine B(E2) values for ^{9}Be by looking at those deviations from Rutherford scattering which occur because of quadrupole excitation from its ground state. However, our preliminary calculations indicate that the effect is too small to allow accurate determination of the B(E2).

At Australian National University, Canberra, J.S. Eck is undertaking a systematic study of ^{9}Be scattering, and we are analyzing these data to determine whether ^{9}Be is better characterized as a light ion (like ^{6}Li) or as a heavy ion (like ^{12}C).

9. Atomic Effects in Nuclear Reactions (J.M. Feagin, E. Merzbacher, W.J. Thompson)

We are investigating in detail the feasibility of experiments involving coincidences between nuclear-scattered particles and atomic de-excitation products (x-rays or electrons). A description of this work has been presented at the 5th Conference on Applications of Small Accelerators. The results for resonances are of importance for extracting the widths of the very narrow isospin-forbidden resonances observed in light nuclei with the TUNL high-resolution system.

A paper describing the effects of atomic excitations in β-decay end-point energies, caused by differences between the excitation effects in β-decay and in the (p,n) reactions used to infer the end-point energies, has been submitted to Physics Letters.

10. Coherence Properties of Particle Wave Packets (E.A. Olszewski ((UNC-Wilmington)), W.J. Thompson)

A paper describing results obtained so far for the electron-proton wave packets produced in photo-ionization is in preparation. The possibility of coherence experiments with electrons is being investigated.

11. Many-Body Reaction Theory (S.R. Cotanch)

A simple unitary estimate for multi-step processes has been developed. The results have been recently reported[1] and submitted for publication in Physical Review C. The abstract of the manuscript follows:

> "Utilizing the unitary constraint for an N dimensional S-matrix and phase averaging arguments, a simple expression is derived to provide realistic bounds on the exact multi-step transition rate for the general reaction A(a,b)B. The formula, which approximately includes a large class of multi-step processes, is designed for practical upper estimates of cross section variation due to higher-order contributions from N reaction channels. The result establishes model-independent guidelines for the importance of higher-order effects and represents a "sum rule" for multi-step phenomena. Applications to the reactions $^{208}Pb(p,t)^{206}Pb(3^+)$ and $^{48}Ca(^{16}O,^{15}C)^{49}Ti$ which are improbable or forbidden in the one-step DWBA, yields cross section estimates that are within an order of magnitude agreement with observation."

---

[1] S.R. Cotanch, B.A.P.S. 23, 931 (1978)

12. Computer Code Development for Particle Capture and Polarized Charge Exchange Reactions (S.R. Cotanch)

The code RADCAP, which computes direct radiative particle capture processes, has been generalized to a coupled channels capture code (EXCAP) by including the isobaric analogue of the target nucleus. EXCAP now requires input specification of both proton and neutron effective charges as well as parameters for the Lane potential which governs the coupling between target and analogue. Further physical details can be found elsewhere.[1]

The code TWAVE, which computes charge exchange reactions, has also been generalized (TWAVE2) to compute analyzing powers. In addition an isovector spin-orbit interaction $(\vec{l}\cdot\vec{s})\,(t\cdot T)$ term has been included. The physical significance of this operator has been recently investigated in a phenomenological analysis[2]. (See Section M-22.)

These codes have been made available to all TUNL personnel.

13. Kaon-Nucleus Studies (S.R. Cotanch)

Investigations concerning the feasibility of using the K^+ meson (kaon) as a nuclear structure probe have continued. The major results obtained have been reported and have been accepted for publication.[4,5] The respective abstracts follow:

> "The plane wave impulse approximation (PWIA) is assessed for K^+ meson inelastic scattering from ^{16}O by comparison with distorted wave impulse approximation (DWIA) calculations. The K^+-nucleus distortions are directly determined from phenomenological K^+-nucleon amplitudes. For $E_{Lab} \geq 50$ MeV use of plane waves enhances the DWIA cross section less than 50%, an effect size comparable to distorted wave calculations with different sets of K^+-nucleon amplitudes."

> "K^+ meson (kaon) inelastic excitation of low-lying ($E_x = 0 - 15$ MeV) T = 0 collective states in ^{16}O is theoretically studied as a function of energy and momentum transfer. The distorted wave impulse approximation is used to calculate angular distributions and total inelastic cross sections for exciting the first $J^{\pi} = 2^+, 3^-, 4^+$, and 5^- states at lab energies from threshold to 400 MeV. The distortions are represented in a Kisslinger-type optical potential constructed from elementary K^+-nucleon amplitudes. Total nuclear elastic and reaction K^+-nucleus cross sections are computed to demonstrate sensitivity to choice in K^+-nucleon amplitudes. Fermi motion effects are also assessed using a simple averaging

[1] S.R. Cotanch, Phys. Lett. 76B, 19 (1978)
[2] R.C. Byrd, R.L. Walter, S.R. Cotanch, submitted to Phys. Rev. Lett.
[3] S.R. Cotanch, B.A.P.S. 23, 554 (1978)
[4] S.R. Cotanch, Phys. Rev. C18 (October, in press)
[5] S.R. Cotanch, Nucl. Phys. A (in press, late 1978 or early 1979)

procedure. The weak absorption character of the kaon is reflected in the inelastic calculations which predict selective excitation of low spin states at low momentum transfer and high spin states at high momentum transfer."

14. Test of Nuclear Structure Models (S.R. Cotanch, J.M. Lafferty)

Progress is continuing in the study of nuclear clustering (correlations) using a simple few-cluster model.[1] The cluster effective two-body interaction is adjusted[1] such that the important static observed nuclear properties are reproduced. Of current interest are the continuum states above the particle emission threshold. These states are being investigated through particle capture processes. The capture code RADCAP has been modified to include the cluster interaction for both the bound state and the continuum and calculations are presently being performed for the specific reaction (α,γ) on a number of light nuclei. The results of these calculations should not only have ramifications in the area of cluster transfer reactions but also, and perhaps more importantly, should provide new information concerning isoscalar giant resonances. Much of this work will be included in Lafferty's Ph.D. dissertation.

15. Realistic-α Particle Potentials (K.A. Sage, R.Y. Cusson, E.G. Bilpuch)

Keith Sage has completed his thesis on the use of our realistic heavy-ion potential code (Nucl. Phys. A270 (1976) 437). The abstract of his thesis follows.

"Brueckner-Hartree-Fock techniques are applied to the calculation of the heavy-ion interaction potential for six reactions involving combinations of ^{4}He, ^{12}C, ^{14}C, and ^{16}O. The K-matrix model for the Hamiltonian is developed and its parametrisation discussed. A self-consistent method for calculating the spin-orbit interaction is introduced and tested by fitting the nuclear properties over a wide range of nuclei. The cluster potential energy for each reaction studied is found first in an adiabatic approximation and then by using a new overlap technique in a sudden approximation. The formalism for this overlap method, taken from the work of Lowdin, is discussed in detail. The results of the overlap calculation point out the importance of shell effects in the heavy-ion potential. Comparison of the calculated adiabatic and sudden cluster potentials with the work of other authors is discussed.

The use of the adiabatic and sudden potentials as the real part of the optical potential is discussed in detail. Attempts to fit experimental data for ^{12}C + ^{4}He elastic scattering meet with little success, but it is shown that the ^{16}O+^{16}O adiabatic potential should be useful in the optical model fitting

[1] B.Buck and A.A. Pilt, Nucl. Phys. A295, 1 (1978); A280, 133 (1977)

of $^{16}O+^{16}O$ elastic scattering data. The heavy-ion optical potentials obtained here are compared with the optical potentials calculated by other authors."

16. Nuclear Rotational-Vibrational Collective Motion with Non Vanishing Vortex Momentum (B. Buck,* L.C. Biedenharn, R.Y. Cusson)

A paper giving a new and elegant derivation of the kinetic energy collective Hamiltonian in the presence of vortex-momentum has been written. The abstract follows.

"A new approach to collective motion is developed which leads naturally and nonredundantly to a separation of the kinetic energy of a many-body system into rotational, vibrational and other intrinsic motions. The results are valid both classically and quantum mechanically and do not require the imposition of approximate constraints."

17. Dynamics of Heavy Ion Reactions in a Realistic Time Dependent Hartree-Fock Model (R.Y. Cusson, J.A. Maruhm ((U. of Frankfurt)), V. Maruhn ((U. of Giessen)), H.W. Meldner ((LLL)), G. Gomesdel Campo ((ORNL)))

A paper entitled "Direct Inelastic Scattering of $^{14}N + ^{12}C$ in a 3-dimensional Time-dependent Hartree-Fock Scheme" will appear shortly in Phys. Rev. C. The abstract follows.

"Momentum space three-dimensional time-dependent Hartree-Fock (TDHF) calculations are performed on $^{12}C+^{14}N$ and $^{16}O+^{16}O$ collisions. The potential is the simplified Skyrme interaction which gives the single-particle potential $V_N(r) = - a\, p(\vec{r}) + b\, p^2(\vec{r})$, and includes the direct part of the Coulomb interaction. We use a predictor corrector method to step in time and a fast Fourier transform (FFT) method to compute the kinetic energy in momentum space. Three types of events are obtained: vibrational instability scattering at low impact parameters b, near orbiting at medium b values, and rotational instability scattering beyond that. The discussion points out that further improvements will require a fusion window and quantal corrections for angular and energy uncertainties which go beyond the TDHF method."

In addition a paper entitled "Analysis of The $^{14}N+^{12}C$ Heavy Ion Reaction" has been submitted to Phys. Rev. Lett. The abstract follows.

---

* On leave from Oxford University

"The ^{14}N (E_{lab} = 106 and 167 MeV) + C heavy ion reaction is analyzed in terms of a modified version of the semiclassical scattering model of Broglia followed by an evaporation calculation. The deflection and energy loss functions are taken from recent TDHF calculations. The complete fusion amplitude vs. the angular momentum ℓ is obtained phenomenologically. A comparison between the model predictions and experiment is made for the following quantities: the total integrated cross sections for production of a fragment with given Z, $\sigma(Z)$; energy distributions $(d^2\sigma/d\Omega dE)_Z$ at fixed laboratory angle and fragment charge; angular distribution $(d\sigma/d\Omega)_Z$ at fixed fragment charge Z and integrated over energy. The agreement is satisfactory. It is concluded that the Z spread observed in this reaction comes only from evaporation effects in the highly excited reaction fragments produced in the original inelastic collision."

An invited paper entitled "Heavy Ion Cluster in The TDHF Approximation" was published in the Proceedings of the 3rd International Conference on Clustering Aspects of Nuclear Structure, U. of Winniped, June 1978. The abstract follows.

"The Time-Dependent Hartree-Fock method is used to produce time dependent graphical representations of the density contours of the binary cluster in the reactions ^{14}N(112 MeV) + ^{12}C, ^{16}O(384 MeV) + ^{16}O, and ^{20}Ne(164 MeV)+ ^{58}Ni. Alpha clustering and multipole shape vibrations are seen. Predictions for $d\sigma/d\Omega$, $d\sigma/dZ_f$, and $d^2\sigma(E_f)d\Omega dE_f|_{Z_f}$ are obtained in the case of ^{14}N + ^{12}C and found to agree well with available experimental data. It is concluded that cluster dynamics play an essential role in heavy-ion reactions."

Lastly a paper entitled: "TDHFB Calculations of Heavy Element Fusion and Fission Phenomena" has been submitted to Phys. Rev. Letters. The abstract follows.

"Time dependent Hartree-Fock-Bogoliubov calculations in three dimensions are reported for the fusion of two ^{118}Pd isotopes and subsequent fission of the compound nucleus ^{236}U. Constant strength pairing, simplified Skyrme plus Yukawa and Coulomb interactions were included. A new result is the appearance of (non-axial) surface oscillations in the compound or fissioning systems."

18. Single Nucleon Induced Fission (R.Y. Cusson, H.W. Meldner, ((L.L.L.)), D. Epperson, F.O. Purser, C. Kalbach, H.W. Newson)

The Ph.D. thesis of D. Epperson has been completed on the analysis of multiple chance proton induced fission. The occurence of a low mass shoulder in the fission fragment mass distribution could signify that a weak branch for heavy element decay is the emission of p-f shell nuclei. The abstract follows.

> "The Cyclo-Graaff facility of the Triangle Universities Nuclear Laboratory, located at Duke University, was used to make fission fragment energy correlation measurements for three isotopes of uranium. From these measurements, fission fragment mass yield distributions have been determined. The proton induced fission of the ^{236}U and ^{235}U targets used incident proton energies ranging in energy from 6.25 MeV to 30.0 MeV in energy steps of 0.25 MeV to 1.0 MeV. Protons ranging in energy from 6.5 MeV to 14.5 MeV were used on the ^{234}U target. A total of ninety-nine fragment energy correlation measurements were made with the three targets. Commercially avaiable heavy ion silicon surface barrier detectors were used to detect the fission fragments. The uranium targets were supplied by Oak Ridge National Laboratory and were of isotopic purity greater than ninety-nine percent.
>
> For incident proton energies greater than approximately 7 MeV, neutron emission competes favorably with fission for all of the uranium isotopes. Therefore, to obtain mass distributions due solely to the first chance fission of ^{237}Np, ^{236}Np, ^{235}Np, and ^{234}Np from sharp excitation energy states ranging from below the fission barrier to 20 MeV, a method for separating experimental multichance fission mass yields was developed. This method utilizes a statistical formalism to describe the decay of the excited compound nucleus through fission, neutron emission, or gamma emission. Neighboring isotopes provide self-consistency checks. A comparison is also made with published neutron induced fission mass yield data.
>
> First chance mass yields from sharp states of excitation energy are presented for ^{237}Np, ^{236}Np, ^{235}Np, and ^{234}Np for excitation energies ranging from approximately 4 MeV to 20 MeV. Preliminary evidence for an enhanced fragment yield in the region of the doubly magic nucleus A = 78 (Z = 28, N = 50) is also shown. The effects of preequilibrium neutron emission for excitation energies between 12 MeV and 33 MeV are also discussed."

In addition, the code NIFTE7D is being used in systematic studies of n-induced fission parameters. An invited paper for the IAEA Symposium on Physics and Chemistry of fission in Julich, May 79 is being prepared. The abstract follows.

"A progress report on current results of neutron fission cross section calculations is given. This is part of a more general program which combines various semi-empirical nuclear theories for the calculation of all significant cross sections for heavy elements exposed to typical thermonuclear neutron spectra. The computer code development was motivated by many interests, e.g., in both laser fusion and in thermo-nuclear macro-explosions neutron fluences can be high enough to result in significant nuclear transmutations, especially in high-Z targets. A theoretical analysis of these processes requires cross sections for fission, capture, (n,p), (n,n'), (n,2n), etc., reactions for a large number of isotopes for most of which no data are available. Other applications are found in the calculation of neutron reactions, the actinide waste problem of the nuclear power industry, astrophysical r-process calculations, the neutron capture synthesis of very heavy, possibly superheavy nuclei, etc.

Since neutron-rich isotopes have a decreasing neutron-emission threshold (Fermi energy) as more neutrons are added the number of evaporated neutrons for incident energies of order 15 MeV can be as high as 3 to 4 before fission takes place. Earlier attempts at a calculation of multiple-chance fission were limited to two neutron evaporations because of the claimed necessity of performing a very time-consuming multi-dimensional energy integral to obtain the multiple chance fission probability. A major new feature of our code is the use of a recursive algorithm for computing the (n-1st) - chance fission given the results of the nth-chance case. Thus, the size of the calculation is linear in the number of chances and it becomes possible to take into account as many neutron evaporations as required before fission of γ-emission.

A statistical model is used for the calculation and the recursive algorithm for including the effects of higher-chance fission on the lower-chance fission and neutron-emission probabilities. The correct inclusion and/or prediction of shell structure shifted threshold positions (fission barrier heights) is clearly most important in achieving any accuracy. Empirical rules are used for the evaluation of the compound nucleus level density at the fission saddle point. Pre-equilibrium processes are taken into account via the Griffin model. The complete code is designed to predict multiple-chance neutron-induced fission, neutron capture, multiple neutron emission, (n,p) and (n,α) reactions. Our goal is the extension of the ENDL-type cross section libraries used in thermonuclear Monte-Carlo calculations to include uranium and several transuranium isotopes of

interest, up to A ≈ 260. Some sample results are presented for the fission of the various isotopes of U, from A = 233 to A = 253. The calculated energy-dependence of the neutron-induced fission of $^{235-239}$U is compared with experimental data."

19. Low Energy Behavior of Fusion Barriers in Heavy Ion Reactions (W.M. Howard ((LLL)), R.Y. Cusson, M. Arnould ((U. of Bruxelles)))

A paper entitled "Fusion of Light Ion Systems at Energies Near and Below the Coulomb Barrier" has been published in the *Proceedings of the International* Workshop on Gross Properties of Nuclei and Nuclear Excitations VI, Hirschegg, Austria, 1978 (Ed. H. von Groote). The introductory paragraph follows.

> "Experimental fusion cross sections for light ion systems at energies below the Coulomb barrier become available in greater and greater number, and provide a stringent test of the macroscopic and microscopic physics involved in models of heavy-ion reactions. Measurements and predictions of the fusion cross sections for $^{12}C + ^{12}C$, $^{12}C + ^{16}O$ and $^{16}O + ^{16}O$ are also of major importance in astrophysics.
>
> Up to now, the theoretical models do not account very well for the energy behavior of the function $S(E) \equiv E\sigma(E)x \exp(2\pi\eta)$, where E is the center of mass energy, $\sigma(E)$ the corresponding fusion cross section and η the Sommerfeld-Coulomb parameter. In this work a simple macroscopic model is adopted for the description of fusion, and its predictions are compared with experimental data."

20. Coupled Channel Analysis of Neutron Inelastic Scattering Data (H.H. Hogue, R.Y. Cusson, H.W. Newson)

Elastic and discrete inelastic neutron differential scattering cross sections for ^{6}Li and ^{7}Li in the 7-14 MeV energy range have been described using the rotational coupled channels model of Tamura.[1] The improved version of Tamura's computer program: JUPITOR KARLSRUHE VERSION[2] was used to perform the calculations. Two modifications of the program proved necessary: (1) For the ^{7}Li calculations a change was required to permit calculation of scattering by states of the K = 1/2 band where the spin 1/2 member of the band is not the ground state. (2) An error affecting the calculation for targets with non-zero integral spin, such as ^{6}Li, was eliminated. A paper describing the results of the calculations is being prepared for publication.

---

[1] Taro Tamura, Rev. Mod. Phys. 37 (1965) 679

[2] H. Rebel and G.W. Schweimer, Kernforshungszentium Karlsruhe Report No. KFK 1333, 1970

21. Inverse Bound State Problem (Brian Buck, J. Spencer ((Oxford)), R.Y. Cusson, L.C. Biedenham)

Methods have been developed for the study of the inverse bound state problem, i.e., if one knows the energy levels of a system, certain strong conditions on the form of the potential have been obtained. The method has been applied to understand why smooth deep local potentials possess extended rotational band spectra. (Varenna Lectures, Course 62, Enrico Fermi Summer School, Varenna, Italy ((1976)). Work is in progress to apply these conditions to ptoblems of nuclear and particle physics.

22. Consistent Lane Model Analyses of The Complete ^{9}Be + Nucleon Data Set (R.C. Byrd, R.L. Walter, S.R. Cotanch)

It has long been recognized that global optical model systematics suggest a symmetry dependence in the neutron and proton potentials. This implicit relationship is formally expressed in the Lane model, which further predicts isospin coupling to the quasi-elastic (p,n) reaction. This model forms the basis of subsequent applications of explicit isospin constraints to optical model analyses which include the (p,n) channel. Although it is clear from these analyses and global symmetry-dependent elastic models that the Lane assumptions are generally valid, the conclusions have been inconsistent in approach and limited in scope. As a result, no definitive test exists of the Lane model's ability to predict a complete set of observables for (p,p), (p,n), and (n,n) reactions with a single consistent potential. It is therefore not known whether the isospin constraints will allow description of such a full data set with agreement comparable to that of single-channel analyses. Such a determination is the immediate goal of our Lane model program, and we feel that our success shows the elegance that the constrained, coupled approach brings to the optical model.

We divide this report into two sections, the first of which includes the results reported last year. Its basic assumption, guided by Hartree-Fock calculations, is that the symmetry potential for light nuclei such as ^{9}Be should be broadly surface-peaked. Our initial results were that such a potential allows an excellent description of most of the ^{9}Be + nucleon data over the 11 to 15 MeV energy range. Specifically, the (p,p), (n,n), and (p,n) cross sections σ_{pp}, σ_{nn}, and σ_{pn} and the (p,p) analyzing powers A_{pp} are well represented. However, no simultaneous description of the (p,n) analyzing powers A_{pn} could be found. (Bull. Am. Phys. Soc. 23, 926 (1978).

An intensive effort was made next to explain the A_{pn} results. Reanalysis after we included in the model a symmetry spin-orbit term $V^{1}_{s.o.}(\vec{l}\cdot\vec{s})(\vec{T}\cdot\vec{T})$ showed that excellent agreement could be obtained for the complete set of observables near 13 MeV, as shown in Fig. M22-1a. It was found, however, that this solution cannot be satisfactorily extended to neighboring energies. Our conclusion concerning the analysis with surface symmetry potentials is that excellent agreement is obtained without the $V^{1}_{s.o.}$ term for all but the A_{pn} results. Further, addition of this term allows good description of the complete data set (but only at a single energy). Results of these analyses were submitted to Physical Review Letters but have now been held up

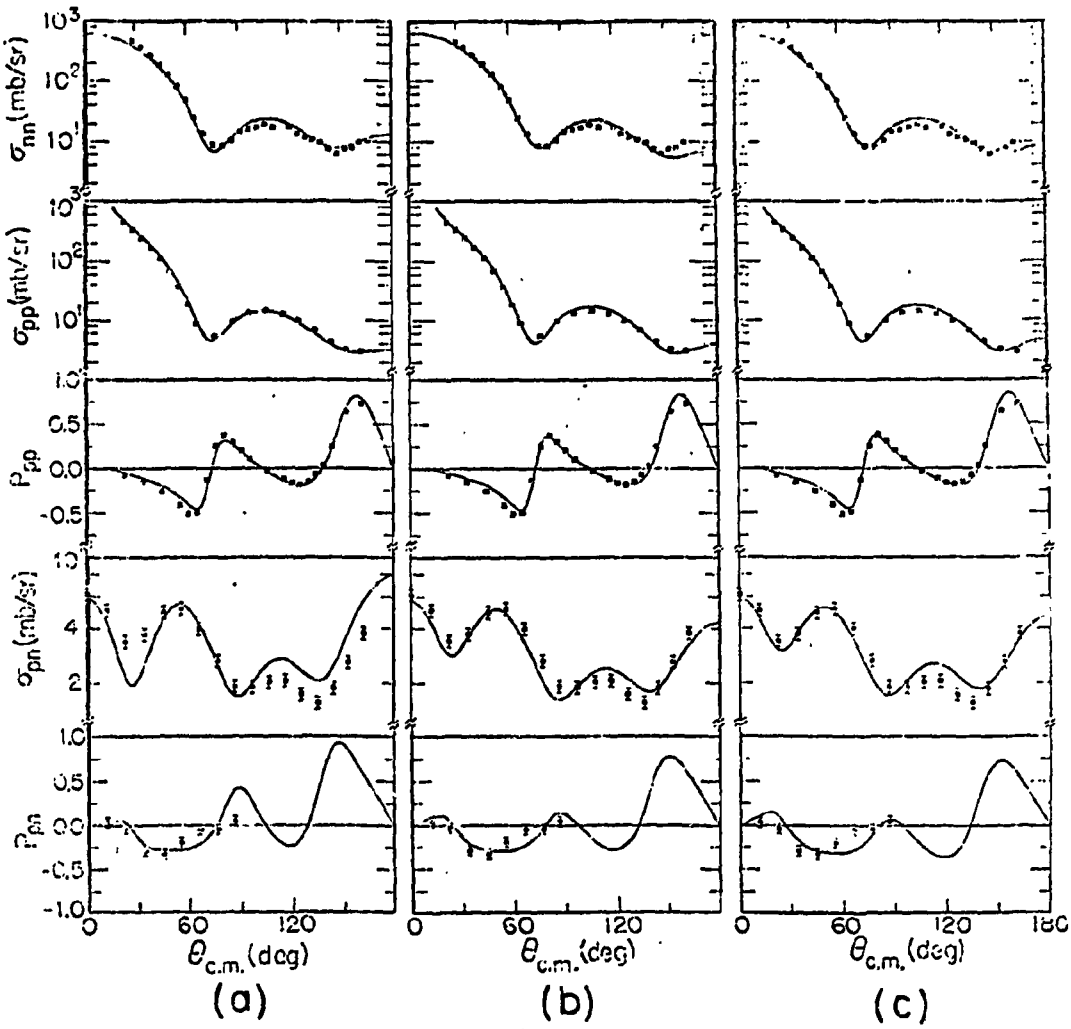

Fig. M22-1 Lane model calculations of ^{9}Be + nucleon results near 13 MeV using different assumptions. (a) Surfaced-peaked real symmetry term with symmetry spin-orbit potential. (b) Volume real symmetry term with symmetry spin-orbit potential. (c) Volume real symmetry term without spin-orbit potential.

by us because of results from a continuation of the analysis as described below.

The second set of analyses were based on a real symmetry potential with a volume shape. We present here two solutions. The first is an optical potential constrained to constant geometries, linearly-varying strengths, and small spin-orbit and Coulomb correction terms. The results, shown in Figure M22-2,

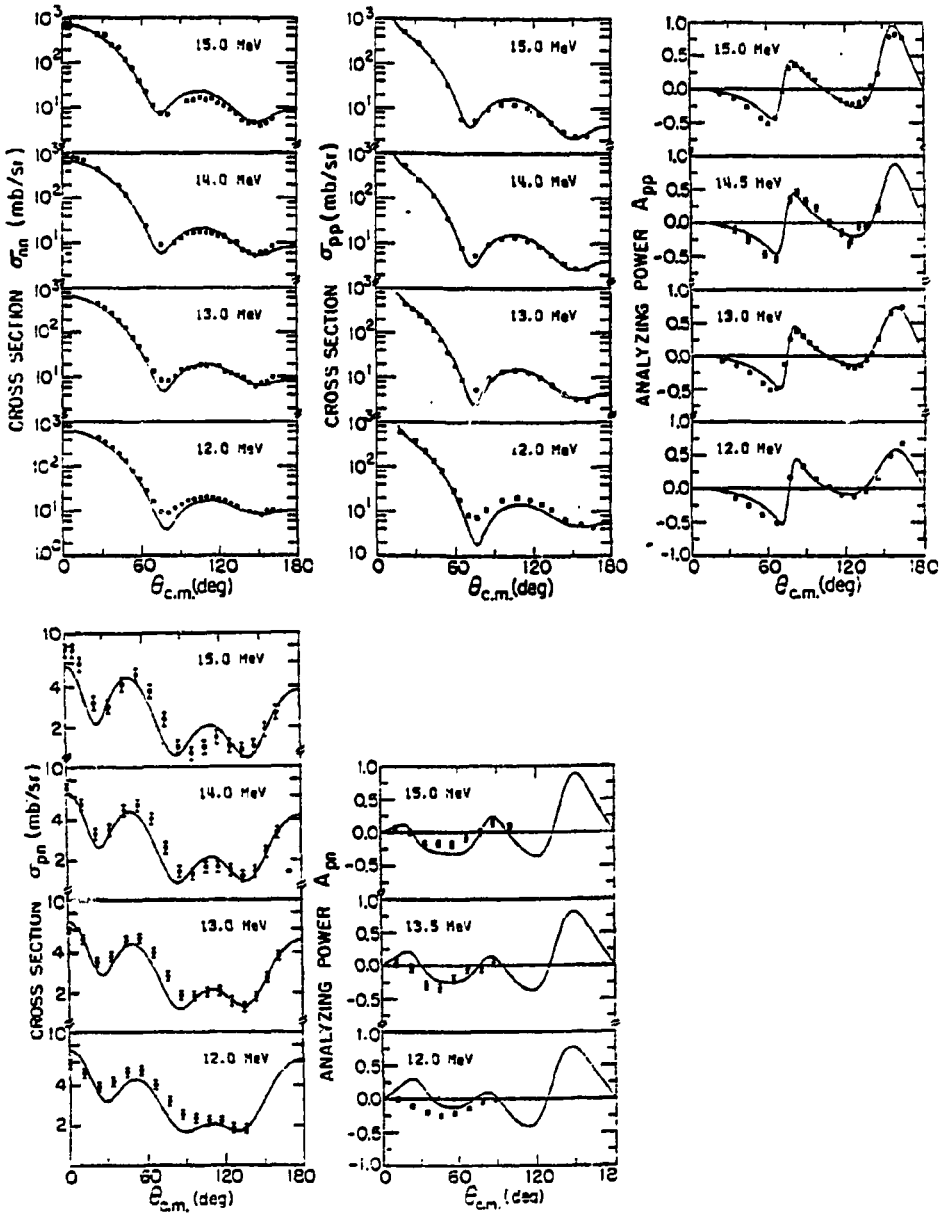

Fig. M22-2 Predictions of observables for the ^{9}Be + nucleon system from 12.0 to 15.0 MeV using a single Lane potential with constant geometries, linearly varying strengths, and a volume real symmetry term.

are a dramatic improvement over the previous surface-peaked solution, both in quality of agreement and energy range of applicability which now extends from 12 to 15 MeV. The second volume analysis used a published energy-dependent optical model for $^{9}Be(p,p)$ as a starting potential. Within the quality of the overall data set, over the full 8- to 15-MeV range the agreement shown in Fig. M22-3

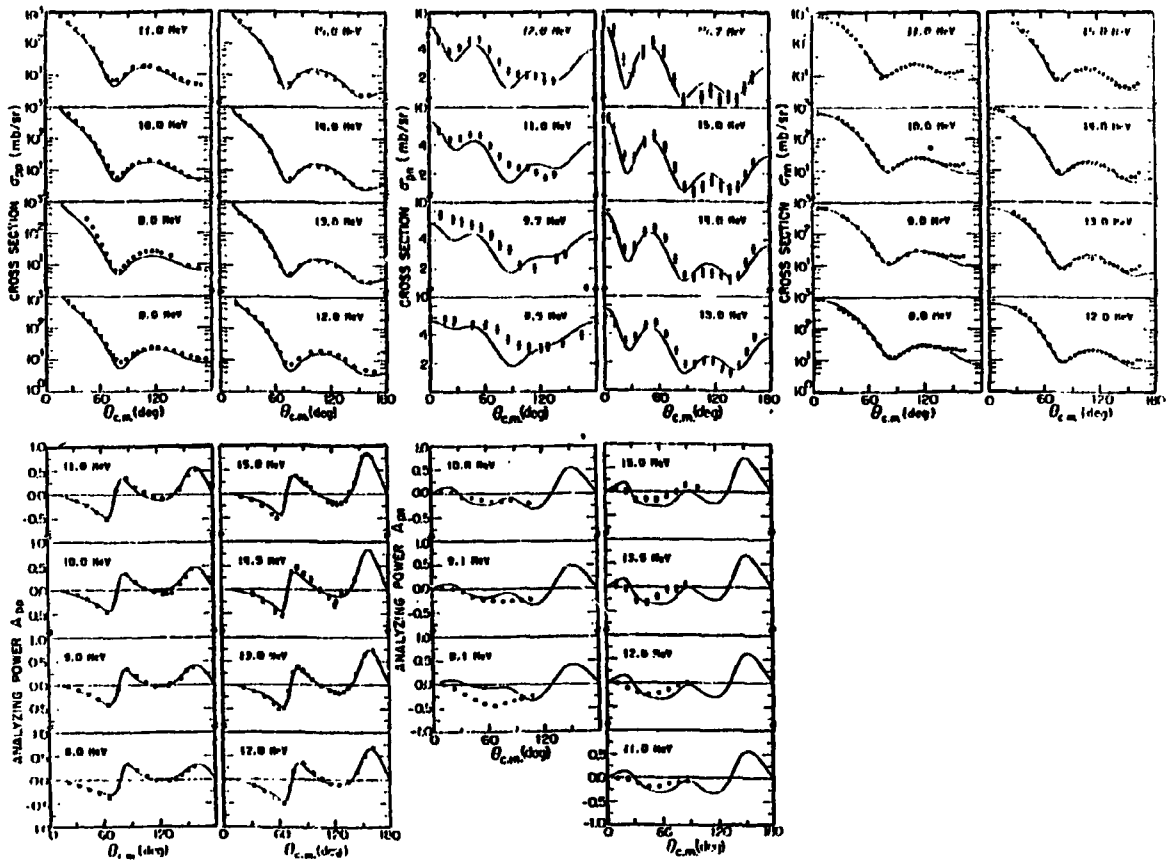

Fig. M22-3 Predictions of observables for the ^{9}Be + nucleon system from 8 to 15 MeV using a single Lane potential with smoothly energy-dependent parameters and a volume real symmetry term.

is indeed comparable to that of single-channel analyses which span a wide energy range.

Our conclusion is thus that the Lane model appears to be as valid as the optical potentials that it connects. These results were presented at the Livermore conference on the optical model and (p,n) reactions and at the 1978 meeting of the American Physical Society Division of Nuclear Physics at Asilomar.

Current analysis is focussed on resolving details of the Lane potentials discussed above. As illustration, Fig. M22-1 shows the best descriptions of the 13-MeV data obtained with three different assumptions. Part (a) shows the prediction using spin-orbit and surface real symmetry potentials. Part (b) gives the similar results with a volume shape, and Part (c) gives the results for a volume shape without spin-orbit $V'_{s.o.}$. Clearly, no unambiguous determination of the necessity of various features can be made, even in our severely constrained analysis. Future studies are anticipated on heavier targets such as the Sn isotopic sequence or the heavy, spherical ^{208}Pb nucleus. Such systems may eliminate some difficulties associated with the highly-deformed ^{9}Be target and answer questions about Coulomb effects which negligible in light nuclei.

23. Angular Distributions for Preequilibrium Emitted Particles* (C. Kalbach)

A phenomenological approach for the calculation of angular distributions of particles emitted in the preequilibrium phase of nuclear reactions is being studied. Experimental angular distributions of preequilibrium particles from a variety of reactions are being analyzed in terms of Legendre polynomials, and the systematics of the resulting coefficients are quite striking. These coefficients will be used in conjunction with a new version of the Griffin model preequilibrium code PRECO which keeps track of how much of the reaction cross section has passed only through a series of unbound states. Kerman and Feshbach[1] have suggested that this part of the cross section should have forward peaked angular distributions, while the remainder should exhibit symmetry about 90° in the center of mass.

24. Shell Effects in Preequilibrium Reactions* (C. Kalbach)

Work is in progress to implement the shell-shifted equi-spacing model for the calculation of particle-hole state densities in the Griffin preequilibrium model. All pertinent equations have been derived and are being programmed. This work requires a complete reworking of the computer code since, for the calculation of shell effects, it is necessary to keep track of the proton and neutron degrees of freedom separately. When this work is completed the validity of the Griffin model should be extended to include both light ($A \lesssim 40$) and also heavier nuclei in the vicinity of nuclear shell closures.

---

* This work is being performed on a consulting basis for Westinghouse Hanford Co.

[1] C. Kalbach, Nuov. Cim. 29A (1975) 283

25. Exciton Number Dependence of The Griffin Model Two-Body Matrix Element (C. Kalbach)

The exciton number dependence of the residual two-body matrix element has been determined using published particle-hole pair creation rates obtained from semi-phenominological calculations. The previous energy dependence of the mean squared matrix element has been replaced by a dependence on the average excitation energy per degree of freedom, E/n. For E/n less than 7 MeV or greater than 15 MeV, the form of the energy dependence has been slightly modified. These changes result in a factor of three reduction in the predicted Griffin model composite nucleus equilibration times but in only minor changes in the calculated energy spectra for emitted particles. This work has been published in Z. Phys. A 287 (1978) 319.

26. Non-Equilibrium Reaction Mechanisms for Loosely Bound Projectiles (C. Kalbach)

A study has been made of the dominant non-equilibrium reaction mechanisms for charged particle emission in d and τ induced reactions. The results of simple statistical calculations are compared with experimental angle-integrated energy spectra appearing in the literature. A consistent picture of the reactions involved can be obtained by including the following spectral components: (1) Griffin model preequilibrium, (2) nucleon transfer in the form of stripping, pickup and exchange, (3) inelastic scattering and knockout involving nucleon clusters, and (4) projectile breakup. Simple methods for calculating these components are presented. This work has been submitted for publication. Preprints are vailable on request.

27. Dynamical Two-Center Shell Model and Unified Treatment of Heavy-Ion Scattering and Transfer Reactions (J. Y. Park, W. Scheid ((Univ. of Giessen)), W. Greiner ((Univ. of Frankfurt)))

The two-center shell model, which was mostly used for static calculations up to now, has been extended to a dynamical model. Scattering and transfer reactions induced by heavy ions are described in a unified fashion using the dynamical two-center shell model. Molecular wave functions are constructed from the two-center wave functions, taking into account the antisymmetrization of the valence nucleons and symmetrization of the cores. Elastic and inelastic scattering and one-nucleon transfer reactions are considered in the coupled-channel formalism. The advantage of using the two-center molecular wave functions lies in the fact that already a large fraction of the interaction between the nucleons and the cores is contained in the two-center potential. Polarization or dynamical orientation effects are also included due to the dependence of the molecular wave functions on the relative coordinate. Another advantage of the two-center molecular treatment is that it eliminates the problem of non-orthogonality of the channel bound-state wave functions in the conventional one-center formulations. The present formulation, which includes explicitly the coupling between the direct and transfer channels, is especially convenient to study the effects of transfer channels on the scattering of heavy ion systems and the antisymmetrization effects. A report on this work was given at the International Conference on Nuclear Structure in Tokyo, Japan.

28. Two-Center Level Structure and the Landau-Zener Excitation Mechanism in Heavy Ion Collisions (J.Y. Park, W. Greiner ((Univ. of Frankfurt)), W. Scheid ((Univ. of Giessen)))

According to the Landau-Zener mechanism in atomic collisions, excitations occur mainly in avoided level crossings, causing the system to jump from one energy surface to another. In order to examine the possibility of the Landau-Zener excitation mechanism in asymmetric heavy ion collisions we have calculated single-particle energies as a function of the internuclear separation distance R for several target projectile combinations, such as $^{13}C + ^{16}O$, $^{12}C + ^{17}O$, $^{9}Be + ^{16}O$ and $^{8}Be + ^{17}O$. The asymmetric two-center shell model which includes $\vec{\ell} \cdot \vec{s}$ and ℓ^2 terms is used to calculate the single particle energies. The parameters of the two-center potential are determined by fitting the experimental level structure near the Fermi levels of the separated nuclei ($R \to \infty$) and the corresponding compound nucleus ($R \to 0$). Our calculations suggest that the cross sections for the excitation and transfer of nucleons in these reactions should exhibit certain enhancements as function of the heavy ion energies which arise due to avoided level crossings in the two-center energy level diagrams. It would be a unique signature for the formation of nuclear molecular orbits if the promotion process for nucleons could be detected in the excitation and transfer cross sections. Such experiments, which can give an answer to the important problem of the existence of molecular orbits in nuclear heavy ion collisions, are proposed. A report on this work was given at the American Physical Society meeting

in Washington.

29. Quasimolecular States in the ^{12}C - ^{12}C System (J.Y. Park, W. Greiner ((Univ. of Frankfurt)), W. Scheid ((Univ. of Giessen)))

Structure of non-statistical origin in the ^{12}C - ^{12}C cross section near the Coulomb barrier has been interpreted as quasimolecular resonances. We have applied the molecular-type adiabatic potential, which reproduced the position and the spacing of the observed sub-coulomb resonances well,[1] for the explanation of the resonances above the Coulomb-barrier up to $E_{C.M.}$ = 14 MeV. We have coupled the first excited 2^+-state on the elastic channel and obtained intermediate structures in the cross sections at energies at which the conditions for the double resonance effect are fulfilled. The effects of the coupling on the reflection and transition coefficients are studied systematically. The abstract of this work, published in Physical Review, is:

> "Quasimolecular resonance structures in the ^{12}C-^{12}C system are studied in the framework of the coupled channel formalism in the energy range $E_{C.M.}$ = 5-14 MeV. The influence of the coupling of the first excited 2^+ state in ^{12}C on the resonance structures is investigated by choosing various types of coupling potentials. The intermediate structures in the reflection and transition coefficients and cross sections can be interpreted with the double resonance mechanism."

A review of this topic was given as an invited talk at the Iowa Workshop on Double Folding Potentials for Heavy Ion Interactions, March 31-April 1, 1978.

30. Application of The Dynamical Two-Center Shell Model to the ^{13}C + ^{13}C Scattering (G. Terecki ((Univ. of Giessen)), W. Scheid ((Univ. of Giessen)), J.Y. Park)

The dynamics of the valence nucleon in the nucleus-nucleus scattering is described by the dynamical two-center shell model with molecular wave functions. The Hamiltonian operator contains the couplings which arise due to the rotation of the molecular coordinate systems (centrifugal and Coriolis terms) and the shift of the nuclear center (radial coupling). The effects of these couplings on the elastic and inelastic scattering of the ^{13}C + ^{13}C system are investigated. Further the theory of dynamical two-center shell model has been generalized to treat the neutron transfer and elastic and inelastic scattering in a unified fashion. A report on this work was given at the German Physical Society meeting in Berlin.

---

[1] J.Y. Park et al., Phys. Rev. C10 (1974) 967

31. Helicity Formulation of Collisions for Systems with Channel Spins One and Two (G.J. Grube, J.Y. Park)

Advances in the field of polarized heavy ions have given added importance to the collision problem between particles with spin one or larger spins. Apart from its simple mathematical elegance the helicity formalism is easily adaptable for the scattering problems with arbitrary spin. We have obtained in the helicity formalism explicit expressions for the scattering amplitudes in terms of the phase shifts for systems with channel spin up to two. The expressions involve only a sum over the total angular momentum J, instead of the five sums in the customary formalism. Some recursion formulae for the reduced rotational wave functions which are useful in the applications are also obtained. The present formalism is especially convenient and advantageous for scattering involving a large number of partial waves as in heavy ion scattering at medium and high energies. It can greatly reduce computational efforts to study, for example, the effects of spin dependence in the nucleus-nucleus interaction for scattering of two spin one particles, such as d, ^{6}Li, ^{14}N, ^{32}P as well as scattering of spin 1/2 particles with spin 3/2 particles, such as ^{7}Li, ^{9}Be, ^{11}B and ^{23}Na.

32. Theory of Nucleon Transfer in The Dynamical Two-Center Shell Model (J.Y. Park, W. Scheid ((Univ. of Giessen)), W. Greiner ((Univ. of Frankfurt)))

A paper with the above title has been submitted to Physical Review. The abstract follows:

> "The theory of nucleon transfer in heavy ion reactions is formulated on the basis of the molecular particle-core model for a system consisting of two cores and one extra-nucleon. The extra-nucleon is described by the molecular wave functions of the asymmetric two-center shell model (ATCSM). The core can be collectively excited and are treated with vibrator-rotator models. The potentials for shape polarization are contained in the ATCSM and the interaction between the cores. The excitation and transfer of the extra-nucleon is induced by the radial and rotational couplings. The coupled channel equations which include the recoil effects in first approximation are derived in a form suitable for numerical calculations of cross sections."

APPENDIX I

A. PUBLISHED TUNL JOURNAL ARTICLES AND ARTICLES BY TUNL PERSONNEL
January 1978-December 1978

1. High-Resolution Study of the $^{26}Mg(p,p)$ Reaction, C.R. Westerfeldt, G.E. Mitchell, E.G. Bilpuch, and D.A. Outlaw, Nucl. Phys. A303 (1978) 111.

2. New Probe of Line Broadening with Resolvable Fine Structure: The "Off-Diagonal Strength Function", A.M. Lane, T.R. Dittrich, G.E. Mitchell, and E.G. Bilpuch, Phys. Rev. Letters 41 (1978) 454.

3. A Pulsed Beam Time Pickoff System for Nanoampere Beams, P.W. Lisowski, R.L. Walter, S.A. Wender, and T.B. Clegg, Nucl. Instr. and Methods 146 (1977) 477.

4. The Analyzing Power $A_y(\theta)$ for the Elastic Scattering of 12-MeV Neutrons from Deuterons, W. Tornow, P.W. Lisowski, R.C. Byrd, and R.L. Walter, Nucl. Phys. A296 (1978) 23.

5. Neutron Emission in Strongly Damped Collisions of ^{86}Kr on ^{166}Er at 602 MeV, Y. Eyal, A. Gavron, I. Tserruya, Z. Fraenkel, Y. Eisen, S. Wald, R. Bass, C.R. Gould, G. Kreyling, R. Renfordt, K. Stelzer, R. Zitzmann, A. Gobbi, U. Lynen, H. Stelzer, I. Rode, R. Bock, Phys. Rev. Letters 41 (1978) 625-628.

6. Neutron Multiplicities in Inelastic Collisions of ^{132}Xe with ^{197}Au, C.R. Gould, R. Bass, J.V. Czarnecki, V. Hartmann, K. Stelzer, R. Zitzmann, Y. Eyal, Zeitschrift für Physik A284 (1978) 353-354.

7. Confirmation of 8^+ Assignment to the 11.86 MeV Level in ^{24}Mg, S.A. Wender, C.R. Gould, D.R. Tilley, D.G. Rickel, R.W. Zurmühle, Phys. Rev. C17 (1978) 1365-1367.

8. Angular Distribution Measurements for Radiative Capture of Fast Neutrons by ^{40}Ca, H.R. Weller, R.A. Blue, P.L. von Behren, N.R. Roberson, C.R. Gould, D.R. Tilley, S.A. Wender, Phys. Rev. C17 (1978) 1260-1263.

9. Differential Elastic and Inelastic Scattering of 7- to 15-MeV Neutrons from Beryllium, H.H. Hogue, P.L. von Behren, D.H. Epperson, S.G. Glendinning, P.W. Lisowski, C.E. Nelson, H.W. Newson, F.O. Purser, W. Tornow, C.R. Gould, L.W. Seagondollar, Nucl. Science and Engineering 68 (1978) 38-42.

10. Determination of Angular Momentum Transfers for (d,α) Reactions Using Polarized Beams, E.J. Ludwig, T.B. Clegg, W.W. Jacobs, and S.A. Tonsfeldt, Phys. Rev. Letters 40 (1978) 441.

11. A Vector Polarized Beam Study of Fluctuations in $^{28}Si + \vec{d}$, R. Henneck, T.B. Clegg, R. Haglund, and E.J. Ludwig, Nucl. Phys. A298 (1978) 189.

12. Polarized Proton Capture on ^{59}Co, J.D. Turner, C.P. Cameron, H.R. Weller, N.R. Roberson, D.R. Tilley, Phys. Rev. C17 (1978) 1853.

APPENDIX I (Continued)

PUBLISHED TUNL JOURNAL ARTICLES AND ARTICLES BY TUNL PERSONNEL

13. Polarized Proton Capture in The Giant Dipole Resonance Region, H.R. Weller, N.R. Roberson, and S.R. Cotanch, Phys. Rev. C18 (1978) 65.

14. Elastic Scattering of Polarized Protons from ^{13}C for $9.1 < E_p < 18.4$ MeV, H.R. Weller, J. Szucs, P.G. Ikossi, J.A. Kuehner, D.T. Petty, and R.G. Seyler, Phys. Rev. C18 (1978) 1120.

15. Quadrupole Radiation in Fast Neutron Capture on ^{40}Ca, S.A. Wender, N.R. Roberson, M. Potokar, H.R. Weller, D.R. Tilley, Phys. Rev. Lett. 41 (1978) 1217.

16. Large Charge Exchange Corrections to Direct Photonuclear Processes, S.R. Cotanch, Phys. Lett. 76B (1978) 19.

17. Plane Waves for Kaon-Nucleus Reactions, S.R. Cotanch, Phys. Rev. C18 (1978) 1941.

18. Projectile Fluorescence Yields in Heavy Ion Collisions, J.A. Tanis and S.M. Shafroth, Phys. Lett. 67A (1978) 124.

19. Target Thickness Dependence of Radiative Electron Capture in Heavy Ion Collisions, J.A. Tanis and S.M. Shafroth, Phys. Rev. Lett. 40 (1978) 1174.

20. Neutron Spectra from Deuteron and Proton Bombardment of Thick Lithium Targets: Potential for Neutron Therapy, C.E. Nelson, F.O. Purser, P. von Behren, and H.W. Newson, Physics in Medicine and Biology 23 (1978) 39.

21. Exciton Number Dependence of The Griffin Model Two-Body Matrix Element, C. Kalbach, Z. Phys. A287 (1978) 319.

APPENDIX I (Continued)

B. JOURNAL ARTICLES ACCEPTED FOR PUBLICATION

1. Study of Inelastic Proton Amplitudes for a Fragmented Analogue State in ^{45}Sc, G.E. Mitchell, T.R. Dittrich, and E.G. Bilpuch, accepted for publication in Zeitschrift für Physik.

2. The $^{2}H(p,\gamma)^{3}He$ Reaction Using Polarized and Unpolarized Protons, D.M. Skopik, H.R. Weller, N.R. Roberson, and S.A. Wender, accepted for publication in Phys. Rev. C.

3. Discovery of the 2^+ T=2 state in ^{28}Si, H. Zarek, T. Drake, and H.R. Weller, accepted for publication in Phys. Rev. C.

4. Spins And Parities of Low-Lying States in ^{77}Kr from The $^{78}Kr(\vec{d},t)^{77}Kr$ Reaction, R.R. Cadmus, T.B. Clegg, E.J. Ludwig, and S.A. Wender, accepted for publication in Nuclear Physics.

5. Physics with Polarized Nuclei, W.J. Thompson and T.B. Clegg, to be published in Phys. Today, January 1979.

6. Elastic and Inelastic Scattering of 7- to 14-MeV Neutrons from Lithium-6 and Lithium-7, H.H. Hogue, P.C. von Behren, D.W. Glasgow, S.G. Glendinning, P.W. Lisowski, C.E. Nelson, F.O. Purser, W. Tornow, C.R. Gould, and L.W. Seagondollar, accepted for publication in Nucl. Sci. and Engineering.

7. Selective Excitation in Kaon-Nucleus Inelastic Scattering, S.R. Cotanch, accepted for publication in Nucl. Phys. A.

8. Comment on "Complex Particle Emission in The Pre-equilibrium Exciton Model", C. Kalbach, accepted for publication in Phys. Rev. C.

9. Resonant Raman Scattering of X-rays: Evidence for K-M Scattering, A.F. Kodre and S.M. Shafroth, accepted for publication in Phys. Rev. A.

10. Projectile K X-ray Production in Thin Solid Targets, J.A. Tanis and S.M. Shafroth, accepted for publication in Japanese Journal of Applied Physics.

11. Q Values in β^+-Decay, (p,n), and (^{3}He,t) Reactions, E. Merzbacher, J.M. Feagin and W.J. Thompson, accepted for publication in Phys. Lett. B.

12. Atomic Data Related to X- and XUV-Radiation, Katharine Way, accepted for publication in Japanese Journal of Applied Physics and Atomic Data and Nuclear Data Tables.

APPENDIX I (Continued)

C. JOURNAL ARTICLES SUBMITTED FOR PUBLICATION

1. Measurements of the Reactions $^{15}N(\gamma, d_0)^{13}C$ and $^{13}C(\vec{d}, \gamma_0)^{15}N$ in The Giant Resonance Region, D.M. Skopik, J.J. Murphy, II, H.R. Weller, R.A. Blue, N.R. Roberson, S.A. Wender and D.R. Tilley, submitted to Phys. Rev. C.
2. Polarization Transfer in $(\vec{d}, n)$ Reactions on Light Nuclei at $\theta = 0°$, P.W. Lisowski, R.C. Byrd, G. Mack, and R.L. Walter, submitted to Nucl. Phys.
3. Detailed Study of the Lane Potential: Multi-Channel and Polarization Constraints, R.C. Byrd, R.L. Walter, and S.R. Cotanch, submitted to Phys. Rev. Letters.
4. Non-equilibrium Reaction Mechanisms for Loosely Bound Projectiles, C. Kalbach.
5. Simple Unitary Estimate for Multistep Processes, S.R. Cotanch, submitted to Phys. Rev. C.
6. Widths of K- Vacancy Excited States by Resonant Raman Scattering of X-rays, A.F. Kodre and S.M. Shafroth, submitted to Phys. Rev. A.
7. L_1-L_2 $M_{4,5}$ and L_1-L_3 $M_{4,5}$ Coster-Kronig Transitions Thresholds in The Region $37 \leq Z \leq 56$, B.L. Doyle and S.M. Shafroth, submitted to Phys. Rev. A.

APPENDIX II

INVITED TALKS, CONFERENCE AND TECHNICAL REPORTS AND BOOK CHAPTERS BY TUNL PERSONNEL

January 1978-December 1978

1. High Resolution Proton Resonance Studies, G.E. Mitchell (invited talk, Small Accelerator Conference) Bull. Am. Phys. Soc. 23, 1023 (1978).

2. Experimental Demonstration of Phase Relations for Common Doorway States, G.E. Mitchell, T.R. Dittrich, and E.G. Bilpuch, presented at Third International Symposium of Neutron Capture Gamma-Ray Spectroscopy, Brookhaven National Laboratory, Sept. 18-22, 1978, to be published.

3. Evidence for an E2 Resonance Observed by Radiative Capture of Fast Neutrons by ^{40}Ca, N.R. Roberson, M. Potokar, D.R. Tilley, S.A. Wender and H.R. Weller, to be published in "Proceedings of the Third International Symposium on Neutron Capture Gamma-Ray Spectroscopy and Related Topics", Sept., 1978.

4. Extension of the Lane Model to Light Nuclei, Roger C. Byrd, Richard L. Walter, and Stephen R. Cotanch, to be published in Lecture Notes in Physics 84, Springer-Verlag, Heidelberg, ed. by H. Zankel.

5. Recent Advances in Neutron Polarization Studies, Invited talk at Washington American Physical Society Meeting by Richard L. Walter, Bull. Am. Phys. Soc. 23, 610 (1978).

6. Particle Induced X-Ray Emission Analysis - PIXEA, R. L. Walter and R.D. Willis, Chapter 6 in Practical Spectroscopy Series, Vol. 2 (Marcel Dekker, Inc., New York) ed by L.S. Birks and H.K. Herglotz, p. 123 (1978).

7. Results of a Self-Consistent Application of the Lane Model to a Complete Data Set, R.C. Byrd, Conference on The (p,n) Reaction and Its Connection to the Nucleon-Nucleus Optical Model at Livermore Lawrence Laboratory, Oct. 1978.

8. Comparison Between Polarization and Analyzing Power Functions for (p,n) Reactions, R.L. Walter, Conference on The (p,n) Reaction and Its Connection to the Nucleon-Nucleus Optical Model at Livermore Lawrence Laboratory, Oct. 1978.

9. Inner-shell Vacancy Production by Charged Particles, Lecture notes for Nordic Spring Symposium at Geilo, Norway, April 1978, Eugen Merzbacher, submitted for publication.

10. Brownian Motion of a Quantum Oscillator and Random Walk in Phase Space, Eugen Merzbacher, to be published in Festschrift for Julian Schwinger, 1979.

11. Atomic Excitation Effects on Nuclear Resonances and Q Values, Eugen Merzbacher, J.M. Feagin, W.J. Thompson, Extended Abstract for Fifth Conference on Applications of Small Accelerators, Denton, Texas, November 1978, to be published in Proceedings of IEEE.

APPENDIX II (Continued)

INVITED TALKS, CONFERENCE AND TECHNICAL REPORTS AND BOOK CHAPTERS BY TUNL PERSONNEL

12. Resonant Raman X-ray Scattering: New Directions, A.F. Kodre and S.M. Shafroth, IEEE, Transactions on Nuclear Science, Invited talk, S.M. Shafroth.

13. Effect of Target Thickness on Characteristic Projectile X Rays and REC in Ion Atom Collisions, J.A. Tanis and S.M. Shafroth, IEEE, Transactions on Nuclear Science, Invited Talk, J.A. Tanis.

14. Resonant Raman X-ray Scattering, S.M. Shafroth, Colloquium, Catholic University, March 1978.

15. Non-equilibrium Reaction Mechanisms in Light Ion Induced Reactions, C. Kalbach, presented at Crocker Nuclear Laboratory, University of California at Davis.

16. Non-equilibrium Reaction Mechanisms in Light Ion Induced Reactions, C. Kalbach, presented at E Division, Lawrence Livermore Laboratory.

17. The Griffin Model: Myths and Methods of Nuclear Reactions, C. Kalbach, presented at the Physics Department, Oregon State University.

18. Proton Capture, H.R. Weller, Invited talk at Photonuclear Gordon Conference, August, 1978.

APPENDIX III

ABSTRACTS OF CONTRIBUTED PAPERS PRESENTED AT AMERICAN PHYSICAL SOCIETY AND OTHER MEETINGS

1. High Resolution Study of the $^{26}Mg(p,p)$ Reaction, C.R. Westerfeldt, G.E. Mitchell, D.A. Outlaw, and E.G. Bilpuch, Bull. Am. Phys. Soc. 23, 520 (1978).

2. High Resolution Proton Inelastic Scattering on ^{46}Ti, J.R. Chandler, G.E. Mitchell, and E.G. Bilpuch, Bull. Am. Phys. Soc. 23, 521 (1978).

3. High Resolution Proton Inelastic Scattering on ^{48}Ti, W.K. Wells, E.G. Bilpuch and G.E. Mitchell, Bull. Am. Phys. Soc. 23, 521 (1978).

4. A High Resolution Study of the Lowest $1/2^+$ Analogue State in ^{91}Nb, M.E. Bleck, W.K. Wells, D.A. Outlaw, C.R. Westerfeldt, E.G. Bilpuch and G.E. Mitchell, Bull. Am. Phys. Soc. 23, 554 (1978).

5. Discovery of the 2^+ T=2 State in ^{28}Si, H. Zarek, B. Pich, S. Yen, T. Drake, J. Szvcs and H.R. Weller, Bull. Am. Phys. Soc. 22, 995 (1977).

6. Angular Distribution Measurements for the $^{40}Ca(n,\gamma_0)^{41}Ca$ Reaction, S.A. Wender, N.R. Roberson, H.R. Weller, M. Potokar, D.R. Tilley, M. Jensen, Bull. Am. Phys. Soc. 23, 507 (1978).

7. Polarized Proton Capture on ^{13}C, J.D. Turner, N.R. Roberson, S.A. Wender, H.R. Weller, D.R. Tilley, Bull. Am. Phys. Soc. 23, 602 (1978).

8. Polarized Proton Capture Studies at the Triangle Universities Nuclear Laboratory, H.R. Weller, Bull. Am. Phys. Soc. 22, 1259 (1977).

9. The $^{78}Kr(\vec{d},p)^{79}Kr$ Reaction Using Vector-Polarized Deuterons, B.C. Burks, R.R. Cadmus, T.B. Clegg and E.J. Ludwig, Bull. Am. Phys. Soc. 23, 954 (1978).

10. A Deuteron Vector and Tensor Polarimeter Employing the $^3He(d,p)^4He$ Reaction, S.A. Tonsfeldt, T.B. Clegg and E.J. Ludwig, Blacksburg, Va. meeting of the American Physical Society, 26-28 Oct. 1978.

11. An Energy Calibration of the TUNL Van de Graaff System, J.F. Wilkerson, T.B. Clegg and E.J. Ludwig, Blacksburg, Va. meeting of the American Physical Society, 26-28 Oct. 1978.

12. Neutron Multiplicities in Inelastic Collisions of ^{132}Xe with ^{197}Au, C.R. Gould, R. Bass, J.V. Czamecki, V. Hartman, K. Stelzer, R. Zitzmann, Y. Eyal, Bull. Am. Phys. Soc. 23, 523 (1978).

13. Neutron Scattering from ^{11}B, C.R. Gould, S.G. Glendinning, H.H. Hogue, C.E. Nelson, A. Beyerle, S. El-Kadi, H.W. Newson, F.O. Purser, L.W. Seagondollar, Bull. Am. Phys. Soc. 23, 635 (1978).

14. Parity Experiments in Atomic Hydrogen and Deuterium, C.E. Weinman, E.S. Fry, R.W. Dunford, R.R. Lewis, W.L. Williams and T.B. Clegg, Bull. Am. Phys. Soc. 23, 39 (1978).

APPENDIX III (Continued)

ABSTRACTS OF CONTRIBUTED PAPERS PRESENTED AT AMERICAN PHYSICAL SOCIETY AND OTHER MEETINGS

15. Investigation of Several Ion Sources for Producing Metastable Hydrogen Beams, S.M. Mitchell, T.B. Clegg and H.L. Manning, Bull. Am. Phys. Soc. 23 (1978), Blacksburg, Va.

16. Lane Model Analysis of (p,p), (p,n_0), and (n,n) Reactions on ^{9}Be, R.C. Byrd, R.L. Walter and S.R. Cotanch, Bull. Am. Phys. Soc. 23, 526 (1978).

17. Cross-Section Measurements for (p,n) Reactions on ^{9}Be, ^{13}C, and ^{15}N from 10 to 16 MeV, R.L. Walter, R.C. Byrd, C.E. Floyd, P.P. Guss, and R.K. Murphy, Bull. Am. Phys. Soc. 23, 926 (1978).

18. Evidence for Surface-Peaked Real and Spin-Orbit Symmetry Potentials in the Optical Model, R.C. Byrd, R.L. Walter, and S.R. Cotanch, Bull. Am. Phys. Soc. 23, 926 (1978).

19. Direct and Preequilibrium Reactions with Loosely Bound Projectiles, C. Kalbach, Bull. Am. Phys. Soc. 23, 571 (1978).

20. Kaon Excitation of High Spin States, S.R. Cotanch, Bull. Am. Phys. Soc. 22, 1021 (1977).

21. Unitary Estimate for Multistep Processes, S.R. Cotanch, Bull. Am. Phys. Soc. 23, 931 (1978).

22. Toward a More Detailed Understanding of Ion-Atom Collisions, E. Merzbacher, Bull. Am. Phys. Soc. 23, 1020 (1978).

23. Calculation of Atomic Alignment in Head-on Collisions with Charged Particles, E. Merzbacher and M.W. Clark, abstract for SESAPS meeting, October 1978, to be published in Bull. Am. Phys. Soc.

24. Quantum Equations of Motion in Accelerated Reference Frames, E. Merzbacher and T.K. Wu, abstract for SESAPS meeting, 1978. To be published in Bull. Am. Phys. Soc.

25. High Resolution Measurement of Chlorine Projectile K_α X Rays, J.A. Tanis, E. Drane, A. Kodre, S.M. Shafroth, Bull. Am. Phys. Soc. 23, 597 (1978).

26. Comparison of Radiative Electron Capture by Cl Ions in C and Cu, S.M. Shafroth, A. Kodre, J.A. Tanis, J. Willis, and R. Mowat, Bull. Am. Phys. Soc. 23, 598 (1978).

27. X-Ray Scattering in the Vicinity of the K Edge, A.F. Kodre and S.M. Shafroth, Bull. Am. Phys. Soc. 23, 622 (1978).

28. Projectile Fluorescence Yield in Heavy Ion Collisions, J.A. Tanis and S.M. Shafroth, Program and Abstracts, International Conference on X-ray and XUV Spectroscopy, Sendai, Japan, Aug. 28-Sept. 1, 1978, pg. 201.

APPENDIX III (Continued)

ABSTRACTS OF CONTRIBUTED PAPERS PRESENTED AT AMERICAN PHYSICAL SOCIETY AND OTHER MEETINGS

29. Target Thickness Dependence of Radiative Electron Capture in Heavy Ion Collisions, J.A. Tanis and S.M. Shafroth, Program and Abstracts, International Conference on X-ray and XUV Spectroscopy, Sendai, Japan, Aug. 28-Sept. 1, 1978, p. 240.

    Resonant Raman X-ray Scattering as Below-Threshold Excitation of X-Ray Line Spectra, A.F. Kodre and S.M. Shafroth, Program and Abstracts, International Conference on X-ray and XUV Spectroscopy, Sendai, Japan, Aug. 28-Sept. 1, 1978, p. 267.

30. Apparatus for the Detection and Analysis of X-ray Induced Electron Emission, J.K. Swenson, A.F. Kodre and S.M. Shafroth, Program, Southeastern Section of the American Physical Society, 26-28 Oct. 1978, p. 22.

31. Curved Crystal X-ray Spectrometer of Target and Projectile Cl K Satellites, J.A. Tanis, J. Willis, A. Kodre, S. M. Shafroth and R. Mowat, Program, Southeastern Section of the American Physical Society, 26-28 Oct. 1978, p. 22.

32. Resonant Raman X-Ray Scattering, A. Kodre and S.M. Shafroth, Bull. Am. Phys. Soc. 23, 1045 (1978).

33. Unified Description of Target and Projectile X Rays vs. Target Thickness, J.A. Tanis and S.M. Shafroth, Bull. Am. Phys. Soc. 23, 1053 (1978).

34. A Study of the Temperature Dependence of K X-Ray Fluorescence in V_2O_5, A. Kueny, C.V. Briscoe, A. Kodre and S.M. Shafroth, Annual Meeting, North Carolina Academy of Sciences, Wake Forest Univ., April 7, 8, 1978.

35. Potassium K Satellite Production by Incident Cl Ions, E. Drane, J.M. Feagin, S.M. Shafroth and J.A. Tanis, Annual Meeting, North Carolina Academy of Sciences, Wake Forest Univ., April 7, 8, 1978.

36. Resonant Raman Scattering of X-Rays, A. Kodre and S.M. Shafroth, Annual Meeting, North Carolina Academy of Sciences, Wake Forest Univ., April 7, 8, 1978.

APPENDIX IV

Articles Published, January 1978-December 1978
in Journal edited at TUNL by K. Way

Atomic Data and Nuclear Data Tables

Vol. 20, No. 2

Energy Levels and Classifications of Doubly-Excited States in Two-Electron Systems with Nuclear Charge, Z = 1, 2, 3, 4, 5, below the N = 2 and N = 3 Thresholds
L. Lipsky, R. Anania, and M.J. Conneely

Higher-Order Corrections to Level Energies of Muonic Atoms
G.A. Rinker and R.M. Steffen

Screening Constants for the Helium and Lithium Isoelectronic Sequences
K.-N. Huang

Bremsstrahlung Energy Spectra from Electrons of Kinetic Energy 1 keV $\leq T_1 \leq$ 2000 keV Incident on Neutral Atoms $2 \leq Z \leq 92$
R.H. Pratt, H.K. Tseng, C.M. Lee, L. Kissel, C. MacCallum, and M. Riley

Vol. 20, No. 3

E2, M1 Multipole Mixing Ratios in Even-Even Nuclei, $58 \leq A \leq 150$
K.S. Krane

Gamma-Ray and Half-Life Data for the Fission Products
J. Blachot and C. Fiche

Vol. 20, No. 4

Semiempirical Auger-Electron Energies for Elements $10 \leq Z \leq 100$
F.P. Larkins

Vol. 20, No. 5

Ranges of Projectiles with $8 \leq Z \leq 20$ in Ti, Fe, Ni, Cu, Ag, and Au for Energies of 0.0125 to 12.0 MeV/Nucleon
L. Winsberg

Steady-State Radiative Cooling Rates for Low-Density, High-Temperature Plasmas
D.E. Post, R.V. Jensen, C.B. Tarter, W.H. Grasberger, and W.A. Lokke

APPENDIX IV (Continued)

Vol. 20, No. 5 (con't)

Quasi-Ground, Quasi-Beta, and Quasi-Gamma Bands
M. Sakai and A.C. Rester

Vol. 20, No. 6

Positron-Annihilation Data Tables
R.M. Singru, K.B. Lal, S.J. Tao, and R.M. Lambrecht

Extended Tables for Plane-Wave Born-Approximation Calculations of Direct Coulomb Ionization of the K-Shell by Charged Particles
R. Rice, G. Basbas, and F.D. McDaniel

Longitudinal Development of Electromagnetic Cascades in Lead, Iron, Copper, and Air
D. Adler, B. Fuchs, and K.O. Thielheim

Lifetimes of Doubly-Excited States of Atomic Helium
W. Shearer-Izumi

Cross Sections for the Photoionization of $H_2(X\,^1\Sigma_g^+, v_i = 0\text{-}14)$ with the Formation of $H_2^+(X\,^2\Sigma_g^+, v_f = 0\text{-}18)$, and Vibrational Overlaps and R^n-Centroids for the Associated Vibrational Transitions
M.R. Flannery, H. Tai, and D.L. Albritton

Vol. 21, No. 1

Internal Conversion Coefficients for E5 and M5 Nuclear Transitions, $30 \leq Z \leq 104$
I.M. Band, M.B. Trzhaskovskaya, and M.A. Listengarten

Wavelengths and Transition Probabilities of Satellites to Resonance Lines of H- and He-Like Ions
L.A. Vainshtein and U.I. Safronova

Momentum-Transfer Cross Sections for Electron Collisions with Atoms and Molecules: Revision and Supplement, 1977
Y. Itikawa

Relativistic Dirac-Fock-Slater Orbital Binding Energies and One-Electron Transition Energies: Cu XVI-XIX, Zn XVII-Zn XX, Ag XI-Ag XIX, and Sn XVIII-Sn XXIII
K. Rashid

APPENDIX IV (Continued)

Vol. 21, Nos. 2-3	Internal Conversion Coefficients for All Atomic Shells ICC Values for Z = 30-67 F. Rösel, H.M. Fries, K. Alder, and H.C. Pauli
Vol. 21, Nos. 4-5	Internal Conversion Coefficients for All Atomic Shells ICC Values for Z = 68-104 F. Rösel, H.M. Fries, K. Alder, and H.C. Pauli

APPENDIX V

Ph.D. DISSERTATIONS - 1978

A High Resolution Study of the Lowest $1/2^+$ Analogue State in ^{91}Nb, Mark Eric Bleck (Duke University)

Channel Spin Mixing Ratios in High Resolution Proton Inelastic Scattering on ^{46}Ti, John Russell Chandler (North Carolina State University)

High Resolution Proton Inelastic Scattering on ^{56}Fe and ^{48}Ti, William Kent Wells (Duke University)

The Giant Dipole Resonance Region of ^{14}N Polarized and Unpolarized Proton Capture Measurements, James David Turner (Duke University)

Systematics of Mass Yield Distributions for The Nuclear Fission of Neptunium, Dennis Harley Epperson (Duke University)

Isospin in (p,n) Reactions between Mirror Nuclei: The Lane Model and Comparison between Polarizations and Analyzing Powers, Roger C. Byrd (Duke University)

MASTER OF SCIENCE THESES - 1978

Spectroscopic Factors for The ^{207}Pb(d,t)^{206} Reaction from Analysis of Polarized Deuteron Data, James Willis (University of North Carolina, Chapel Hill)

APPENDIX VI

TUNL SEMINARS 1978

1. Brian Buck, Oxford University (1/12/78)
   Why Do Smooth Local Potentials Give Rise to Rotational Bands?
2. Daniel E. Murnick, Bell Laboratories (1/19/78)
   Laser-induced Nuclear Orientation: An Intersection of Laser and Nuclear Spectroscopy
3. Henry R. Weller, University of Florida (2/7/78)
   Giant Resonances in Nuclei: Past, Present and Future
4. David G. Mavis, Stanford University (2/9/78)
   An Update on The Feasibility and Application of Polarized Atomic Beam Targets
5. Daniel F. Coope, University of Kentucky (2/14/78)
   Collective Excitations in Low Energy Neutron Scattering
6. Francis Perey, Oak Ridge National Laboratory (2/15/78)
   Evidence For and Speculations About Unexplained Naturally Occuring Radioactivities
7. Richard E. Anderson, University of Colorado (2/21/78)
   Fragmentation of Elementary Nuclear Modes--Weak Coupling Model Revisited
8. Hans-Otto Meyer, Institut Für Physik, Basel (2/28/78)
   Elastic Scattering and Asymptotic Nuclear Wavefunctions
9. Henry H. Hogue, Duke University (4/6/78)
   Fast Neutron Scattering Cross Section Measurements in P Shell Nuclei
10. Roger C. Byrd, Duke University (4/13/78)
    Lane Model Description of ^{9}Be + Nucleon Interactions
11. Charles E. Ragan, Los Alamos Scientific Laboratory (4/20/78)
    Shock Wave Experiments in The 20 MBar Pressure Region Using Underground Nuclear Explosions
12. Dennis H. Epperson, Duke University (6/29/78)
    Systematics of Mass Yield Distributions for The Nuclear Fission of Neptunium
13. Erhard Steffens, Max Planck-Institut für Kernphysik, Heidelberg (7/6/78)
    Experiments at Heidelberg with the Polarized Alkali Source
14. Thomas B. Clegg, University of North Carolina - Chapel Hill (9/14/78)
    Physics with Polarized Beams
15. Thomas Bauer, LASL and Centre d'Etudes Nucleaires de Saclay, Paris (9/19/78)
    A Study of (p,d) Reactions on Targets for A = 6 to 40 with Protons at 800 MeV
16. W. J. Thompson, University of North Carolina-Chapel Hill (9/28/78)
    Polarized Reflections from Bad Honnef

APPENDIX VI (Continued)

TUNL SEMINARS 1978

17. Klaus Wienhard, Justus-Leibig Institüt-Giessen, W. Germany (10/5/78)
Nuclear Resonance Fluoresence Scattering with Polarized and Unpolarized Photons

18. H. Klein, Braunschweig, W. Germany (10/10/78)
Neutron Experiments at the Physikalishe Technische Bundesanstalt

19. Henry R. Weller, Duke University (10/19/78)
The $(\vec{p},\gamma)$ Capture Reaction--A Review

20. Ray V. Poore, Los Alamos Scientific Laboratory (10/24/78)
The New LASL Computing System

21. Daniel J. Horen, Oak Ridge National Laboratory (10/26/78)
Definitive Identification of M1 Radiating States in Lead Isotopes by Means of High Resolution Neutron Transmission and Scattering Measurements

22. Steven M. Shafroth, University of North Carolina-Chapel Hill (11/2/78)
A Short Summary of The Sendai, Japan Conference on X-ray and XUV Spectroscopy

23. Thomas B. Clegg, University of North Carolina-Chapel Hill (11/9/78)
Thoughts on Accelerator and Ion Source Technology after The Recent SNEAP Meeting at Oak Ridge

24. N. Russell Roberson, Duke University (11/16/78)
The (n,γ) Capture Program at TUNL

25. Fred H. Schmidt, University of Washington, Seattle (11/21/78)
Tandem Van de Graaff Accelerators and Radio-Chronology--An Unlikely Wedding

26. Dean Haldeson, Florida State University (11/30/78)
Applications of The Center-of-Mass-Corrected Continuum Shell Model

27. G. A. Keyworth, Los Alamos Scientific Laboratory (12/7/78)
Fission with Polarized Neutrons and Polarized Targets

28. Peter Schwandt, Indiana University Cyclotron Facility (12/7/78)
Intermediate Energy Nuclear Physics at The Indiana Cyclotron

29. Chris Bottcher, Oak Ridge National Laboratory (12/14/78)
Coherent Effects in Heavy-Ion Atom Collisions

30. M. A. M. Shahabuddin, McMaster University (12/19/78)
A Comparison of (t,α) and (p,α) Reactions in The Transitional Nuclei